

The Pennsylvania State University
The Graduate School
Department of Crop and Soil Sciences

**COUPLING SOIL NITROGEN CYCLING AND HYDROPEDELOGY WITHIN
FORESTS AND AGROECOSYSTEMS**

A Dissertation in
Soil Science
by
Michael J. Castellano

Submitted in Partial Fulfillment
of the Requirements
for the Degree of

Doctor of Philosophy

December 2009

The dissertation of Michael J. Castellano was reviewed and approved* by the following:

Jason P. Kaye
Assistant Professor of Biogeochemistry
Dissertation Advisor
Co-Chair of Committee

Hangsheng Lin
Associate Professor of Hydropedology/ Soil Hydrology
Co-Chair of Committee

Elizabeth W. Boyer
Associate Professor of Forest Resources

Gary W. Petersen
Distinguished Professor Emeritus of Soil and Land Resources

John P. Schmidt
Adjunct Associate Professor of Soil Science

David M. Sylvia
Professor of Soil Microbiology
Head of the Department of Crop and Soil Sciences

*Signatures are on file in the Graduate School

ABSTRACT

Humans have doubled natural inputs of mineral nitrogen to terrestrial Earth, and these inputs are accelerating. Greater than 1/3 of this human-derived nitrogen reaches surface and ground waters, creating significant environmental problems such as the hypoxic zones in the Chesapeake Bay and Gulf of Mexico and the pollution of drinking waters. However, human-derived mineral nitrogen is necessary for the maintenance of human health; synthetic ammonia-based fertilizers account for approximately 40% of global human protein consumption.

The vast majority of human-derived mineral nitrogen travels through the soil prior to reaching surface and ground waters. Within the soil, mineral nitrogen is transformed and transported by a variety of water-dependent mechanisms. I explicitly linked biogeochemical and hydrological nitrogen cycling mechanisms at different scales and in different ecosystems. I used a variety of approaches including meta-analysis, laboratory experimentation and field observation.

At the global scale, I demonstrate that within-site spatial variation in soil solution nitrate, dissolved organic nitrogen and saturated hydraulic conductivity are similarly related to soil clay content. Clay content explained greater than 1/3 of within-site spatial variation in nitrate, dissolved organic nitrogen and saturated hydraulic conductivity. These relationships suggest that soil hydrology, as mediated by clay content, may be a significant mechanism affecting variation in soil solution nitrogen. Moreover, these data show that the heterogeneity of an important resource, soil solution N, is a predictable function of clay content.

Across an artificially drained agroecosystem landscape I examined biogeochemical and hydrological controls on the magnitude and timing of nitrous oxide flux from the soil. I collected soil columns from three landscape positions that vary in hydrological and biogeochemical properties. Across all landscape positions, there was a positive linear relationship between total soil nitrogen and the log of cumulative nitrous oxide emissions ($r^2 = 0.47$; $p = 0.0132$). Within individual soil columns, nitrous oxide flux was a Gaussian function of water filled pore space and matric potential during drainage. These data demonstrate that biogeochemical properties control the absolute magnitude of nitrous oxide flux while hydrological properties control the timing of nitrous oxide flux. The Gaussian relationship between nitrous oxide flux and matric potential reveal that water filled pore size is the hydrological property controlling the relative magnitude of soil nitrous oxide flux across all soils; using these data I identified that maximum nitrous oxide flux occurs when pores $>40 \mu\text{m}$ have drained.

Within a northeastern United States deciduous forest, I monitored soil solution ammonium and nitrate concentrations as well as volumetric soil water content across two environmental gradients: a 30 meter catenary hillslope and 300 meter silt-to-sand soil texture gradient. Across the gradients, soil solution nitrate and ammonium increased downslope and with sand content. Immobilization of nitrate and ammonium into insoluble organic nitrogen compounds could not explain this pattern. In contrast, nitrogen mineralization could help to explain this pattern; in situ net ammonification rates were positively correlated with sand content.

TABLE OF CONTENTS

LIST OF FIGURES	vii
LIST OF TABLES	x
ACKNOWLEDGEMENTS	xi
Chapter 1 Coupling nitrogen biogeochemistry and hydrology: justification and importance	1
Chapter 2 Global within-site variance in soil solution nitrogen and hydraulic conductivity are correlated with clay content	5
Abstract.....	5
Introduction.....	6
Methods	9
Data Retrieval	9
Determination of Variation.....	10
Determination of Soil Texture.....	12
Data Analysis.....	13
Results.....	15
Discussion.....	20
Literature Cited.....	25
Chapter 3 Hydrological and biogeochemical controls on the timing and magnitude of nitrous oxide flux across an agricultural landscape	32
Abstract.....	32
Introduction.....	32
Methods	36
Field Location & Sample Collection.....	36
Sample Treatment.....	37
Experimental Protocol	40
Data Analyses	42
Results.....	43
Discussion.....	49
Cumulative N ₂ O Emissions	50
Relative Magnitude of N ₂ O Emissions.....	51
Literature Cited.....	55
Chapter 4 Nitrogen transport and transformation along gradients of topography and soil texture.....	61
Abstract.....	61

Introduction.....	62
Methods	65
Field Site	65
Experimental Design	68
Monitoring Equipment	71
Laboratory and Field Analyses.....	72
Statistical Analysis	75
Results.....	75
Soil Properties	75
Throughfall	76
Soil Solution	78
Soil Volumetric Water Content	82
Net Ammonification and Net Nitrification.....	83
Insoluble Organic Nitrogen	84
Discussion.....	87
Soil Solution Nitrogen.....	88
Ammonium and Nitrate Immobilization	89
Conclusion.....	90
Literature Cited.....	91
Chapter 5 Conclusions	97
Literature Cited.....	99
Appendix A.	100
Appendix B.	113
Appendix C.	114
Appendix D	121

LIST OF FIGURES

- Figure **2-1**: Nitrate (NO_3), dissolved organic N (DON) and K_s (soil saturated hydraulic conductivity) coefficients of variation and corresponding clay contents. Each triangle represents an independent report. The bold, solid lines correspond to modeled data from a 4 parameter Gaussian function $y = y_o + ae^{\left[-0.5\left(\frac{x-x_o}{b}\right)^2\right]}$. Nitrate, $r^2 = 0.35$, $p < 0.0001$; DON, $r^2 = 0.53$, $p < 0.0001$; K_s , $r^2 = 0.39$, $p = 0.0001$. The smaller dashed lines represent the 95% and 5% confidence intervals of the regression modeled data. 16
- Figure **2-2**: Inset: Mean (se) nitrate and DON CVs from the same lysimeters within reports (paired t-test $n = 23$; $p = 0.072$). However, the difference in magnitude of variation was a function of clay content. On the y-axis, zero corresponds to no difference between nitrate and DON CVs. The bold curve represents modeled data from the exponential function $y = ae^{-bx}$ ($r^2 = 0.30$; $p = 0.007$). 19
- Figure **2-3**: Paired comparison of nitrate and DON CVs (mean, se) from reports that compared soil solution N between young or recently harvested forests and old forests (paired t-test; nitrate $n = 8$, $p = 0.033$; DON $n = 4$; $p = 0.038$).... 20
- Figure **3-1**: Schematic of a 30 x 30 cm soil column drawn to scale. 47
- Figure **3-2**: The log of cumulative N_2O flux as a linear function of total soil nitrogen ($r^2 = 0.47$; $p = 0.0132$). Circles indicate Ditch, triangles indicate Near-Ditch and Squares indicate Middle-Field. 47
- Figure **3-3**: Nitrous oxide flux as a function of water filled pore space and matric potential for Block 2 soil columns. Circles indicate Ditch, triangles indicate Near-Ditch and squares indicate Middle-Field. The x-axis for matric potential has been truncated to increase clarity. Bold lines indicate a 3 parameter Gaussian model fit to the data. See Table 2 for r^2 and p values. See Appendix 3-1 for complete data set for all replicates.. 48
- Figure **3-4**: Water filled pore space at which maximum N_2O flux occurred (WFPS_{max}) as a function of total porosity ($r^2 = 0.76$; $p = 0.0002$) and bulk density ($r^2 = 0.83$; $p < 0.0001$). Circles indicate Ditch, triangles indicate Near-Ditch and squares indicate Middle-Field. 48

- Figure 3-5: Water retention curves for Block 2 soil columns during the 96 hour experiment. Note different scale among x axes. Dashed reference lines indicate the volumetric soil water content at which maximum instantaneous N_2O flux rate was measured. Ditch and Middle data in smaller symbol size indicate modeled data. All other data were empirically measured. 49
- Figure 4-1: Topographic map including 1 m contour intervals. The general area of occurrence for each soil series is displayed (Joppa, Elsinboro and Evesboro). The general gradient in soil texture is indicated as well. ... 66
- Figure 4-2: Location where the lithified paleosol intersects the soil surface. Inset: Icicle formation as evidence of lateral flow parallel with the hillslope. Bottom right: My conceptual understanding of water flow through the hillslope soils. 68
- Figure 4-3: A) Blue lines indicate monitoring transects that span topographic and texture gradients. Transects are labeled one through eight from the North to South. Red circles indicate each monitoring location (N = 8 Ridgetop, N = 8 Hillslope and N = 8 Toeslope locations). B. Sampling design at each monitoring location (indicated in 4-3 A with red circles). 70
- Figure 4-4: Linear regressions between mean 2009 A horizon tension lysimeter soil solution nitrogen concentrations and sand content. Circles indicate ridgetop position, squares indicate hillslope position and triangles indicate toeslope position. 78
- Figure 4-5: Linear regression between cumulative 2009 A horizon soil solution flux across all sample locations (N = 22; December 2008- August 2009). Circles indicate ridgetop position, squares indicate hillslope position and triangles indicate toeslope position. 79
- Figure 4-6: Linear regression between the $\log(x+1)$ transformed difference between mean 2009 (December 15, 2008-August 24, 2009) zero tension lysimeter nitrate-N concentration and A horizon tension lysimeter nitrate-N (N = 20 pairs) and saturated hydraulic conductivity (Jurinko 2009). Circles indicate ridgetop position, squares indicate hillslope position and triangles indicate toeslope position. Log transformation was necessary due to low y-axis values (Zar 1999). 80
- Figure 4-7: Volumetric water content (black lines), tension lysimeter nitrate-nitrogen (red triangles) concentration and tension lysimeter ammonium-nitrogen (blue squares) concentrations from 2008 sandy-soil A horizon replicates. Arrows indicate periods of decreasing soil moisture that are associated with increasing nitrate-nitrogen concentrations. Blue ovals indicate increases in volumetric water content that are associated with a subsequent decrease in soil solution nitrate-nitrogen concentrations. 81

- Figure 4-8: Linear regression between 3-day net ammonification and sand content. Circles indicate ridgetop position, squares indicate hillslope position and triangles indicate toeslope position. 84
- Figure 4-9: Linear regressions between the transfer of ammonium-¹⁵nitrogen and nitrate-¹⁵nitrogen isotope tracers to insoluble organic nitrogen compounds. Filled circles are ammonium and open circles are nitrate. 86

LIST OF TABLES

Table 2-1 : Four Parameter Gaussian functions fit to soil texture and coefficient of variation (CV) data. See Figure 2 caption for equation.	17
Table 3-1 : Mean and standard error of physical properties at each sample location (n = 4). Different letters within a row indicate a statistically significant difference ($p < 0.05$).	44
Table 3-2 : Mean and standard error of various indices of nitrous oxide flux during the 96-hour experiment. Different letters within a row indicate statistically significant differences ($p < 0.01$). Individual Gaussian model fits (r^2 s) for all individual replicates were significant ($p < 0.0001$). Water filled pore size at maximum N_2O flux indicates the largest pore size that remained filled with water at maximum N_2O flux (i.e. all larger pores were drained at maximum N_2O flux).	45
Table 4-1 : Selected soil properties from transect sample locations displayed in Fig. 4-3. * indicates a location where soil solution and throughfall were not collected.	77
Table 4-2 : Mean (standard error) of soil properties across topographic locations and soil horizons. Three independent 3 x 2 analyses of covariance with topographic location and soil horizon main effects and a sand content covariate demonstrated significant effects of topographic location and soil horizon on all three soil properties ($p < 0.05$). There was no significant interaction effect in any of the analyses. Post hoc analyses of topographic location demonstrated the Toeslope location to be significantly different from the Ridgetop and Hillslope locations for all three dependent variables ($p < 0.05$).	77
Table 4-3 : Mean (standard error) of throughfall and soil solution nitrogen concentrations from December 15, 2008 through August 24, 2009. Letters within column indicate topographic location was a significant source of variation in analyses of covariance. Different letters within columns indicate significant differences between locations ($p < 0.05$).	82
Table 4-4 : Correlation coefficients (R) and probabilities of Type I errors (p) between the transfer of 15 Ammonium-nitrogen and 15 Nitrate-nitrogen isotope tracers into insoluble organic nitrogen and sand content ($g\ kg^{-1}$), carbon-to-nitrogen ratio, and soil organic carbon ($g\ kg^{-1}$).	85

ACKNOWLEDGEMENTS

I thank my family for their commitment to education. I thank my committee members and advisors for their dedication and collegiality. This work was funded by the United States Department of Agriculture Needs Fellowship Program (2005-38420-15774), the United States Department of Agriculture Agricultural Research Service, the National Oceanic & Atmospheric Association National Estuarine Research Reserve Graduate Research Fellowship Program and the National Science Foundation Division of Environmental Biology Doctoral Dissertation Improvement Grant Program.

Chapter 1

Coupling nitrogen biogeochemistry and hydrogeology: justification and importance

Humans have doubled the annual background mineralization of nitrogen through ammonia synthesis, legume cultivation and impure hydrocarbon combustion (Galloway et al. 2008). The magnitude of this anthropogenic change is large: In comparison, humans have only increased the annual mineralization of carbon by approximately ten percent (Smil 2000).

Similar to human-derived carbon mineralization (e.g., hydrocarbon combustion), human-derived nitrogen mineralization can have negative environmental consequences including water pollution, forest mortality and greenhouse gas production (Galloway et al. 2008). However, human-derived mineral nitrogen is necessary for the maintenance of human health; synthetic ammonia-based fertilizers account for approximately 40% of global human protein consumption (Smil 2001). Thus, some societies suffer the environmental consequences of excess mineral nitrogen applications while other societies suffer the health consequences of food shortages and protein deficiencies that could be alleviated with increases in mineral nitrogen fertilizer applications (Vitousek et al. 2009).

In areas that currently receive excess mineral nitrogen inputs, greater than 1/3 of the inputs typically reach surface and ground waters, creating significant environmental problems such as the hypoxic zones in the Chesapeake Bay and Gulf of Mexico and the pollution of drinking waters (Schlesinger 2009). The vast majority of these mineral

nitrogen inputs travel through the soil prior to reaching surface and ground waters.

Within the soil an interaction between biogeochemical and hydrological transformation and transport processes determine an ecosystem's ability to retain mineral nitrogen inputs, preventing transport to surface and ground waters.

My objectives were to examine interactions between biogeochemical and hydrological mechanisms that control the transformation and transport of nitrogen through soil. An improved understanding of these interactions can help to identify the locations and times of disproportionately large mineral nitrogen fluxes, potentially enhancing ecosystem management and modeling capabilities. To achieve these objectives I worked within and across a variety of scales and ecosystems and used approaches including meta-analysis, laboratory experimentation and field observation. This dissertation includes three empirical endeavors that are independently described in Chapters 2-4.

Chapter 2 demonstrates that within-site spatial variation in soil solution nitrate, dissolved organic nitrogen and saturated hydraulic conductivity are similarly related to soil clay content across a diverse array of globally distributed soils. These relationships suggest that that soil hydrology, as mediated by clay content, may be a significant mechanism affecting spatial variation in soil solution nitrogen. Moreover, these data show that the heterogeneity of an important ecosystem resource, soil solution N, is a predictable function of clay content.

Working across a pedologically diverse agricultural catena, Chapter 3 demonstrates that biogeochemistry controls the absolute magnitude of soil nitrous oxide flux while hydrology controls the timing of soil nitrous oxide flux. Moreover, Chapter 3

identifies soil water filled pore size to be the hydrological mechanism that controls the relative magnitude of soil nitrous oxide flux.

Chapter 4 describes patterns in soil solution mineral nitrogen concentrations and volumetric water content across gradients topography and soil texture. A negative relationship between soil solution flux and sand content prevents relatively mineral nitrogen-rich sandy soils from exporting more nitrate and ammonium than mineral nitrogen-poor silty soils.

The final Chapter, 5, unites the core conclusions from Chapters 2-4 within the framework of a coupled conceptual model of hydrological nitrogen transport and biogeochemical nitrogen transformation. Chapter 5 continues to discuss the future of coupled nitrogen cycling and hydrogeology research.

Literature Cited

- Galloway JN, Townsend AR, Erisman JW, Bekunda M, Cai ZC, Freney JR, Martinelli LA, Seitzinger SP, Sutton MA. 2008. Transformation of the nitrogen cycle: recent trends, questions and potential solutions. *Science* 320, 889-892.
- Schlesinger WH. 2009. On the fate of anthropogenic nitrogen. *Proceedings of the National Academy of Sciences* 106, 203-208.
- Smil V. 2000. *Feeding the World: A Challenge for the 21st Century*. The MIT Press, Cambridge, MA 320 pp.
- Smil V. 2001. *Enriching the Earth: Fritz Haber, Carl Bosch and the Transformation of World Food Production*. The MIT Press, Cambridge, MA. 411 pp.

Vitousek PM, Naylor R, Crews T, David MB, Drinkwater LE, Holland E, Johnes PJ, Katzenberger J, Martinelli LA, Matson PA, Nziguheba G, Ojima D, Palm CA, Robertson GP, Sanchez PA, Townsend AR, Zhang FS. 2009. Nutrient Imbalances in Agricultural Development. *Science* 324, 1519-1520.

Chapter 2

Global within-site variance in soil solution nitrogen and hydraulic conductivity are correlated with clay content

Abstract

Nutrient fluxes in terrestrial ecosystems are governed by complex biological and physical interactions. Ecologists' mechanistic understanding of these interactions has focused on biological controls including plant uptake and microbial processing. However, ecologists and hydrologists have recently demonstrated that physical controls are also important. Using a meta-analysis of published data, I show that within-site spatial variation in soil solution N concentrations is a function of soil clay content across a globally diverse array of field sites. Clay content explained 35% and 53% of the coefficient of variation (CV) in soil solution nitrate (NO_3) and dissolved organic nitrogen (DON), respectively. The CV of soil hydraulic conductivity is a similar function of clay content, suggesting that soil hydrology may be a significant mechanism affecting variation in soil solution N. Although vegetation physiognomy and soil C/N ratios are known to affect soil solution N concentrations, neither were significantly related to within-site spatial variation in NO_3 or DON. However, the spatial variation of NO_3 and DON was greater in younger forests than in paired older forests. My data show that the heterogeneity of an important resource, soil solution N, is a predictable function of clay

content. Resource heterogeneity, such as that described here for soil solution N, can affect population, community and ecosystem processes.

Introduction

Studies of ecosystem nutrient cycling and retention have traditionally focused on plant and microbial processes (Vitousek and others 1982; Magill and others 1997; Bohlen and others 2001). However, several recent reviews and empirical studies demonstrate that ecosystem losses of nitrate (NO_3), dissolved organic nitrogen (DON), and dissolved organic carbon are controlled by complex interactions between biological mechanisms (plant and microbial activity) and physical mechanisms mediated by soil hydrology (e.g., Neff and Asner 2001; Qualls 2000; Lohse and Matson 2005; Asano and others 2006; De Schrijver and others 2007; Dittman and others 2007). At the global scale, the relative importance of biological and physical controls on nutrient cycling has not been evaluated across ecosystems. Moreover, with the exception of several well known examples, the identification of global patterns in terrestrial biogeochemistry is hindered by high chemical and physical variation within soils (e.g., Schimel and others 1994; Raich and Potter 1995; Jobbagy and Jackson 2000).

Variation itself is an important yet often overlooked ecosystem property (Kratz and others 2003). Analyses of ecological variability have provided significant insight into population, community, and ecosystem ecology. For example, studies have shown that cross-scale intraspecific variation in population abundance is predictable (Brown and others 1995), biodiversity can promote community stability (Tilman 1999), and

interannual variation in aboveground net primary production is a function of both precipitation variability and potential growth rates (Knapp and Smith 2001). Across ecosystems, variation in properties such as nutrient cycling and productivity is often related to physical attributes including climate and soil (Prentice and others 1992; Schimel and others 1994; Knapp and Smith 2001).

Nutrient loss through the soil is one important ecosystem property that is affected by interactions between soil hydrology and biogeochemistry (Fisher and others 2004). To measure this property, ecologists routinely sample soil solution nitrogen (N). These data are used to develop ecosystem nutrient budgets and determine potential nutrient pollution of ground and surface waters (Chapin and others 2002). Several reviews have synthesized these measurements, focusing on regional patterns of solute concentration, flux and their controls (Kalbitz and others 2000; Qualls 2000; De Schrijver and others 2007). However, to my knowledge, global cross-ecosystem patterns of variability have not been examined.

Here, I test biologically-based and physically-based hypotheses to explain within-site variability of an important ecosystem resource, soil solution N. Two important biologically-based controls on ecosystem N leaching are vegetation physiognomy and soil C/N ratio. Vegetation physiognomy can affect soil solution N through differences in throughfall and litter quality (e.g, Manderscheid and Matzner 1995; Michalzik and others 2001; De Schrijver and others 2007). Soil C/N ratio is negatively correlated with ecosystem nitrate export (Emmett and others 1998; Lovett and others 2002). Due to the correlations between these variables and soil solution N concentrations, I explored the potential for vegetation physiognomy and C/N ratios to account for within-site variation

in soil solution N through the following two hypotheses: 1a) Within-site spatial variation of soil solution N is a function of vegetation physiognomy. 1b) Within-site spatial variation of soil solution N peaks at intermediate soil C/N ratios and is lower in soils with narrow (N availability is consistently high with little variation) or wide (rapid immobilization keeps N low with little variation) C/N ratios.

Alternatively, soil hydrologists have demonstrated that physical structure of soil can affect water and solute transport including dissolved N (e.g., Vervoort and others 1999; Jarvis 2007). Recently, Jarvis (2007) developed a conceptual model that describes soil hydrology and solute transport as a function of soil structure. Soil structure refers to the development of soil aggregates; well structured soils have many aggregates whereas poorly structured soils have few aggregates. The model builds upon the general relationship between soil structure and clay content— soils with moderate clay content are well-structured whereas soils with low clay or high clay contents are poorly structured. Accordingly, the model predicts that, as a result of poor structure, soils with low and high clay contents are dominated by homogenous soil hydrology characterized by equilibrium and matrix flow. In contrast, the model predicts that soils with a quantitatively undefined moderate clay content, and thus good structure, are dominated by heterogeneous soil hydrology characterized by non-equilibrium and preferential (bypass) flow. Thus, I hypothesize: 2a) Within-site spatial variation of soil solution N is a function of clay content peaking at moderate clay contents, but not a function of sand or silt content. Because I posit hydrology is a mechanism affecting variation in soil solution N, I further hypothesize: 2b) within-site spatial variation of soil hydrology (as indexed by saturated hydraulic conductivity) is a similar function of clay content.

Methods

Data Retrieval

To test hypotheses 1 and 2a, I searched the peer-reviewed published literature for papers that report mineral soil solution nitrate (NO_3) and dissolved organic N (DON) sampled by tension lysimeters, zero tension lysimeters, or centrifuge methods. I selected these two biogeochemicals because they differ in biological availability; NO_3 is cycled rapidly and widely used by plants and microbes whereas DON is cycled more slowly and is less biologically available (Neff and others 2003). Because hypothesis 2 addresses the relationship between soil solution and soil structure, I did not include data from lysimeters that sampled surface organic soil horizons that overlay mineral soils. However, I did include data from lysimeters that sampled completely organic soils (i.e. peat soils). I also limited my search to non-agricultural systems because agriculture disturbs soil structure and alters N cycling. Similarly, when experiments compared manipulation treatments to untreated controls, I only used data from the controls. When available, I recorded the time since major disturbance such as forest harvest or fire (Appendix). Two papers reported total dissolved inorganic N ($\text{NH}_4 + \text{NO}_3$); I included these data with reports of NO_3 (Lajtha and others 1995; Dijkstra and others 2007). The inclusion or exclusion of these data did not significantly change my results.

To test hypothesis 2b, I conducted a similar search of the peer-reviewed literature for papers that report saturated hydraulic conductivity (K_s) of surface soils. I selected K_s because this is the most frequently reported soil hydrology variable and the standard for measuring water conductivity due to difficulty in estimating unsaturated conductivity. I

executed this search with the same inclusion rules applied to my search for soil solution N data.

Determination of variation

Several methods are available to measure variation in ecological data (Fraterrigo and Rusak 2008). I used the coefficient of variation (CV) of the mean ($CV = 100 * \frac{\text{standard deviation}}{\text{mean}}$) to standardize and compare within-site spatial variation across studies. The CV has a long history of use in studies of ecosystem variability (e.g., Whittaker and others 1979, Knapp and Smith 2001). Because the CV standardizes for the mean and is a dimensionless number, it permits comparison of variation across ratio scale data with different units and means (Fraterrigo and Rusak 2008). Although the CV can be sensitive to low mean values, I found no correlation between mean soil solution concentrations of NO_3 and DON or rates of K_s and their respective CVs. Calculation of the CV requires the following information: the mean and standard deviation (SD) *or* the mean, standard error (SE) and sample size. I collected these data from tables and figures. I could not include many reports of soil solution N in my analysis because they did not contain these data, or the data were presented in figures that were too small to interpret (e.g., Carnol and others 1997).

Spatial variability in ecosystem properties can be scale dependent (Collins and Smith 2006) and the papers included in my analyses sampled a wide range of spatial scales. Replicate plot sizes ranged from 1-5000m²; total treatment areas ranged from 6-75,000m². However, it was rarely possible to determine the distance between lysimeters

within plots or treatments. In a majority of reports, lysimeters were randomly located within plots. Thus, I made no evaluation of spatial scale on soil solution N CVs.

I required spatial means and errors. Thus, I carefully considered how means and errors were derived in each paper. For example, I could not use data that calculated a mean and error by first averaging replicates within each sample time and then averaging across sample times (e.g., a monthly mean). However, I could use data that were derived from multiple sample times but first averaged across-time within a replicate and then multiple replicates' cross-time means were averaged (i.e., a spatial mean).

Several papers reported the spatial mean and error (SE or SD) for multiple time points (e.g., months, seasons, years). In these cases I used the mean CV of the time points in my analysis by calculating the average CV across time. In two of these papers, the standard error was greater than the mean for a particular point in time. I eliminated these time points from calculation of the CV because they do not significantly differ from zero and it was not clear from the methods whether near-zero means resulted from values near detection limits or from missing data assigned a zero concentration value (e.g., no water collected in the lysimeter; Johnson and others 2001; Brenner and others 2006). This interpretation rule also resulted in the total elimination of NO_3 data from a third paper where the standard error was greater than the mean on all sample dates and the CV was >200% (Asano and others 2006).

If a paper reported the mean and an error for replicate locations (e.g., mean and errors of subsamples within a replicate), I used the treatment CV (and not multiple CVs for each replicate). Several papers provided mean soil solution N and error for multiple

mineral soil depths within a location; in these cases, I determined the CV for each depth and then used the cross-depth mean CV in my analysis.

Determination of Soil Texture

In addition to the CV of soil solution NO_3 , DON and K_s , I also required percent clay (by mass) of the soil. I obtained percent clay data in one of five ways (ordered in preference): 1. reported in the paper, 2. reported in a previously published paper from the same location, 3. contacted the author, 4. published on the USDA NRCS Web Soil Survey (NRCS 2008; <http://websoilsurvey.nrcs.usda.gov/app/>), 5. taken as the mean of the reported soil texture class. The fourth method was used by locating the research site latitude and longitude (typically to seconds) on the Web Soil Survey and retrieving the mean sand, silt and clay contents to lysimeter depth as reported in the Web Soil Survey database. The fifth clay determination method was clearly the least accurate. However, I only used this method for 11% of my data. When I was forced to use this method, I determined soil texture as follows: if soil texture was reported to be “clay loam” I used 33.75% clay because that is the mean clay content for the clay loam soil texture class which has a range from 27.5-40% clay (NRCS 2008). Sand and silt contents were determined the same way for each textural class. Soil clay content typically varies with depth; accordingly, I used the depth-weighted mean soil texture to lysimeter depth when possible.

Data Analysis

To evaluate hypothesis 1a (“within-site spatial variation of soil solution N is a function of vegetation physiognomy”), I sorted each report of soil solution NO_3 and DON into one of seven vegetation physiognomy groups (Conifer; Hardwood-Deciduous; Hardwood-Evergreen; Grassland; Savanna-Shrubland; Mixed Conifer-Deciduous and Heath). Then, using two individual one-way analyses of variance (ANOVA), I independently analyzed the dependent variables NO_3 CV and DON CV across the between subject factor vegetation physiognomy. I selected the seven physiognomy groups because two have been used to evaluate the effect of vegetation physiognomy on soil solution N concentrations (i.e., Hardwood-Deciduous and Conifer; e.g., Currie and others 1996; De Schrijver and others 2007); the other four groups separated the remaining data between well accepted global biomes (Prentice and others 1992). Although Savanna-Shrubland and Heath are both dominated by a shrub physiognomy, the Savanna Shrubland sites were dominated by nonericaceous species whereas the Heath sites were dominated by ericoids.

To evaluate hypothesis 1b (“within-site spatial variation in soil solution N peaks at intermediate soil C/N ratios”) and 2a (“within-site spatial variation in soil solution N is a function of clay content”), I again independently analyzed NO_3 and DON data. Using Sigmaplot®, I fit the percent clay (x) and CV (y) data to several Gaussian and lognormal functions exhibiting a single maximum. I did not formally select among curve-fitting options because my interest was in determining whether non-linear relationships existed, rather than defining a specific non-linear curve. However, I did examine the residuals of

these curves to determine the modeled data's fit throughout the data range. I also examined the relationships between NO_3 and DON CVs and sand and silt content although these data were not available for seven reports. To evaluate hypothesis 2b, (“within-site spatial variation of soil saturated hydraulic conductivity is a function of clay content”), I fit K_s CVs and clay, sand and silt content to the same functions I used for NO_3 and DON.

I used a subset of reports to 1) evaluate the relative magnitude of NO_3 and DON CVs for cases when lysimeter water was analyzed for both N species, 2) compare the relative magnitude of NO_3 or DON CVs between young or recently harvested forests and paired older forests and 3) compare the relative magnitude of NO_3 or DON CVs between unmanipulated controls and paired N addition treatments (Appendix A). Twenty-five reports analyzed lysimeter water for both NO_3 and DON. Nine reports compared NO_3 and four reports compared DON between young or recently harvested forests and older forests on the same soils. Four reports compared NO_3 and four reports compared DON between unmanipulated controls and paired mineral N addition treatments on the same soils. I used paired t-tests to make all of these comparisons. I also used a majority of reports to search for a general effect of time since major disturbance across all reports (i.e., forest harvest, fire or cessation of cropping; Appendix A).

The distributions of data did not significantly differ from the normal distribution according to the Kolmogorov-Smirnov test for normality of distributions ($p > 0.1$; Zar 1997) and variance was not significantly different between groups (t-tests and ANOVA). Sample sizes in analyses of variance for vegetation physiognomy were not equal.

However, equal sample sizes are not required for single-factor ANOVA although they do diminish statistical power (Zar 1997).

To evaluate hypothesis 1a (“within-site spatial variation of soil solution N is a function of vegetation physiognomy”), I sorted each report of soil solution NO_3 and DON into one of seven vegetation physiognomy groups (Conifer; Hardwood-Deciduous; Hardwood-Evergreen; Grassland; Savanna-Shrubland; Mixed Conifer-Deciduous and Heath). Then, using two individual one-way analyses of variance (ANOVA), I independently analyzed the dependent variables NO_3 , CV, and DON CV across the between subject factor vegetation physiognomy. I selected the seven physiognomy groups because two have been used to evaluate the effect of vegetation physiognomy on soil solution N concentrations (i.e., Hardwood-Deciduous and Conifer; e.g., Currie and others 1996; De Schrijver and others 2007); the other four groups separated the remaining data between well accepted global biomes (Prentice and others 1992). Although Savanna-Shrubland and Heath are both dominated by a shrub physiognomy, the Savanna Shrubland sites were dominated by nonericaceous species whereas the Heath sites were dominated by ericoids.

Results

I found 36 papers that met my requirements for soil solution N data. These papers included a total of 98 independent reports of NO_3 (61) and DON (37) representing different soils and vegetation physiognomies. Geographically, my data set includes representatives from Africa, Asia, Europe, North America, and South America.

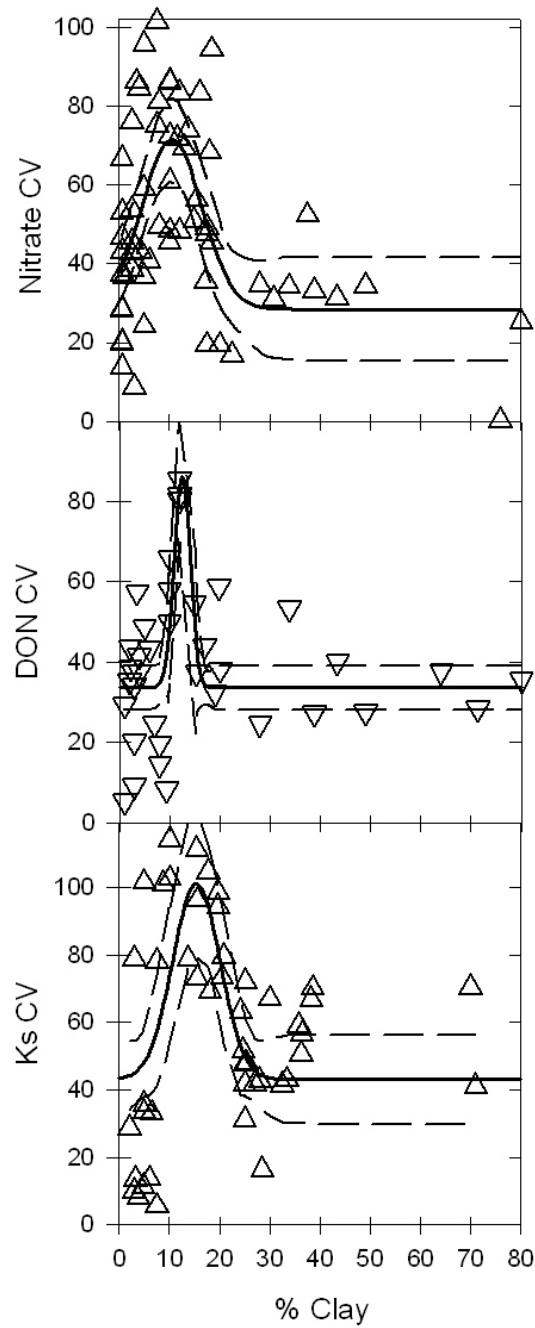


Figure 2-1. Nitrate (NO_3), dissolved organic N (DON) and K_s (soil saturated hydraulic conductivity) coefficients of variation and corresponding clay contents. Each triangle represents an independent report. The bold, solid lines correspond to modeled data from a 4 parameter Gaussian

$$\text{function } y = y_o + ae \left[-0.5 \left(\frac{x - x_o}{b} \right)^2 \right]. \text{ Nitrate, } r^2 = 0.35, p < 0.0001; \text{ DON, } r^2 = 0.53, p < 0.0001; K_s,$$

$r^2 = 0.33, p = 0.0008$. The smaller dashed lines represent the 95% and 5% confidence intervals of the regression modeled data.

Ecologically, these data are distributed across forest, grassland and wetland biomes from the tropics to the sub-arctic. However, there was no effect of vegetation physiognomy or soil C/N ratios on NO_3 or DON CVs (data not shown). Although not included in my hypotheses, I also found no effect of time since disturbance, or total C or total N on soil solution N CVs.

I found 25 independent papers that met my requirements for K_s data. These papers included a total of 46 independent reports. Similar to reports of soil solution N, these data were widely distributed both geographically and ecologically (Appendix A). Although the number of samples and replicates varied across the reports of NO_3 , DON and K_s , I found no affect of these variables on CVs.

The relationship between clay content and the CVs of soil solution NO_3 , DON and K_s significantly fit both Gaussian and lognormal distributions (Fig. 2-1). However, no variable's distribution significantly differed from the normal distribution ($p > 0.2$); thus I display the data as fit by a 4-parameter Gaussian function. Percent clay of the soil accounted for greater than 1/3 of the variation in the CV of mean soil solution NO_3 and K_s . Peak variation of NO_3 , DON and K_s occurred at $\approx 12\%$ clay content. Clay accounted for more variation within NO_3 , DON and K_s CVs than either sand or silt (Table 1).

Table 2-1: Four Parameter Gaussian function fit to soil texture and coefficient of variation (CV) data. See Figure 2 caption for equation.

	Nitrate CV	DON CV	Saturated Hydraulic Conductivity CV
% Sand	$r^2 = 0.03$ ($p = .6365$)	$r^2 = 0.15$ ($p = 0.1706$)	$r^2 = 0.00$ ($p = 1.0$)
% Silt	$r^2 = 0.13$ ($p = 0.0522$)	$r^2 = 0.08$ ($p = .4367$)	$r^2 = 0.00$ ($p = 1.0$)
% Clay	$r^2 = 0.35$ ($p < 0.0001$)	$r^2 = 0.53$ ($p < 0.0001$)	$r^2 = 0.33$ ($p = 0.0008$)

Considering all data, the magnitude of NO_3 variation was $\approx 26\%$ greater than DON. The arithmetic mean CV of NO_3 and DON were 49.84 % and 39.57%, respectively. Limiting the comparison to NO_3 and DON CVs from the same samples within reports, NO_3 CVs were higher. However, the difference in magnitude between NO_3 and DON CVs was also a function of clay content. At low clay content, NO_3 CVs were typically greater than DON CVs, whereas at higher clay contents NO_3 and DON CVs were more similar (Fig 2-2). Although there was no effect of time since major disturbance across all sites (Appendix A), in paired plots both NO_3 and DON variation were lower in older forests compared to young or recently harvested forests (Fig 2-3). I found no effect of mineral N additions on NO_3 or DON CVs ($p > 0.2$; data not shown). However, the sample size ($n = 4$) for mineral N addition comparisons was extremely limited.

Although my hypotheses did not address mean concentrations of NO_3 and DON, and my data set was not assembled to identify patterns in mean concentrations of soil solution N across sites, I found no correlation between clay content and mean concentrations of soil solution NO_3 and DON. Similarly, there was no effect of vegetation physiognomy on mean concentrations.

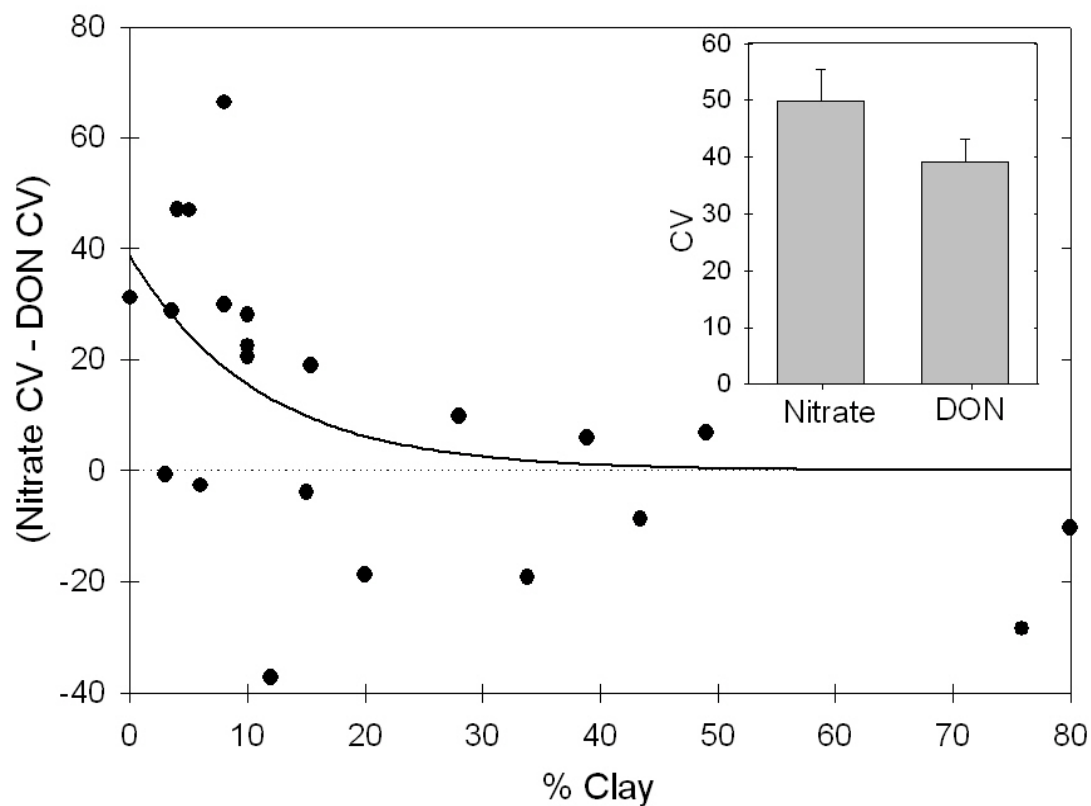


Figure 2-2: Inset: Mean (se) nitrate and DON CVs from the same lysimeters within reports (paired t-test $n = 23$; $p = 0.072$). However, the difference in magnitude of variation was a function of clay content. On the y-axis, zero corresponds to no difference between nitrate and DON CVs. The bold curve represents modeled data from the exponential function $y = ae^{-bx}$ ($r^2 = 0.30$; $p = 0.007$).

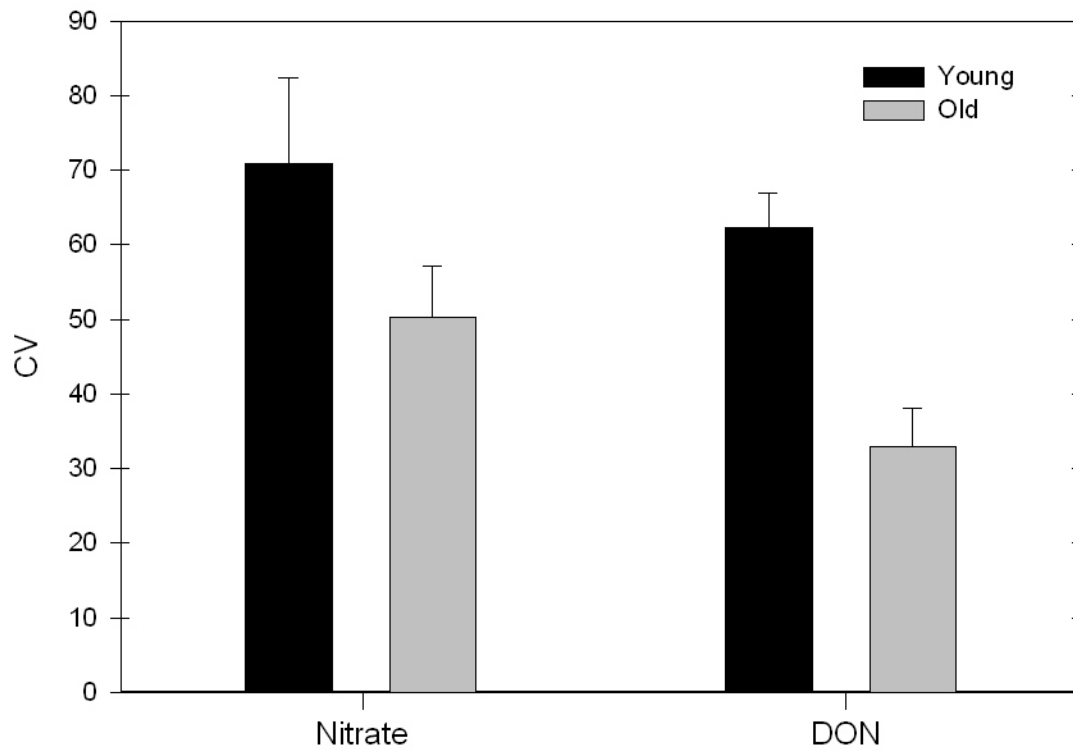


Figure 2-3: Paired comparison of nitrate and DON CVs (mean, se) from reports that compared soil solution N between young or recently harvested forests and old forests (paired t-test; nitrate $n = 8$, $p = 0.033$; DON $n = 4$; $p = 0.038$).

Discussion

For the dataset assembled here, I reject my hypotheses that the coefficient of variation in soil solution N is related to vegetation physiognomy or soil C/N ratios. In contrast, I found significant correlations between clay content and within-site variation of NO_3 , DON, and K_s . Thus I cannot reject my second hypothesis; clay content, through its impact on hydrology, appears to be an important determinant of within-site variation in soil solution N concentrations. Soil solution N CVs are well-fit by several functions exhibiting a single maximum, suggesting that concentrations are more spatially variable

at intermediate clay contents ($\approx 10\text{-}15\%$). My DON data represent a limited sample size and should be interpreted with caution.

Although I cannot rule out additional mechanisms beyond vegetation physiognomy, soil C/N ratio, total C and total N, the coincident peaks and similar functional relationships between clay and the CVs of K_s , NO_3 and DON suggest that the mechanistic basis for the clay- NO_3 CV and clay-DON CV relationships is hydrological. Hydrological controls on variation in soil solution N may ultimately be the result of physical and biological interactions. For example, soil structure may influence the variation in mass flux of water and its transport of soil solution N. In contrast, hydrology may impact the diversity and heterogeneity of the microbial communities that form NO_3 and DON. Similarly, differences in soil solution N CVs between young and old forests could be the result of physical and biological mechanisms. Harvesting methods physically alter soil structure, which can result in greater soil solution N variation; harvesting also reduces vegetative uptake, which can result in greater soil solution N variation (Guo and others 2004). Nonetheless in my dataset, clay content appears to be working as a proxy for both direct and indirect effects of soil hydrology on soil solution N variation.

That a single variable (clay content) can explain a large portion of the variability in CV in soil solution N is an important discovery. However, a substantial fraction of variation in CVs was not explained by clay. What mechanisms can account for this residual variance? Sand and silt contents explained only a small (although sometimes significant) proportion of the variation in soil solution N CVs and K_s CVs. This affirms, as suggested by Jarvis (2007), that clay plays a greater role affecting soil hydrology than

either silt or sand. Vegetation physiognomy can also be ruled out as a dominant control. However, many complex biogenic and physiogenic processes and properties govern heterogeneity in soil structure and hydrology. For example, the abundance of mineral particles $> 2\text{mm}$ are not included in soil texture measurements. Similarly, root density and size as well as soil macrofauna can affect soil structure and hydrology (Wilding & Lin 2006). Accordingly, I expect that a significant proportion of the unexplained variation in CVs are due to these site-specific variables that affect soil hydrology but are not explained by clay content. This is particularly likely for K_s and DON which are largely controlled by physical mechanisms (Vervoort and others. 1999; Kalbitz and others 2000).

Chemical mechanisms may also account for the observed relationship between clay content and variation in soil solution N as well as unexplained variation. Soil pH, clay mineralogy and organic matter composition can control the microbial transformation and solid-solution exchange of dissolved N species (De Nobili and others 2002). In particular, DON is a heterogeneous group of molecules that interact with soil solids in different ways. For example, these molecules contain hydrophobic and hydrophilic species (Huygens and others 2008). In particular, interactions between clay mineralogy and NO_3 and DON may account for unexplained variation in CVs.

In the case of NO_3 , a significant proportion of the unexplained variation is likely due to its active biological cycling. Many plants and soil microorganisms use NO_3 as a source of N. In contrast, DON is chemically heterogeneous; a significant fraction of DON is recalcitrant to microbial degradation, and only a small portion of DON is available for direct biological uptake (i.e., amino acids; Chapin and others 2002; Neff and

others 2003). Accordingly, NO_3 turnover is faster than DON turnover and it is probable that the greater biological availability of NO_3 is responsible for the larger (relative to DON) variation observed for NO_3 at low clay contents. This interpretation of the relationship between NO_3 and DON variation is similar to the traditional comparison of biologically reactive chemicals with a conservative tracer (typically Cl^-): molecules that are susceptible to rapid biological cycling have greater variation in mean concentration than tracers. Manderscheid and Matzner (1995) found a strong correlation between Cl^- in throughfall and soil solution, but no correlation between NO_3 in throughfall and soil solution. Several reviews also indicate that hydrology can control soluble nutrient transport through the soil (Kalbitz and others 2000, Neff and Asner 2001, Qualls 2000). My interpretation is also consistent with the occurrence of biological hotspots and hot moments of N cycling that increase the heterogeneity of reactive N distribution in the soil (McClain and others 2003). I cannot isolate the mechanism driving the negative exponential relationship between the difference in magnitude of NO_3 and DON CVs and clay content (Fig 2-2). Biological mechanisms, physical mechanisms, chemical mechanisms, or their interaction could have resulted in this observation.

Nitrate CVs in my data (range: 0.16-101.54%) were generally within the range reported from single-site studies that were conducted with an objective to characterize spatial variability in soil nitrate concentrations in lysimeter and salt extracted solutions (Robertson and others 1988, CV = 65%; Manderscheid and Matzner 1995, CV = 44.5-75.8%; Rothe and others 2002, CV = 20-129%). One such report from a relatively high-clay soil (19.8%) that did not meet my data inclusion rules found much higher NO_3 spatial variation (Asano and others 2006, CV > 200%). These data may reflect an

unusually well structured high-clay soil. Although most high-clay soils are poorly structured, exceptions do occur and they might not fit within the patterns observed in my data set. My lowest NO_3 CV values ($< 1\%$) were much lower than these single-site studies because none of them were conducted on extremely high or low clay content soils that I found to be characterized by lower spatial variation.

Soil texture, and clay content in particular, have proven to be a useful proxy for hydrology and robust predictor of global ecological and hydrological properties including soil carbon storage (Jobbagy and Jackson 2000), plant resource limitation (Paruelo and others 1999), dominant vegetation physiognomy (Prentice and others 1992) and water storage (Saxton and others 1986). My results extend soil texture's utility to describe ecosystem resource heterogeneity. Soil N availability can limit both plant and microbial growth in terrestrial ecosystems (Kaye and Hart 1997), so my data have important implications for variation in plant and microbial activity across sites. For example, spatial heterogeneity of soil resources has recently been proposed to explain why net N mineralization is a good predictor of plant-available N in some ecosystems, and a poor predictor of plant-available N in other ecosystems (Schimel and Bennett 2004). My data add to this new component of soil N cycling theory by showing that soil solution N will be more patchy, or spatially heterogeneous, in sites with intermediate clay content. In these ecosystems, I would expect a diverse array of soil microsites that enable both oxidative (e.g. nitrification) and reductive (e.g. denitrification) microbial processes to occur in different soil patches (Schimel and Bennett 2004). In contrast, soils with very high or low clay content will have less spatial variation in soil solution N, which would lead to decreased heterogeneity in microbial processes.

Resource heterogeneity can shape ecosystems' productivity, diversity, function and structure (e.g., Hutchings and others 2003; Maestre and Reynolds 2007). These processes operate across scales from physiology (Jackson and Caldwell 1996) to ecosystems (Anderson and others 2004). For example, spatial variation in soil solution N can control population, community and ecosystem structure as well as function (Sulkava and Huhta 1998; Ettema and Wardle 2002; Anderson and others 2004). My data should encourage further testing of resource heterogeneity hypotheses in natural systems without manipulation.

Literature Cited

- Anderson TM, McNaughton SJ. 2004. Scale-dependent relationships between the spatial distribution of a limiting resource and plant species diversity in an African grassland ecosystem. *Oecologia* 139:277-287.
- Asano Y, Compton JE, Church MR. 2006. Hydrologic flowpaths influence inorganic and organic nutrient leaching in a forest soil. *Biogeochemistry* 81:191-204.
- Bohlen PJ, Groffman PM, Driscoll CT, Fahey TJ, Siccama TG. 2001. Plant-soil-microbial interactions in a northern hardwood forest. *Ecology* 82:965-978.
- Brown JH, Mehlman DW, Stevens GC. 1995. Spatial variation in abundance. *Ecology* 76:2028-2043.
- Brenner RE, Boone RD, Jones JB, Lajtha K, Ruess RW. 2006. Successional and physical controls on the retention of nitrogen in an undisturbed boreal forest ecosystem. *Oecologia* 148:602-611.

- Carnol, M, Ineson P, Anderson JM, Beese F, Berg MP, Bolger T, Couteaux MM, Cudlin P, Dolan S, Raubuch M, Verhoff HA. 1997. The effects of ammonium sulphate deposition and root sinks on soil solution chemistry in coniferous forest soils. *Biogeochemistry* 38:255-280.
- Collins, SL, Smith MD. 2006. Scale-dependent interaction of fire and grazing on community heterogeneity in tallgrass prairie. *Ecology* 87:2058-2067.
- Chapin FS III, Matson PA, Mooney HA. 2002. *Principles of Terrestrial Ecosystem Ecology*. Springer. NY, USA.
- Currie WS, Aber JD, McDowell WH, Boone RD, Magill AH. 1996. Vertical transport of dissolved organic C and N under long-term N amendments in pine and hardwood forests. *Biogeochemistry* 35:471-505.
- De Nobili M, Francaviglia R, Sequi P. 2002. Retention and mobility of chemicals in soil. Violante A, Huang PM, Bollag J-M, Gianfreda L, editors. *Developments in Soil Science, Volume 28 A*. Amsterdam: Elsevier Science. p171-196.
- De Schrijver A, Geudens G, Augusto L, Staelens J, Martens J, Wuyts K, Gielis L, Verheyen K. 2007. The effect of forest type on throughfall deposition and seepage flux: a review. *Oecologia* 153:663-674.
- Dijkstra FA, West JB, Hobbie SE, Trost JB, Reich PB. 2007. Dissolved inorganic and organic N leaching from a grassland field experiment: interactive effects of plant species richness, atmospheric [CO₂] and N fertilization. *Ecology* 88:490-500.
- Dittman JA, Driscoll CT, Groffman PM, Fahey TJ. 2007. Dynamics of nitrogen and dissolved organic carbon at the Hubbard Brook Experimental Forest. *Ecology* 88:1153-1166.

- Emmett BA, Boxman D, Bredemeier M, Gundersen P, Kjonaas OJ, Moldan F, Schleppi P, Tietema A, Wright RF. 1998. Predicting the effects of atmospheric nitrogen deposition in conifer stands: evidence from the NITREX ecosystem-scale experiments. *Ecosystems* 1:352-360.
- Ettema CH, Wardle DA. 2002. Spatial soil ecology. *Trends in Ecology and Evolution* 17:177-183.
- Fisher SG, Sponseller RA, Heffernan JB. 2004. Horizons in biogeochemistry: flowpaths to progress. *Ecology* 85:2369-2379.
- Fraterrigo JM, Rusak JA. 2008. Disturbance-driven changes in the variability of ecosystem patterns and processes. *Ecology Letters* 11:756-770.
- Gou, D, Mou P, Jones RH, Mitchell RB. 2004. Spatio-temporal patterns of soil available nutrients following experimental disturbance in a pine forest. *Oecologia* 138:613-621.
- Hutchings MJ, John EA, Wijesinghe DK. 2003. Toward understanding the consequences of soil heterogeneity for plant populations and communities. *Ecology* 84:2322-2334.
- Huygens D, Boeckx P, Templer P, Paulino L, van Cleemput O, Oyarzun C, Muller C, Godoy R. 2008. Mechanisms for retention of bioavailable nitrogen in volcanic rainforest soils. *Nature Geoscience* 1:543-548.
- Jackson RB, Caldwell MM. 1996. Integrating resource heterogeneity and plant plasticity: Modeling nitrate and phosphorus uptake in a patchy soil environment. *Journal of Ecology* 84:891-903.

- Jarvis NJ. 2007 A review of non-equilibrium water flow and solute transport in soil macropores: principles, controlling factors and consequences for water quality. *European Journal of Soil Science*. 58:523-546.
- Jobbágy EG, Jackson RB. 2000. The vertical distribution of soil organic carbon and its relation to climate and vegetation. *Ecological Applications* 10:423-436.
- Johnson DW, Susfalk RB, Dahlgren DA, Caldwell TG, Miller WW. 2001. Nutrient fluxes in a snow-dominated, semi-arid forest: Spatial and temporal patterns. *Biogeochemistry* 55:219-245.
- Kalbitz K, Solinger S, Park JH, Michalzik B, Matzner E. 2000. Controls on the dynamics of dissolved organic matter in soils: A review. *Soil Science* 165:277-304.
- Kaye JP, Hart SC. 1997. Competition for nitrogen between plants and soil microorganisms. *Trends in Ecology and Evolution* 12:139–143.
- Knapp AK, Smith MD. 2001. Variation among biomes in temporal dynamics of aboveground primary production. *Science* 291:481-484.
- Kratz TK, Deegan LA, Harmon ME, Lauenroth WK. 2003. Ecological variability in space and time: Insights gained from the US LTER program. *Bioscience* 53: 57-67.
- Lajtha K, Seely B, Valiela I. 1995. Retention and leaching losses of atmospherically-derived nitrogen in the aggrading coastal watershed of Waquoit Bay, MA. *Biogeochemistry* 28:33-54.

- Lohse KA, Matson PA. 2005. Consequences of nitrogen additions for soil processes and soil solution losses from wet tropical forests. *Ecological Applications* 15:1629-1648.
- Lovett, GM, Weathers, KC, Arthur, MA. 2002. Control of nitrogen loss from forested watersheds by soil carbon:nitrogen ratio and tree species composition. *Ecosystems* 5:712-718.
- Maestre FT, Reynolds, JF. 2007. Amount or pattern? Grassland responses to the heterogeneity and availability of two key resources. *Ecology* 88:501-511.
- Magill AH, Aber JD, Hendricks JJ, Bowden RD, Melillo JM, Steudler P. 1997. Biogeochemical response of forest ecosystems to simulated chronic nitrogen deposition. *Ecological Applications* 7:402-415.
- Manderscheid B, Matzner E. 1995. Spatial and temporal variation of soil solution chemistry and ion fluxes through the soil in a mature Norway Spruce (*Picea abies* (L.) Karst.) stand. *Biogeochemistry* 30:99-114.
- McClain ME, Boyer EW, Dent CL, Gergel SE, Grimm NB, Groffman PM, Hart SC, Harvey JW, Johnston CA, Mayorga E, McDowell WH, Pinay G. 2003. Biogeochemical hot spots and hot moments at the interface of terrestrial and aquatic ecosystems. *Ecosystems* 6: 301-312.
- Michalzik B, Kalbitz K, Park JH, Solinger S, Matzner E. 2000. Fluxes and concentrations of dissolved organic carbon and nitrogen- a synthesis for temperate forests. *Biogeochemistry* 52:173-205.

- NRCS 2008. Soil Survey Staff, Natural Resources Conservation Service, United States Department of Agriculture. Web Soil Survey. <http://websoilsurvey.nrcs.usda.gov/>
Accessed: Nov. 2008.
- Neff JC, Asner GP. 2001. Dissolved organic carbon in terrestrial ecosystems: Synthesis and a model. *Ecosystems*. 4: 29-48.
- Neff JC, Chapin III FS, Vitousek PM. 2003. The role of dissolved organic nitrogen in nutrient retention and plant mineral nutrition; reconciling observations with ecological theory. *Frontiers in Ecology and Environmental Science*. 1: 205-211.
- Paruelo JM, Lauenroth WK, Burke IC, Sala OE. 1999. Grassland precipitation use efficiency varies across a resource gradient. *Ecosystems* 2:64-68.
- Prentice IC, Cramer W, Harrison SP, Leemans R, Monserud RA, Solomon AM. 1992. A global biome model based on plant physiology and dominance, soil properties and climate. *Journal of Biogeography* 19:117-134.
- Qualls RG. 2000. Comparison of the behavior of soluble organic and inorganic nutrients in forest soils. *Forest Ecology and Management* 138:29-50.
- Raich JW, Potter CS. 1995. Global patterns of carbon dioxide emissions from soils. *Global Biogeochemical Cycles* 9:23-36.
- Rothe A, Huber C, Kreutzer K, Weis W. 2002. Deposition and soil leaching in stands of Norway spruce and European Beech: Results from the Hogwald research in comparison with other European case studies. *Plant and Soil* 240:33-45.
- Robertson GP, Huston MA, Evans FC, Tiedje JM. 1988. Spatial variability in a successional plant community: Patterns of nitrogen mineralization, nitrification, and denitrification. *Ecology* 69:1517-1524.

- Saxton KE, Rawls WJ, Romberger JS, Papendick RI. 1986. Estimating generalized soil-water characteristics from texture. *Soil Science Society of America Journal* 50:1031-1036.
- Schimel DS, Braswell BH, Holland EA, McKeown R, Ojima DS, Painter TH, Parton WJ, Townsend AR. 1994. Climatic, edaphic and biotic controls over storage and turnover of carbon in soils. *Global Biogeochemical Cycles* 8:279-293.
- Schimel JP, Bennett J. 2004. Nitrogen mineralization: Challenges of a changing paradigm. *Ecology* 85:591-602.
- Sulkava P, Huhta V. 1998. Habitat patchiness affects decomposition and faunal diversity: a microcosm experiment on forest floor. *Oecologia* 116:390-396.
- Tilman, D. 1999. The ecological consequences of changes in biodiversity: A search for general principles. *Ecology* 80:1455-1474.
- Vervoort RW, Radcliffe DE, West, LT. 1999. Soil structure development and preferential solute flow. *Water Resources Research* 35:913-928.
- Vitousek, PM, Gosz JR, Grier CG, Melillo JM, Reiners WR. 1982. A comparative analysis of potential nitrification and nitrate mobility in forest ecosystems. *Ecological Monographs* 52:155-177.
- Whittaker RH, Likens GE, Bormann FH, Eaton JS, Siccama TG. 1979. The Hubbard Brook Ecosystem Study: Forest nutrient cycling and element behavior. *Ecology* 60:203-220.
- Wilding, LP, Lin HS. 2006. Advancing the frontiers of soil science towards a geoscience. *Geoderma* 131:257-274.
- Zar JH. 1999. *Biostatistical Analysis*. Prentice Hall, NJ, USA.

Chapter 3

Hydrological and biogeochemical controls on the timing and magnitude of nitrous oxide flux across an agricultural landscape

Abstract

Anticipated increases in precipitation intensity due to climate change may affect hydrological controls on soil N₂O fluxes, resulting in a feedback between climate change and soil greenhouse gas emissions. I evaluated soil hydrology controls on N₂O emissions during experimental water table fluctuations in large, intact soil columns that were amended with 100 kg ha⁻¹ KNO₃-N. Soil columns were collected from three landscape positions that vary in hydrological and biogeochemical properties (N = 12 columns). I flooded columns from bottom to surface to simulate water table fluctuations that are typical for this site, and expected to increase given future climate change scenarios. After the soil was saturated to the surface, I allowed the columns to drain freely while monitoring volumetric soil water content, matric potential, and N₂O emissions over 96 hours. Across all landscape positions and replicate soil columns, there was a positive linear relationship between total soil N and the log of cumulative N₂O emissions ($r^2 = 0.47$; $p = 0.013$). Within individual soil columns, N₂O flux was a Gaussian function of water filled pore space (WFPS) during drainage (mean $r^2 = 0.90$). However, instantaneous maximum N₂O flux rates did not occur at a consistent WFPS, ranging from 63 to 98% WFPS across landscape positions and replicate soil columns. In contrast, instantaneous maximum N₂O flux rates occurred within a narrow range (-1.88 to -4.48

kPa) of soil matric potential that approximated field capacity. The relatively consistent relationship between maximum N₂O flux rates and matric potential indicates that water filled pore *size* is an important factor affecting soil N₂O fluxes. These data demonstrate that matric potential is the strongest predictor of the timing of N₂O fluxes across soils that differ in texture, structure and bulk density.

Introduction

The atmospheric concentration of N₂O, a radiatively important gas, is increasing at an accelerating rate due to fertilizer use and fuel combustion (Galloway et al. 2008). Anticipated changes in precipitation patterns may affect soil N₂O emissions. Across the globe, the frequency of intense precipitation events is expected to increase (Kunkel et al. 2008). In low elevation coastal plain ecosystems, intense precipitation events can result in rapid water table fluctuations that temporarily saturate surface soils (Vadas et al. 2007). These events represent short periods of time with reducing conditions and high rates of microbial denitrification and N₂O production (Davidson 1991; McClain et al. 2002; Groffman et al. 2009). High water content in surface soils promotes reducing conditions and accompanying microbial denitrification respiratory processes.

Accordingly, water filled pore space (WFPS) is the primary independent variable used in empirical analyses of N₂O fluxes from agricultural soils (e.g., Linn & Doran 1984; Conen et al. 2000; Dobbie & Smith 2003; del Prado et al. 2006; Ruser et al. 2006). In agricultural systems, substrate availability is typically not limiting and WFPS frequently explains substantial variation in soil N₂O fluxes. In fact, univariate analysis of

WFPS can account for greater variation in N_2O flux than multivariate analyses that include additional variables such as temperature and nitrate concentrations (Dobbie & Smith 2003).

Nonetheless, WFPS can leave unexplained variation in N_2O emissions even when substrate availability does not appear to be limiting (Shepherd et al. 1991; Clayton et al. 1997). Davidson (1991) hypothesized that the relative magnitude of soil N_2O flux is a Gaussian function of WFPS; and this relationship has received some implicit empirical support (Schmidt et al. 2000; del Prado et al. 2006; Petersen et al. 2008). However, laboratory and field experiments across a broad array of soils have found that N_2O flux is an exponential or positive linear function of WFPS (e.g., Dobbie et al. 1999; Breuer et al. 2000; Smith et al. 2003; Ball et al. 2008; Beare et al. 2009; Chapuis-Lardy et al. 2009; Hayakawa et al. 2009). The inconsistent support for a Gaussian relationship between WFPS and N_2O flux may be due to insufficient sampling during brief periods of high WFPS in field experiments. On the other hand, a portion of the unexplained variation in the relationship between WFPS and N_2O flux may be due to the biophysical complexity of intact soils.

Matric potential (water potential of the bulk soil) is a thermodynamically-based property that provides a common basis for predicting the maximum activity of individual microbial processes across soil types (Sommers et al. 1981). Although WFPS has been used as an easy-to-measure substitute for matric potential (Franzluebbers 1999), it does not consistently relate to thermodynamically available water across soil types due to differences in soil texture and structure (Farquharson & Baldock 2008). For example, the presence of macropores may preclude relationships between WFPS and N_2O flux because

macropores drain rapidly while smaller intra-aggregate pore spaces maintain high water content and continue to provide favorable conditions for N₂O production (Conen et al. 2003; Syväsalö et al. 2004). In this case, macropore drainage reduces WFPS but the matric potential of the bulk soil remains largely unchanged. Additionally, differences in soil texture can modulate the relationship between WFPS and N₂O flux because soil texture affects the relationship between WFPS and matric potential (Schjønning et al. 2003).

Experimental manipulations based on climatic events that are expected to increase with global change will improve my modeling capabilities and understanding of potential climate change feedbacks. Many such events, including water table fluctuations into surface soils, represent times of large N₂O flux known as “hot moments” and are underrepresented in ecosystem models (Groffman et al. 2009). To advance my empirical understanding of the relationship between soil hydrology and N₂O flux, I simulated water table fluctuations in replicate, fertilized (100 kg ha⁻¹KNO₃-N) soil columns while measuring volumetric soil content, WFPS, matric potential and N₂O flux at high temporal resolution. I hypothesized 1) N₂O flux is a Gaussian function of WFPS and matric potential (Davidson 1991; Franzluebbers 1999) and 2) matric potential is a more accurate predictor of maximum N₂O flux than WFPS (Franzluebbers 1999).

Methods

Field Location & Sample Collection

This research was conducted on soils collected from a ditch-drained agroecosystem at the University of Maryland Eastern Shore Research Farm in Princess Anne, MD USA (38°12'22'' N, 75° 40'35'' W; 5 m elevation above mean absolute sea level). At this site, mean annual precipitation and temperature are 1110 mm and 13°C. Soil samples were collected from a field that is maintained in a maize (*Zea mays* L.)/wheat (*Triticum aestivum* L.)/soybean (*Glycine max* (L.) Merr.) rotation. Soils belong to the poorly drained Othello series (Fine-silty, mixed, active, mesic Typic Endoaquults) and are extensively ditched to drain excess water. The field is bound by two privately maintained ditches (<1.5m deep) that drain to a larger municipally maintained ditch (>2m deep) that ultimately drains to the Chesapeake Bay. For >20 years, these soils have received regular applications of poultry manure and commercial fertilizer N at rates often exceeding crop demand (e.g., 50-150 kg N ha⁻¹). Soil inorganic N is dominated by NO₃ (Schmidt et al. 2007). Detailed site information can be found in Kleinman et al (2007).

I divided the field into four blocks that each included private-ditch, near-ditch and middle-field landscape locations. Within each block, one intact replicate soil column (28 cm in diameter x 30 cm deep) was extracted from each landscape location (N = 12). Soil coring sites were randomly selected within each block. A 30 x 30 cm schedule 80 PVC cylinder was pushed into the soil by a 2-Mg drop weight that was slowly lowered onto the upright cylinder. To prevent soil compaction, the drop weight was not allowed to contact the soil column surface. Soil columns were also visually inspected for evidence

of compaction after sampling (i.e. comparison of soil column depth and extraction hole). Columns were extracted by removing the soil adjacent to the submerged cylinder and then tilting the cylinder to cleanly break contact between the soil column and the underlying subsoil. Subsequently, columns were inverted and washed sand was poured into the voids created by the separation of the soil at the column bottom (Fig 3-1). A layer of nylon drain fabric was placed over the sand as a retainer, followed by a 30-cm diameter PVC disk, perforated with roughly 60, 0.2-cm perforations. The disk was held in place by a PVC cap sealed to the cylinder with silicone. With cap in place, the columns were returned to their original upright position. To allow drainage and flooding, a hole was drilled into the cap and fitted with a 1-cm PVC nozzle. Soil columns were transported to the laboratory and maintained at saturation when not in use for experimentation or instrument installation. No plants were allowed to grow in soil columns after collection. At each soil column collection site, I also sampled a separate 5 x 30 cm companion soil core that was used to measure bulk density, particle size distribution as well as total organic C and total N on dried, ground samples with a dry combustion elemental analyzer. There is no inorganic C in these soils.

Sample Treatment

I used the drainage nozzle at the bottom of the soil column containers to manipulate the water table. Based on field data from groundwater monitoring wells (Vadas et al. 2007), I flooded soil columns from the bottom to surface by applying a positive head of water to the soil column drainage nozzle. To do this, I connected the soil

column drainage nozzle to an 18.9 L bucket containing a solution of 0.0001M CaSO_4 that was elevated above the soil surface. I used CaSO_4 at this concentration because it provided a close match to the groundwater monitoring well chemistry measured at the site.

To monitor volumetric soil water content (VWC) and matric potential in the soil columns, I inserted soil water content sensors and tensiometers through the side of each column at 10 cm and 20 cm depths. On opposite sides of the soil columns, I drilled two 2.54 cm diameter holes through the PVC soil column container. Using a steel replica of the soil water content sensors I created a pilot hole in which the soil water content sensor was inserted. Using a drill bit that was 0.16 cm diameter smaller than the tensiometers, I drilled a pilot hole into the soil in which tensiometers were inserted. Insertion sites were sealed with a rubber stopper and silicone caulk. Wires connecting the soil water content sensors to data loggers ran through the rubber stoppers. Similarly, the tensiometers extended through the rubber stoppers. An example soil column is depicted in Figure 1.

Soil water content sensors obtained VWC by measuring the soil dielectric constant (Decagon Devices, Inc. Pullman, WA). In homogenized, 2-mm sieved soils I calibrated the soil water content sensors to be accurate within 2.5% VWC. Tensiometers were fabricated from polyvinyl chloride (PVC) tubing, ceramic cups and rubber septa. The 1-bar straight-walled ceramic cup (Soil Moisture Equipment Corp, Santa Barbara, CA) was glued flush against one end of the PVC tube and firmly inserted into the soil. A rubber septum was fitted on the exposed end of the PVC tube and sealed with vacuum grease. A pressure transducer was fitted to each tensiometer through the rubber septum and also sealed with vacuum grease. Pressure transducers were calibrated on a

monometer in cm H₂O; these data were converted to kPa. Prior to experimentation, the tensiometers were filled with de-aired water. Tensiometers were fragile and prone to fracture at the connection between ceramic cup and PVC tube. Due to the fragility of tensiometers and initial data that indicated 20-cm tensiometer readings were not correlated with surface gas flux, I eliminated 20-cm tensiometers from the experiment reported herein. Soil water content sensors and tensiometers were connected to dataloggers that recorded at one minute intervals (Campbell Scientific Inc., Logan, UT).

To determine total porosity and saturation for each soil column, I maintained a 2 cm head of water above the soil surface until constant VWC was obtained (>1 week). Using these data, I calculated WFPS ($WFPS = \text{volumetric soil water content} / \text{maximum volumetric soil water content}$). Using matric potential data from tensiometers and the capillarity equation (Jury & Horton 2004), I determined water filled pore radius as:

$$r = \frac{2\sigma}{\rho gh}$$

where σ is the surface tension of water, ρ is the density of water, g is the acceleration of gravity and h is the hydraulic head (matric potential). For a given value of r , all pores of a radius $>r$ are assumed to be drained.

Nitrous oxide flux from the soil columns was measured from a static flux chamber that was fitted to the top of each soil column with a model 1412 Infrared Photoacoustic Spectroscopy (PAS) gas analyzer (Innova Air Tech Instruments, Ballerup, Denmark). One flux-chamber lid was fabricated from a round PVC collar with an inner diameter of 28 cm and inner height of 9 cm. The lid was vented, insulated with aluminum foil, and contained three sampling ports. During flux measurement, the lid

was sealed to the soil column and connected in a closed-loop system with the PAS gas analyzer. Total measurement time was 10 minutes with 2 minute sampling intervals and a sampling rate of 1.8 L minute⁻¹. Between measurements, soil columns were open to the atmosphere. Nitrous oxide fluxes were obtained by fitting a linear regression of gas concentration against time after chamber closure and calculated as:

$$F = \frac{\Delta C}{\Delta t} \times \frac{V}{A} \times \rho \times \alpha$$

where F is the gas production rate for N₂O (μg N₂O-N m⁻² hr⁻¹), $\Delta C/\Delta t$ denotes the increase/decrease of N₂O concentration (C) in the chamber over time (t), V is the chamber volume (m³), A is the chamber cross-sectional surface area (m²), and ρ is the density of gas at 20 °C and 0.101 MPa (1 mole per 24.04 m³), and α is the N₂O-N mass conversion coefficient 28/44. The density of gas was calculated based on 20°C and not the actual air temperature because the PAS instrument calculated the concentration of each gas at 20°C. However, all measurements were conducted in a laboratory with relatively constant air temperature (18-20 °C).

Experimental Protocol

Field monitoring at the research site indicates that intense precipitation events can result in rapid water table fluctuations that briefly saturate surface soils (hours-days; Vadas et al. 2007). I simulated water table recession by allowing columns to drain freely after columns were completely saturated. I focused my research on the evaluation of relationships between soil hydrology and N₂O flux during water table recession because

this allowed us to start from a thermodynamically similar hydrological condition (i.e. saturation).

I flooded soil columns until they reached 100% WFPS (as indicated by soil water content sensors) and the water table was approximately 5 mm above the soil surface. After columns were saturated, I injected $100 \text{ kg ha}^{-1} \text{ KNO}_3\text{-N}$ into the top 15 cm of each column using 19 gauge through hole side-port spinal needles (Popper & Sons. Inc., New Hyde Park, NY). To evenly distribute the KNO_3 solution, I applied 20 equally spaced 2 mL injections per column. Immediately after injecting the KNO_3 solution, I opened the soil column drainage nozzles and allowed columns to drain freely under the combined pressure potentials produced by gravity and the underlying sand substrate (see column description above). Although the $\text{KNO}_3\text{-N}$ solution injections did slightly increase matric potential and volumetric soil moisture, the increase was small and did not persist for >10 min in any column. After ponded water drained from the soil column surfaces ($\approx 10\text{-}15$ mins), I began to measure N_2O flux from the soil columns as frequently as possible over the course of 96 h. During this time VWC (10 and 20 cm) and matric potential data (10 cm) were automatically recorded at one minute intervals. Volumetric soil water content was converted to WFPS as described above. Soil temperature was periodically monitored with a food thermometer and ranged from $15\text{-}16^\circ\text{C}$. I conducted this procedure on four separate occasions, once per block of soil columns. This allowed us to maximize the number of N_2O flux measurements per soil column.

Data Analyses

I calculated 96 h cumulative N₂O fluxes by plotting instantaneous (10 min) N₂O flux against time, linearly interpolating between flux measurements, and integrating the area under the curve (Dobbie & Smith 2003). Cumulative N₂O fluxes were log(X+1) transformed because the range of data was large and within-landscape-location variance was correlated with the mean (Zar 1999). I analyzed data with regression and analysis of variance (ANOVA). I examined the effect of landscape position on cumulative N₂O fluxes, soil texture, bulk density, total C, total N, and C/N ratio with ANOVA and Fisher's Least Significant Difference post-hoc. I also compared the WFPS, matric potential and maximum water filled pore size at which maximum instantaneous N₂O fluxes occurred between landscape positions with ANOVA and Fisher's Least Significant Difference post-hoc. Finally, I regressed cumulative N₂O flux against soil properties with univariate and multivariate step-wise linear regression.

A 3-parameter Gaussian function was fit to WFPS and N₂O flux as well as matric potential and N₂O flux:

$$y = ae \left[-0.5 \left(\frac{x - x_o}{b} \right)^2 \right]$$

I did not perform a comparison of model fits or describe parameters due to the high temporal resolution of my data. I used the Gaussian function to confirm the conceptual relationship between soil water content and N₂O flux (Davidson 1991).

In some cases, tensiometers malfunctioned during the 96 h experiment. In these cases I modeled the missing matric potential data with existing matric potential and

volumetric soil water content data. Modeled data accounted for <20% of total matric potential data. The soil-specific water content release curve was modeled using the Brooks and Corey (1964) equation:

$$h = h_b \left(\frac{(\theta_s - \theta)}{(\theta_s - \theta_r)} \right)^{-1/\lambda}$$

where h is the soil matric potential, h_b is the bubbling pressure, θ is the volumetric water content, θ_s is the saturated water content, θ_r is the residual water content and λ is a fitting exponent. Saturated water content (θ_s) was taken from the measured drainage curve, and a Monte Carlo approach was used to determine the remaining 3 parameters (θ_r , h_b and λ). One hundred thousand (100,000) iterations were run to adequately explore the possible range of the three parameters. The parameter set with the lowest root mean square error between the measured and modeled matric potential was chosen for prediction of the missing matric potential data.

Results

Soil physical and chemical properties differed across the landscape (Table 3-1). Ditch soils had the greatest total N, total C, pore space and lowest bulk density. I measured N₂O flux approximately 102 times per soil column during the 96 h experiment. These measurements were focused on the initial drainage period when VWC, matric potential and N₂O flux change most rapidly. Cumulative N₂O-N flux over 96 h was greatest in Ditch and Near-Ditch soils (Table 3-2). Across soil columns and landscape positions, there was a positive linear relationship between total N and the log of

cumulative N₂O flux (Fig 3-2). However, no other measured variables explained significant variation in cumulative N₂O flux across soil columns in univariate or multivariate linear regressions.

Table 3-1: Mean and standard error of physical properties at each sample location (n = 4). Different letters within a row indicate a statistically significant difference (p < 0.05).

Soil Properties	Landscape Locations		
	Ditch	Near-Ditch	Middle-Field
Sand (g kg ⁻¹)	220.5 ^{ab} (31.0)	171.5 ^b (31.7)	249.0 ^a (10.7)
Silt (g kg ⁻¹)	553.0 (32.1)	588.5 (32.1)	567.8 (17.7)
Clay (g kg ⁻¹)	226.5 ^a (12.3)	239.9 ^a (13.9)	183.1 ^b (15.8)
Bulk Density (g cm ⁻³)	0.69 ^a (0.08)	1.20 ^b (0.04)	1.20 ^b (0.03)
Total Pore Space (cm ³ cm ⁻³)	0.4812 ^a (0.0000)	0.3257 ^b (0.0000)	0.3301 ^b (0.0020)
Total N (g kg ⁻¹)	1.73 ^a (0.09)	1.29 ^b (0.15)	1.36 ^b (0.07)
Total C (g kg ⁻¹)	15.64 ^a (1.18)	11.07 ^b (1.72)	13.86 ^{ab} (1.30)
C/N	9.007 ^b (0.227)	8.416 ^b (0.414)	10.132 ^a (0.431)

Within soil columns, N₂O flux was well fit by Gaussian functions of WFPS at 10 cm and matric potential at 10 cm (Fig 3-3, Tables 3-2). Within-soil-column N₂O flux could be fit by a Gaussian function of WFPS at 20 cm, but the fits were consistently poor (data not shown). From hereon, “WFPS” and “matric potential” refer to the 10 cm depth. Although WFPS accounted for a large proportion of within-column variation in N₂O flux (Table 2), maximum instantaneous N₂O flux across all columns occurred at a broad range of WFPS (range = 0.63-0.98 cm³ cm⁻³). Maximum instantaneous N₂O flux occurred at lower WFPS in Ditch soils compared to Near-Ditch and Middle-Field soils (Table 3-2).

Two soil properties were associated with this difference: Total porosity and bulk density were associated with variation in the WFPS at which maximum N₂O flux occurred (Fig. 3-4). However, these relationships were largely driven by mean differences among the soils of the different landscape positions, rather than true linear relationships. Matric potential typically accounted for less within-column variation in N₂O flux rate than WFPS (mean $r^2 = 0.83$). However, relative to WFPS, maximum N₂O flux rates occurred at a consistent matric potential (mean = -3.75 kPa; range across all 12 replicates was -1.88 to -4.66 kPa; Fig. 3-3). This matric potential corresponds to a mean pore radius of 39.58 μm , indicating that maximum N₂O flux occurs when pore sizes > 39.58 μm have drained. The matric potential at which maximum instantaneous N₂O flux occurred was not significantly different between landscape positions ($p > 0.5$). In contrast, the WFPS at which maximum instantaneous N₂O flux occurred was significantly different between landscape positions ($p < 0.01$).

Maximum instantaneous rates of N₂O flux occurred near field capacity in all columns and landscape positions (Fig. 3-5). Nitrous oxide flux data could not be pooled across soil columns and fit by Gaussian functions of WFPS and matric potential because cumulative N₂O flux varied widely between soil columns (39.56 – 632.17 mg N₂O-N m⁻² 96 h⁻¹). For visual clarity and brevity, Figures 3-3 & 3-5 depict data from block 2 only. All data are included in Appendix B.

Table 3-2. Mean and standard error of various indices of nitrous oxide flux during the 96-hour experiment. Different letters within a row indicate statistically significant differences ($p < 0.01$). Individual Gaussian model fits (r^2 s) for all individual replicates were significant ($p < 0.0001$). Water filled pore size at maximum N_2O flux indicates the largest pore size that remained filled with water at maximum N_2O flux (i.e. all larger pores were drained at maximum N_2O flux).

Nitrous Oxide Flux Indices	Landscape Locations		
	Ditch	Near-Ditch	Middle-Field
Cumulative N_2O Flux ($mg\ N_2O-N\ m^{-2}\ 96\ h^{-1}$)	352.83 ^a (130.94)	314.07 ^{ab} (208.92)	66.73 ^b (10.00)
Mean Fit of N_2O Flux to a Gaussian Function of WFPS (r^2)	0.91 (0.04)	0.89 (0.03)	0.91 (0.03)
Mean Fit of N_2O Flux to a Gaussian Function of Matric Potential (r^2)	0.94 (0.01)	0.81 (0.06)	0.74 (0.05)
WFPS at Maximum N_2O Flux ($cm^3\ cm^{-3}$)	0.660 ^b (0.021)	0.883 ^a (0.043)	0.842 ^a (0.022)
Matric Potential at Maximum N_2O Flux (kPa)	-3.425 (0.416)	-3.695 (0.649)	-4.130 (0.355)
Water Filled Pore Size at Maximum N_2O Flux (μm)	< 42.30 (6.46)	< 42.38 (10.32)	< 34.05 (3.52)

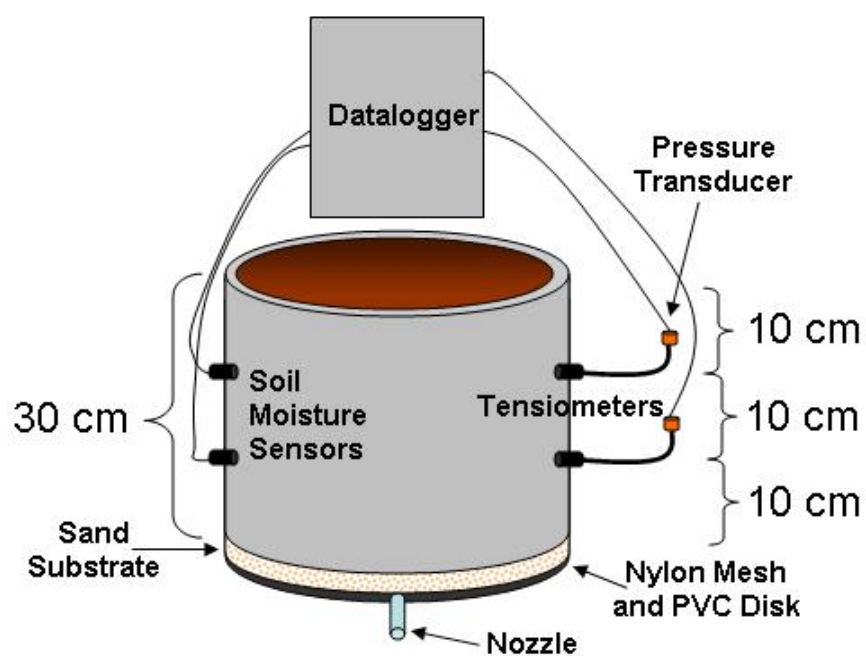


Figure 3-1: Schematic of a 30 x 30 cm soil column drawn to scale.

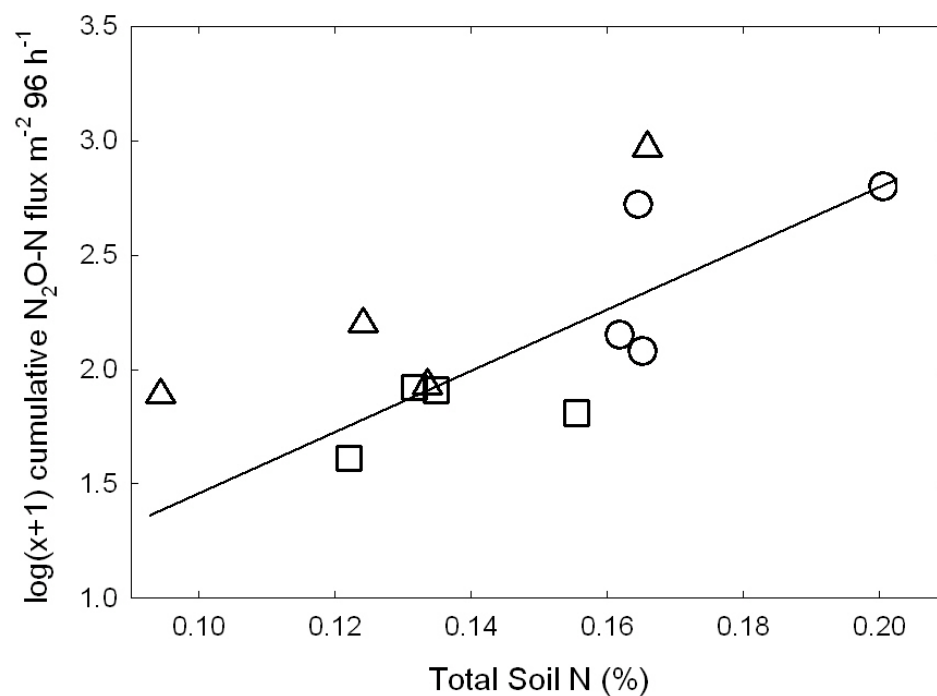


Figure 3-2: The log of cumulative N₂O flux as a linear function of total soil nitrogen ($r^2 = 0.47$; $p = 0.0132$). Circles indicate Ditch, triangles indicate Near-Ditch and Squares indicate Middle-Field.

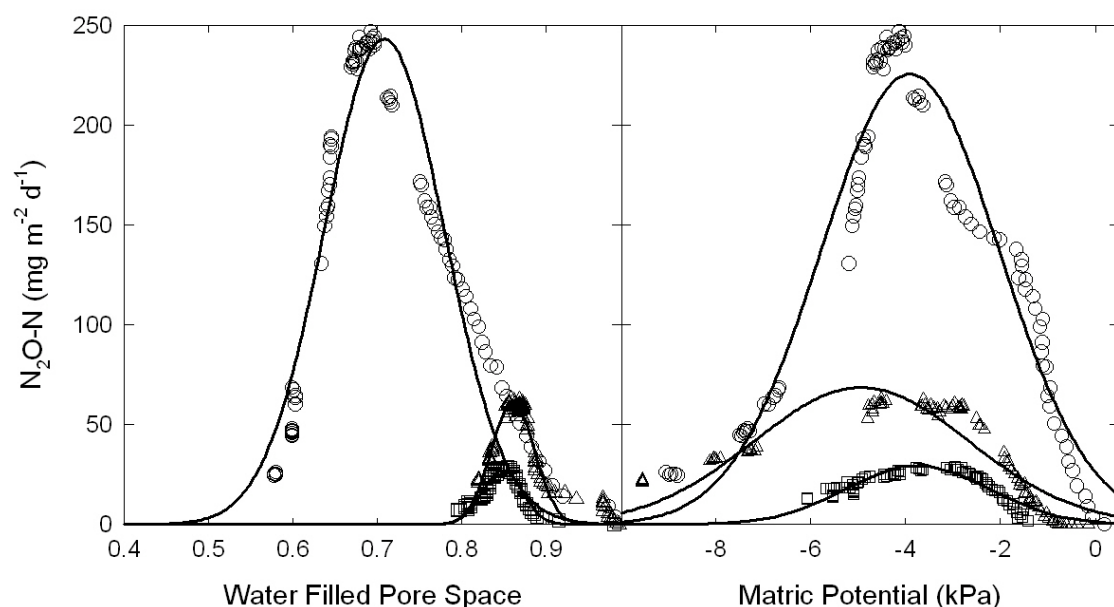


Figure 3-3: Nitrous oxide flux as a function of water filled pore space and matric potential for Block 2 soil columns. Circles indicate Ditch, triangles indicate Near-Ditch and squares indicate Middle-Field. The x-axis for matric potential has been truncated to increase clarity. Bold lines indicate a 3 parameter Gaussian model fit to the data. See Table 2 for r^2 and p values. Appendix 3-1 for complete data set for all replicates.

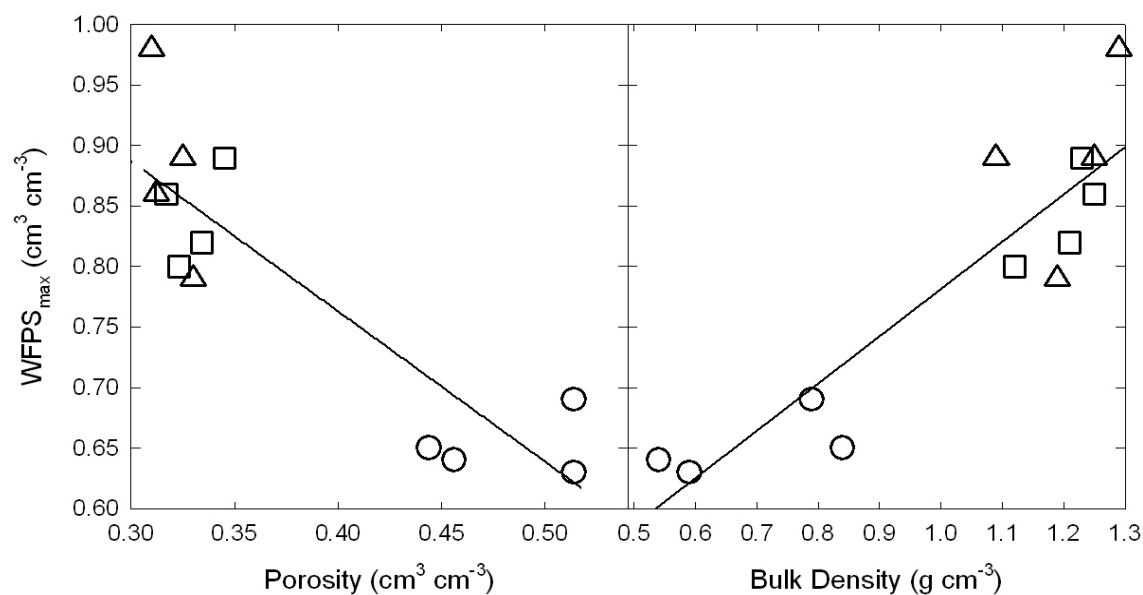


Figure 3-4: Water filled pore space at which maximum N_2O flux occurred (WFPS_{max}) as a function of total porosity ($r^2 = 0.76$; $p = 0.0002$) and bulk density ($r^2 = 0.83$; $p < 0.0001$). Circles indicate Ditch, triangles indicate Near-Ditch and squares indicate Middle-Field.

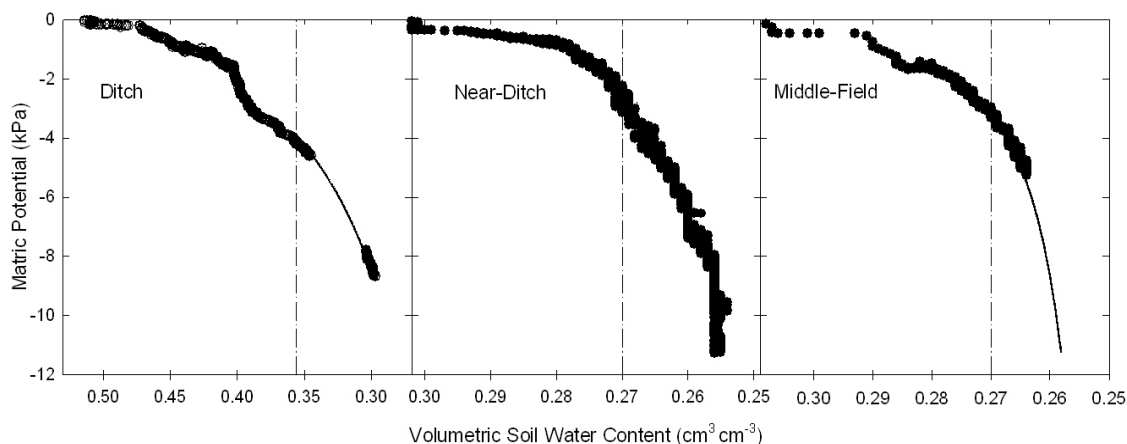


Figure 3-5: Water retention curves for Block 2 soil columns during the 96 hour experiment. Note different scale among x axes. Dashed reference lines indicate the volumetric soil water content at which maximum instantaneous N_2O flux rate was measured. Ditch and Middle data in smaller symbol size indicate modeled data. All other data were empirically measured.

Discussion

I cannot reject my first hypothesis; N_2O flux was a Gaussian function of WFPS and matric potential. Similarly, I cannot reject my second hypothesis; although WFPS accounted for more variation in N_2O flux than matric potential, maximum N_2O flux was more accurately predicted by matric potential (Fig 3-3; Table 3-2). Field soil matric potential can span 5 orders of magnitude (e.g., positive pressures to < -1500 kPa), but my results show that instantaneous maximum N_2O fluxes to occur within an extremely narrow range (-1.88 to -4.66 kPa).

Across all landscape positions and soil columns, total soil N accounted for significant variation in the cumulative amount of N_2O flux (Fig 3-2). Within landscape positions and soil columns, WFPS and matric potential were both good indicators of the

relative magnitude of N_2O flux (Fig 3-3; Table 3-2). Although WFPS is a strong predictor of the relative magnitude of N_2O flux within similar soils, matric potential appears to be a more consistent predictor of the relative magnitude of N_2O flux across different soils (Fig 3-3, Table 3-2). Such a relationship between matric potential and maximum microbial activity has been reported for soil microbial processes including aerobic respiration and nitrification (Franzluebbers 1999). Matric potential can accurately characterize microbial activity because it regulates substrate availability, microbial mobility and intracellular water potential (Stark & Firestone 1995).

Cumulative N_2O Emissions

Surprisingly, there was large variation in the cumulative N_2O flux across landscape positions and replicate soil columns during the 96 h experiment (Table 3-2). I expected much less variation due to the large application of oxidized N (NO_3). The primary control on N_2O flux is the availability of electron acceptors and electron donors. Although I did not measure labile organic C availability, I found no correlation between cumulative N_2O flux and total soil C. In contrast, I found a positive relationship between total soil N and cumulative N_2O flux (Fig 3-2). A positive relationship between microbial biomass and total N may have produced this result; microbial biomass C is positively correlated with aerobic respiration across a broad array of soils although I know of no similar data correlating microbial biomass C and anaerobic respiration or N (Booth et al. 2005). Alternatively, N_2O production may have been limited by oxidized N availability despite the large NO_3 application. Prior to this experiment (oxidized N

additions), N_2O fluxes were one order of magnitude lower during similar water table fluctuations (Castellano et al. unpublished data). It is unknown if larger NO_3 additions would have increased N_2O flux. However, maximum N_2O flux rates in Near-Ditch and Middle-Field soil columns did not approach maximum reported rates of N_2O flux (e.g., Clayton et al. 1997).

Previous work has demonstrated that wide C/N ratios can accurately predict N_2O flux across landscapes (Klemetsson et al. 2005). At wide C/N ratios oxidized N availability is likely to limit N_2O flux and C/N ratios can serve as a proxy for available N. However, at narrow C/N ratios (<15-20), other variables may better predict N_2O fluxes (Klemetsson et al. 2005). The soils studied herein had C/N ratios that ranged from 7.27 to 11.37. As expected, I found no relationship between C/N ratio and cumulative N_2O flux. However, the relationship between total soil N and cumulative N_2O flux (Fig. 3-2) suggests that total soil N may be a more effective predictor of N_2O flux in soils with narrow C/N ratios and a history of N fertilizer application. A similar relationship was found across diverse fertilized agricultural soils with C/N ratios from 13-15 (Syväsalö et al. 2004). In soils with low C/N ratios, a consistently large proportion of total N is likely to be available for mineralization and nitrification, resulting in positive net mineralization and nitrification (Emmett et al. 1998; Lovett et al. 2002).

Relative Magnitude of N_2O emissions

I found strong, consistent evidence that N_2O flux rate is a Gaussian function of WFPS and matric potential at 10 cm depth despite wide variation in flux rates across

landscape positions and soil columns (Fig 3-3; Table 3-2). Many reports suggest that the relationship between WFPS and N_2O flux is positively linear or exponential. In the field, this relationship may be the result of limited data at high WFPS (e.g., Breuer et al. 2000). In the lab, this relationship may be due to the estimation of WFPS from bulk density measurements that are not directly obtained from the soil samples that are analyzed for gas analysis (e.g., Chapuis-Lardy 2009). Sampling of intact soil columns can decrease bulk density and increase total porosity due to incomplete sealing between the soil and column container (Tokunaga 1988).

The conceptual relationship between WFPS and N_2O flux suggests that maximum N_2O occurs at ~60% WFPS (Davidson 1991). However, 60% WFPS is used as an approximation of field capacity rather than an absolute control on maximum N_2O flux rate (Davidson et al. 2000). Field capacity is thought to accurately predict maximum N_2O flux because it represents a soil condition where anaerobic microsites are abundant yet soil aeration is sufficient for N_2O diffusion to the atmosphere prior to further reduction to N_2 (Davidson et al. 2000; Smith et al. 2003). My data appear to be consistent with a control on maximum N_2O flux rate that is related to field capacity; I found that maximum N_2O rates occurred within close proximity to field capacity as indicated by soil water retention curves (Fig 3-5).

Variation in the WFPS at which maximum N_2O flux occurred was associated with differences in total porosity and bulk density (Fig 3-4). These relationships are likely due to the larger pore sizes and greater drainable pore space in Ditch soils compared to Near-Ditch and Middle-Field soils. A large portion of the total porosity in Ditch soils drained freely whereas only a small portion of total porosity drained freely in Near-Ditch

and Middle-Field soils (Fig 3-5; note differences in x-axes scale). Drainable porosity refers to the pore space that drains freely between saturation and field capacity (Weiler et al. 2005). Thus, if maximum N_2O flux is indeed related to field capacity, drainable porosity will be negatively correlated with the WFPS at which maximum N_2O flux occurs. Consistent with this idea, soil compaction reduces drainable pore space and can increase the WFPS at which maximum N_2O flux occurs (Ruser et al. 2006; Ball et al. 2008).

In contrast to WFPS, matric potential offers a consistent thermodynamically-based determinant of maximum N_2O flux across different soil types. The maximum rates of a variety of microbial processes are accurately characterized across soil types by a relatively consistent matric potential (Sommers 1981; Schjønning et al. 2003). I found that maximum N_2O flux occurred within a narrow range of matric potential across soil types (Table 2). As far as I know, the relationship between N_2O flux and matric potential has not been previously examined across soil types and water contents. However, in striking similarity to my results, Smith et al. (1998) reported that N_2O flux in a peaty gleysol soil column was a similar function of matric potential, peaking at -5 kPa. Consistent with these data N mineralization is also a Gaussian function of matric potential, but reaches a maximum at a lower matric potential (i.e., drier soil conditions; -52 kPa, Franzluebbers 1999; -14 to -43 kPa, Schjønning et al. 2003). As suggested by previous work, my data confirms that WFPS can serve as an acceptable proxy for matric potential when comparing soils that have similar texture, structure and bulk density (e.g., Near-Ditch and Middle-Field soils; Franzluebbers 1999). However, the use of a discrete

WFPS to compare N_2O flux across soils that differ in physical properties is likely to produce spurious conclusions regarding the rate and amount of N_2O flux.

My data have implications for future analyses of N gas fluxes within the framework of the “hole-in-the-pipe” (HIP) conceptual model (Firestone & Davidson 1989; Davidson et al. 2000). The HIP model describes the ratio of $\text{NO}:\text{N}_2\text{O}:\text{N}_2$ flux and the relative magnitude of N gas flux from the soil as a function of WFPS. Although WFPS is used as a proxy for water holding capacity and potential limitations are discussed, WFPS was selected because it is relatively easy to measure (Davidson 1991). However, as reported for other microbial processes, matric potential appears to provide a more consistent indicator of the relative magnitude of N_2O flux across different soil types. I recommend that future cross-soil predictions of N_2O flux focus on matric potential as the water scalar that controls the relative magnitude of N_2O flux. It remains unknown if matric potential is a more accurate indicator of the ratio of $\text{NO}:\text{N}_2\text{O}:\text{N}_2$ flux.

My data suggest that future increases in precipitation intensity and frequency of surface soil saturation could increase N_2O fluxes. During drainage, N_2O fluxes were increased above typical fluxes by 1-2 orders magnitude for > 3 days (data not shown). Although hydrological data (e.g. matric potential; Fig. 3) can be used to determine when hot moments of N_2O flux occur, biogeochemical data (e.g. total soil N; Fig. 2) will be required to determine where hot spots of N_2O flux occur. These data must be used in concert to predict and manage terrestrial N_2O emissions.

Literature Cited

- Ball BC, Crichton I, Horgan GW (2008) Dynamics of upward and downward N₂O and CO₂ fluxes in ploughed or no-tilled soils in relation to water-filled pore space, compaction and crop presence. *Soil & Tillage Research*, **101**, 20-30.
- Beare MH, Gregorich EG, St. Georges P (2009) Compaction effects on CO₂ and N₂O production during drying and rewetting of soil. *Soil Biology & Biochemistry*, **41**, 611-621.
- Booth MS, Stark JM, Rastetter E (2005) Controls on nitrogen cycling in terrestrial ecosystems: A synthetic analysis of literature data. *Ecological Monographs*, **75**, 139-157.
- Breuer L, Papen H, Butterbach-Bahl K (2000) N₂O emission from tropical forest soils of Australia. *Journal of Geophysical Research-Atmospheres*, **105**, 26353-26367.
- Brooks RH, Corey AJ (1964) Hydraulic properties of porous media. Hydrology Paper 3, Colorado State University, Fort Collins, CO.
- Clayton H, McTaggart IP, Parker J, Swan L, Smith KA (1997) Nitrous oxide emissions from fertilised grassland: A 2-year study of the effects of N fertiliser form and environmental conditions. *Biology and Fertility of Soils*, **25**, 252-260.
- Conen F, Dobbie KE, Smith KA (2000) Predicting N₂O emissions from agricultural land through related soil parameters. *Global Change Biology*, **6**, 417-426.
- Chapuis-Lardy L, Metay A, Martinet M et al. (2009) Nitrous oxide fluxes from Malagasy agricultural soils. *Geoderma*, **148**, 421-427.

Davidson EA (1991) Fluxes of nitrous oxide and nitric oxide from terrestrial ecosystems.

In: *Microbial Production and Consumption of Greenhouse Gases: Methane, Nitrogen Oxides and Halomethanes* (eds Rogers JE, Whitman WB), pp 219-236. American Society for Microbiology, Washington DC.

Davidson EA, Keller M, Erickson HE, Verchot LV, Veldkamp E (2000) Testing a conceptual model of soil emissions of nitrous and nitric oxides. *Bioscience*, **50**, 667-680.

del Prado A, Merino P, Estavillo JM, Pinto M, Gonzalez-Murua C (2006) N₂O and NO emissions from different N sources under a range of soil water contents. *Nutrient Cycling in Agroecosystems*, **74**, 229-243.

Dobbie KE, McTaggart IP, Smith KA (1999) Nitrous oxide emissions from intensive agricultural systems: variations between crops and seasons, key driving variables, and mean emission factors. *Journal of Geophysical Research* **104**, 26891-26899.

Dobbie KE, Smith KA (2003) Nitrous oxide emission factors for agricultural soils in Great Britain: the impact of soil water-filled pore space and other controlling variables. *Global Change Biology*, **9**, 204-218.

Emmett BA, Boxman D, Bredemeier M, Gundersen P, Kjonaas OJ, Moldan F, Schleppi P, Tietema A, Wright RF (1998) Predicting the effects of atmospheric nitrogen deposition in conifer stands: evidence from the NITREX ecosystem-scale experiments. *Ecosystems*, **1**, 352-360.

Farquharson R, Baldock J (2008) Concepts in modelling N₂O emission from land use. *Plant and Soil*, **309**, 147-167.

- Firestone MK, Davidson EA (1989) Microbiological basis of NO and N₂O production and consumption in soil. In: *Exchange of trace gases between terrestrial ecosystems and the atmosphere*. (eds Andreae MO, Schimel DS), pp 7-21, John Wiley & Sons, NY.
- Franzluebbers AJ (1999) Microbial activity in response to water-filled pore space of variably eroded southern Piedmont soils. *Applied Soil Ecology* **11**, 91-101.
- Galloway JN, Townsend AR, Erismann JW et al. (2008) Transformation of the nitrogen cycle: recent trends, questions, and potential solutions. *Science*, **320**, 889-892.
- Groffman PM, Butterbach-Bahl K, Fulweiler RW et al. (2009) Challenges to incorporating spatially and temporally explicit phenomena (hotspots and hot moments) in denitrification models. *Biogeochemistry*, **93**, 49-77.
- Hayakawa A, Akiyama H, Sudo S, Yagi K (2009) N₂O and NO emissions from an Andisol field as influenced by pelleted poultry manure. *Soil Biology & Biochemistry*, **41**, 521-529.
- Kleinman PJA, Allen AL, Needelman BA et al. (2007) Dynamics of phosphorus transfers from heavily manured Coastal Plain soils to drainage ditches. *Journal of Soil and Water Conservation*, **62**, 171-178.
- Klemetsson L, von Arnold K, Weslien P, Gundersen P (2005) Soil C/N ratio as a scalar parameter to predict nitrous oxide emissions. *Global Change Biology*, **11**, 1142-1147.
- Kunkel KE et al. (2008) Observed changes in weather and climate extremes. In: *Weather and Climate Extremes in a Changing Climate. Regions of Focus: North America, Hawaii, Caribbean, and US Pacific Islands* (eds Karl TR et al.) A Report by the

US Climate Change Science Program and Subcommittee on Global Change Research, Washington, DC.

- Linn DM, Doran JW (1984) Effect of water-filled pore-space on carbon-dioxide production in tilled and nontilled soils. *Soil Science Society of America Journal*, **48**, 1267-1272.
- Lovett GM, Weathers KC, Arthur MA (2002) Control of nitrogen loss from forested watersheds by soil carbon:nitrogen ratio and tree species composition. *Ecosystems*, **5**, 712-718.
- McClain ME, Boyer EW, Dent CL et al. (2003) Biogeochemical hot spots and hot moments at the interface of terrestrial and aquatic ecosystems. *Ecosystems* **6**, 301-312.
- Ruser R, Flessa H, Russow R, Schmidt G, Buegger F, Munch JC (2006) Emission of N₂O, N₂ and CO₂ from soil fertilized with nitrate: Effect of compaction, soil moisture and rewetting. *Soil Biology & Biochemistry*, **38**, 263-274.
- Schmidt U, Thoni H, Kaupenjohann M (2000) Using a boundary line approach to analyze N₂O flux data from agricultural soils. *Nutrient Cycling in Agroecosystems*, **57**, 119-129.
- Schmidt JP, Dell CJ, Vadas PA, Allen AL (2007) Nitrogen export from coastal plain field ditches. *Journal of Soil and Water Conservation*, **62**, 235-243.
- Shepherd MF, Barzetti S, Hastie DR (1991) The production of atmospheric NO_x and N₂O from a fertilized agricultural soil. *Atmospheric Environment Part A-General Topics*, **25**, 1961-1969.

- Smith KA, Ball T, Conen F, Dobbie KE, Massheder J, Rey A (2003) Exchange of greenhouse gases between soil and atmosphere: interactions of soil physical factors and biological processes. *European Journal of Soil Science*, **54**, 779-791.
- Petersen SO, Schjønning P, Thomsen IK, Christensen BT (2008) Nitrous oxide evolution from structurally intact soil as influenced by tillage and soil water content. *Soil Biology & Biochemistry*, **40**, 967-977.
- Sommers LE, Gilmour CM, Wildung RE, Beck SM (1981) The effect of water potential on decomposition processes in soils. In: *Water Potential Relations in Soil Microbiology* (eds Parr JF, Gardner WR, Elliot LF) Soil Science Society of America Special Publication Number 9, WI.
- Syväsalo E, Regina K, Pihaltie M, Esala M (2004) Emissions of nitrous oxide from boreal agricultural clay and loamy sand soils. *Nutrient Cycling in Agroecosystems*, **69**, 155-165.
- Schjønning P, Thomsen IK, Moldrup P, Christensen BT (2003) Linking soil microbial activity to water- and air-phase contents and diffusivities. *Soil Science Society of America*, **67**, 156-165.
- Stark JM, Firestone MK (1995) Mechanisms for soil moisture effects on activity of nitrifying bacteria. *Applied and Environmental Microbiology*, **61**, 218-221.
- Tokunaga, TK (1988) Laboratory permeability errors from annular wall flow. *Soil Science Society of America* **52**, 24-27.
- Vadas, PA, Srinivasan MS, Kleinman PJA, Schmidt JP, Allen AL (2007) Hydrology and groundwater nutrient concentrations in a ditch-drained agroecosystem. *Journal of Soil and Water Conservation*, **62**, 178-188.

Weiler M, McDonnell JJ, Tromp van Meerveld I, Uchida T (2005) Subsurface Stormflow Runoff Generation Processes. In: *Encyclopedia of Hydrological Sciences* (eds Anderson MG), pp1719-1732. Wiley & Sons, NY.

Chapter 4

Nitrogen transport and transformation along gradients of topography and soil texture

Abstract

Soil organic carbon (SOC) and carbon to nitrogen (C/N) ratios often describe a significant amount of variation in ecosystem mineral nitrogen (N) losses and retention. Nonetheless, these variables leave unexplained variation that has been attributed to soil texture. Within a forested catchment that contains similar vegetation, but gradients in topography, soil texture, SOC and C/N ratio, I evaluated controls on N transport and transformation. At this site, soil solution mineral N concentrations were positively correlated with sand content. However, soil solution flux was negatively correlated with sand content. Accordingly, there was no relationship between sand content and mass flux of soil solution N. Differences in mineral N immobilization into insoluble organic N compounds during 3 day field incubations were not correlated with soil texture and thus could not explain the positive relationship between soil solution mineral N concentrations and sand content. In contrast, but consistent with previous work, immobilization of mineral N into insoluble organic N compounds was positively correlated with SOC concentrations. In alternative to N immobilization, N mineralization could help to explain the positive correlation between soil solution mineral N concentrations and sand content; *in situ* 3 day net ammonification was positively correlated with sand content.

Introduction

Human-derived biologically available nitrogen (mineral N) inputs to the biosphere are increasing as a result of impure hydrocarbon combustion and ammonia synthesis (Smil 2001; Galloway et al. 2003). While these inputs have beneficial effects including increased crop production, they also have deleterious effects such as the eutrophication of surface waters. The majority of mineral N inputs to surface waters are from nonpoint terrestrial sources, traveling through soil prior to reaching open water (Carpenter et al. 1998).

Over the past decade ecologists have worked to predict the fate of anthropogenically added N in terrestrial ecosystems. This work has identified a widespread pattern—most ecosystems retain a majority of mineral N inputs, transforming mineral N into relatively non-reactive stable organic N (Aber et al. 1998). Accordingly, only a small fraction of mineral N inputs are leached to groundwaters and surface waters. Mechanistic explanations for these observations focus on biotic and abiotic processes. Biotic mechanisms focus on competition between plants and microbes for mineral N, resulting in tight cycling with little mineral N loss (Kaye & Hart 1997), especially when plant litter and soils have wide C/N ratios (Emmett et al. 1998; Lovett et al. 2002). Abiotic mechanisms focus on the reaction of nitrite, ammonium and labile proteins with aromatic ring structures of phenolic and lignitic soil organic matter, resulting in the formation of decomposition-resistant compounds (Hättenschwiler & Vitousek 2000; Davidson et al. 2003; Fitzhugh et al. 2003), and the association of organic N with soil minerals (Hassink 1997).

Both biotic and abiotic N retention processes are C-dependent: The capacity of biotic mechanisms to sequester N depends on a surplus of microbe-available C and a deficit of microbe-available N. The capacity of abiotic mechanisms to sequester N depends on the availability of C substrate (Stevenson 1994). Consistent with these mechanisms, total N retention (abiotic + biotic immobilization) is well correlated with soil organic carbon (SOC) across a diverse array of sites (e.g., Nadelhoffer et al. 1999; Kaye et al. 2002; Barrett et al. 2002). Soil organic carbon content is typically correlated with soil texture (e.g., Schimel et al. 1994). The high surface area of clay particles promotes the adsorption and physical protection of humic materials, resulting in a positive relationship between clay and SOC (Hassink 1997). Accordingly, there is a strong possibility that texture affects the capacity of soil to retain mineral N inputs. In fact, soil texture has been suggested to obscure or eliminate the expected relationship between C/N ratios and nitrate (NO_3) leaching (Lovett et al. 2004; Templer et al. 2005). Nonetheless, the potential for soil texture to explain variation in temperate forest N retention remains largely unexplored (Pastor et al. 1984; Lovett et al. 2004).

As ecologists have been working to understand biogeochemical controls on ecosystem N retention at the pedon scale, ecologists and hydrologists have been working to understand hydrological controls on mineral N transport through catchments and watersheds. This work has produced several independent reports of low mineral N export during baseflow, contrasted by high mineral N export during storm events, a process termed “flushing” (*sensu* Hornberger et al. 1994). Nitrate flushing has been largely attributed to two hydro-biogeochemical mechanisms that focus on the rapid transport of NO_3 from nutrient-rich surface soils to less biologically active subsoils and open water

(Dittman et al. 2007; van Verseveld et al. 2008). These mechanisms include: 1) The rise and fall of a transient water table that leaches NO_3 from nutrient-rich surface soils to open waters (Boyer et al. 1997), and 2) The occurrence of rapid flowpaths that transport NO_3 vertically from nutrient-rich surface soils to less biologically active subsoils, then laterally downslope (Gaskin et al. 1989; Creed et al. 1996). Rapid flow can occur in soils with coarse soil texture or an abundance of macropores and reduces contact time between water and soil. This mechanism assumes that reduced contact time allows NO_3 to bypass plant and microbial sinks, travelling unabated from nutrient rich surface soils to less biologically active subsoils and open waters (Dittman et al. 2007; McGuire & McDonnell 2007). However, NO_3 flushing is not universally observed, primarily due to plant and microbial N limitation (Hill et al. 1999).

Both ecologically-based N retention and hydrologically-based N flushing mechanisms focus on processes that originate in nutrient-rich surface soils. Nitrogen cycling in these soils can impact surface water N status (Bohlen et al. 2001; Dittman et al. 2007). Ecosystem N retention theory can help to determine *when, where and why* NO_3 flushing occurs. Specifically, it is plausible that interactions between the observed range of N retention efficiency (30-80%) and the timescale of retention (minutes to decades) could be responsible for the inconsistent observation of the NO_3 flushing response. Systems with high N retention efficiency over short timescales would not be expected to exhibit NO_3 flushing.

On the other hand, texture-based NO_3 flushing mechanisms may contribute to unexplained variation in N retention (Templer et al. 2005) and the manifestation of N saturation (Pregitzer et al. 2004). Using a small forested catchment containing large

gradients in soil texture, SOC, and C/N ratios I address the overarching question: How do soil texture, SOC, C/N ratios and nitrate flushing interact to influence ecosystem N retention and mineral N losses?

Methods

Field Site

I sampled an eastern deciduous forested catchment on the western shore of the Chesapeake Bay in Harford County, MD USA (39°27'05"N, 76°16'23"W). The site is approximately 6.5 ha and included within the boundaries of the National Oceanic and Atmospheric Association Chesapeake Bay Maryland National Estuarine Research Reserve. Mean annual maximum and minimum temperatures are 18.2°C and 5.8 °C. Mean annual precipitation is 1164 mm. Within the catchment, I limited my work to the western hillslope (Fig. 4-1) which contains large gradients in soil texture that run parallel (~300 m) and perpendicular (~ 30 m) to the drainage. The soils in this area are mapped (1:15840) to include three individual soil series: Joppa, Elsinboro and Evesboro. The Joppa series includes loamy-skeletal, siliceous, semiactive, mesic Typic Hapludults. The Elsinboro series includes fine-loamy, mixed, semiactive, mesic Typic Hapludults; occurrence of this soil is limited within the study location. The Evesboro soil includes mesic, coated Lamellic Quartzipsamments.

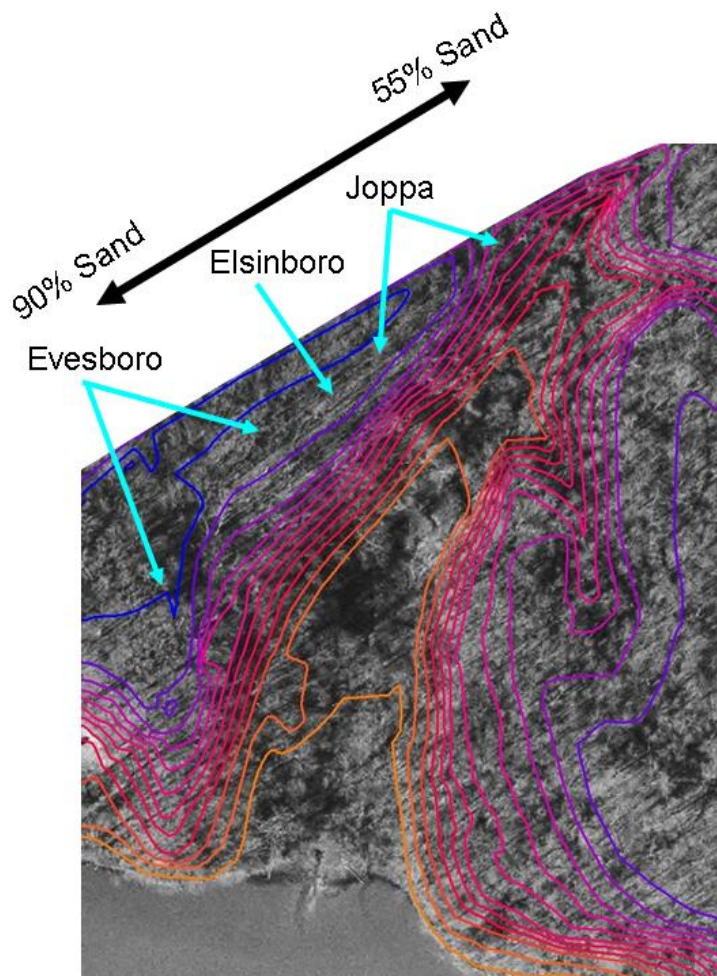


Figure 4-1: Topographic map including 1 m contour intervals. The general area of occurrence for each soil series is displayed (Joppa, Elsinboro and Evesboro). The general gradient in soil texture is indicated as well.

Transitions between the soils of these series are not abrupt. Rather, they comprise a gradient in soil texture that runs parallel to the catchment drainage, spanning approximately 55% sand to >90% sand. Clay content throughout the site is low (<15%). A second gradient in soil texture that runs perpendicular to the drainage is associated with the hillslope (Jurinko 2009). Steep slopes are associated with a downslope increase in sand content whereas shallow slopes are associated with a downslope increase in silt content. Vegetation is relatively homogenous and dominated by *Liriodendron tulipifera*

(Tulip Poplar), *Liquidamber styraciflua* (Sweetgum), *Fagus grandifolia* (Beech), and *Quercus* spp (Oak).

Underlying the catchment soils is a lithified paleosol from the Cretaceous period (T. White, pers. comm.). The lithified paleosol occurs approximately 1 m below the soil surface and runs parallel with the soil surface down the hillslope of the west side of the catchment (Doolittle 2008). In areas, the paleosol intersects the soil surface. After vertical water movement down the soil profile, the lithified paleosol forces lateral water flow parallel to the hillslope (Doolittle 2008; Fig. 4-2). Lateral flow is evidenced by the occurrence of a perennial seep at the toeslope and visual identification of lateral flow (Fig 4-2).

The USDA Natural Resources Conservation Service used ground penetrating radar imaging to map the occurrence of the lithified paleosol on the western side of the catchment. Ground penetrating radar images were collected along seven transects parallel with the hillslope and perpendicular to the catchment drainage. The seven transects were coincident with 7 of 8 sampling transects discussed below. Because the lithified paleosol is much denser than the surface soils, ground penetrating radar could be used to locate the area of density change that corresponded to the soil-paleosol boundary. In select areas, the subsurface layer that was identified as the paleosol by ground penetrating radar was visually confirmed. Figure 4-2 displays a toeslope location where the paleosol intersects the soil surface as well as my resultant conceptual understanding of soil water flow through the hillslope. Ground penetrating radar images are located in the appendix. USDA NRCS soil scientist James Doolittle concluded that the layer, as pictured in Figure 4-2 and Appendix 4-1, influences downslope water flow.

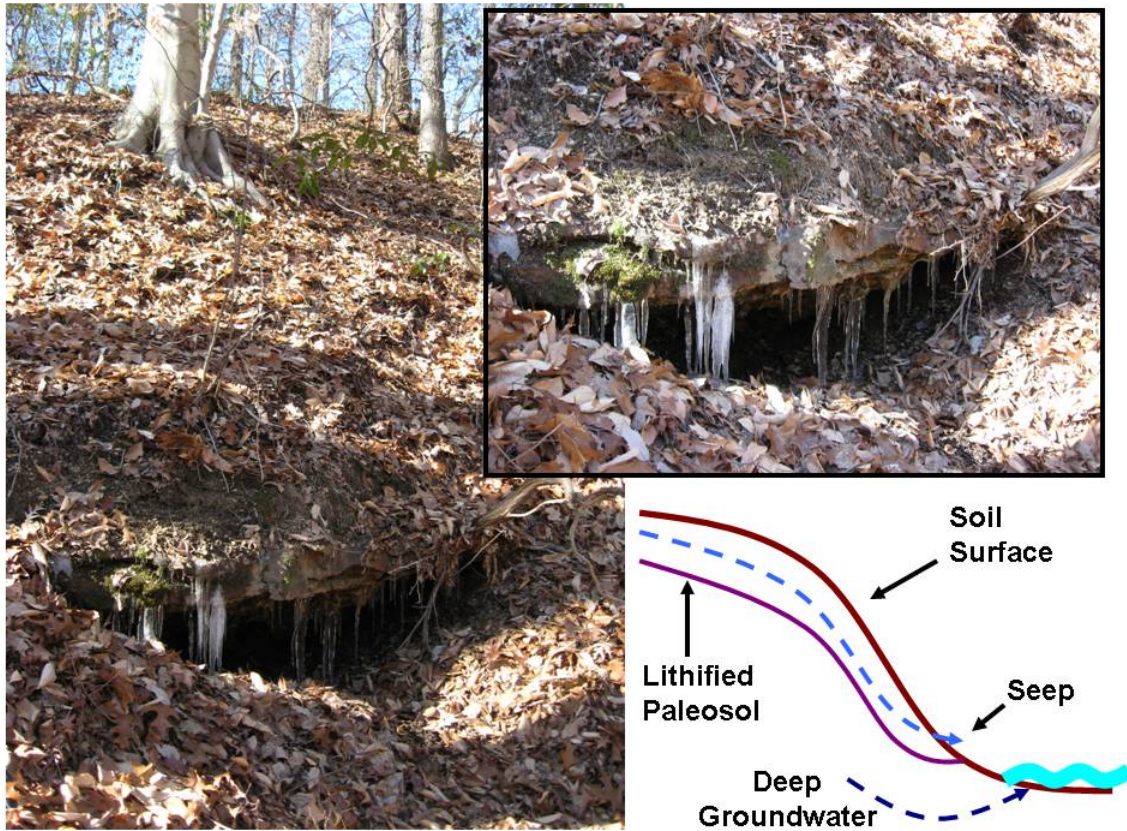


Figure 4-2: Location where the lithified paleosol intersects the soil surface. Inset: Icicle formation as evidence of lateral flow parallel with the hillslope. Bottom right: My conceptual understanding of water flow through the hillslope soils.

Experimental Design

To address my objectives, I used the gradients in soil texture and topography to conduct a regression-based analysis of nitrogen transport and transformation in response to soil texture, soil organic carbon and C/N ratios. In 2008 I conducted pilot monitoring on the ridge top of the west side of the catchment spanning the full texture gradient (Fig 4-1). In November 2007, I installed tension lysimeters at four locations along the texture gradient. At each location I installed two tension lysimeters: one at the bottom of the A soil horizon and a second 1 m below the soil surface (approximating the bottom of the B

soil horizon and soil-paleosol boundary; $N = 8$). All lysimeters were sampled on 10 occasions between January 25, 2008 and August 9, 2008. After the August 9, 2008 sample, the soil became too dry for the tension lysimeters to collect soil solution samples.

Volumetric water content sensors were installed to correspond with each bottom A horizon tension lysimeter. I installed additional volumetric water content sensors at 60 cm below the soil surface to roughly correspond with the deep tension lysimeters (Fig 4-3). The volumetric water content sensors were connected to data loggers that recorded volumetric water content at 10 minute intervals.

In September 2008, I expanded my monitoring efforts to double the ridge top sample size and include the topographic hillslope gradient. To comprise a total of eight sample locations on the ridge top, I added four ridgetop sample locations with A and B horizon tension lysimeters and volumetric water content sensors. At all eight locations I also installed zero tension lysimeters in the bottom the A horizon only (zero tension lysimeters were not installed in the B horizon). Using these eight locations on the ridgetop as start-points, I established eight transects parallel with the hillslope and perpendicular to the drainage. Similar to ridgetop locations, I also installed tension lysimeters and volumetric water content sensors in the A and B horizons as well as zero tension lysimeters in the A horizon at hillslope and toeslope transect locations.

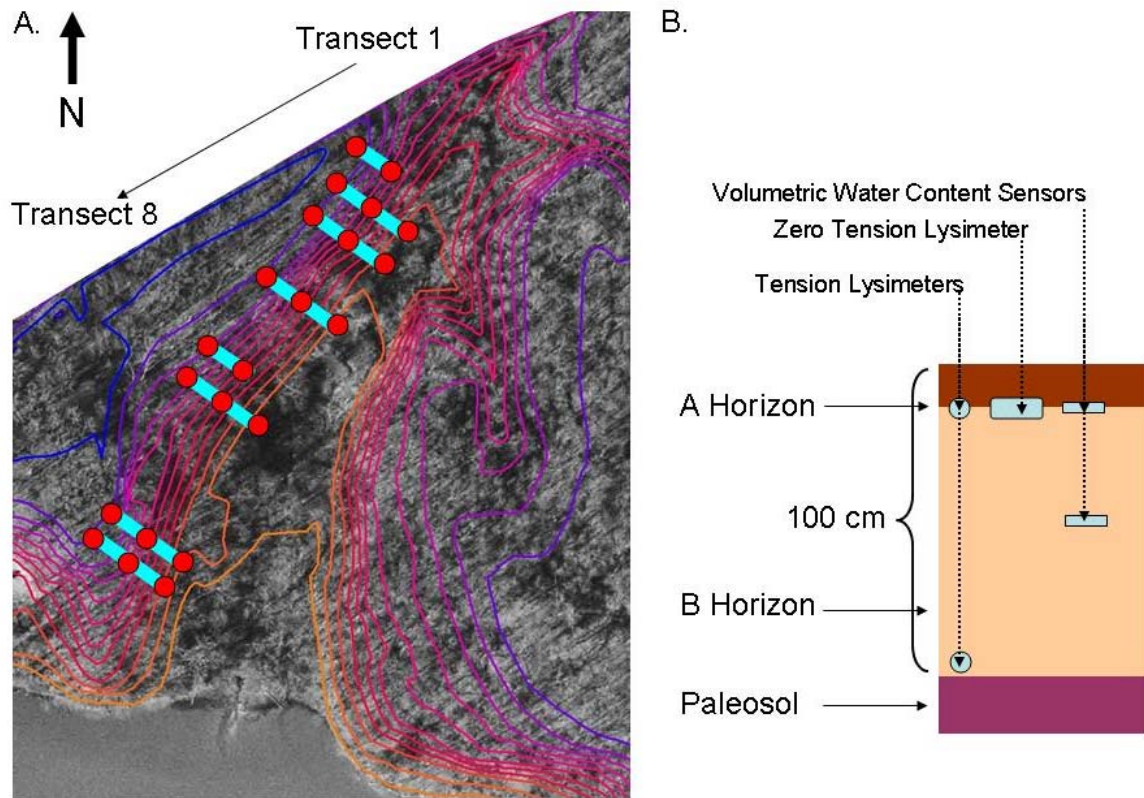


Figure 4-3: A) Blue lines indicate monitoring transects that span topographic and texture gradients. Transects are labeled one through eight from the North to South. Red circles indicate each lysimeter/ volumetric water content monitoring location (N = 8 Ridgetop, N = 8 Hillslope and N = 6 Toeslope locations). B. Sampling design at each monitoring location (indicated in 4-3 A with red circles).

In addition, throughfall collectors were added at all sample locations. At the toeslope location on two transects, I did not install lysimeters, soil moisture sensors or throughfall collectors due to equipment limitations (although I did sample soil properties from these locations; see Laboratory and Field Analyses below). Thus, this final monitoring design included a total of 22 sample locations (Fig 4-3). The sample transects were not evenly spaced because I placed all transects on similar, planar slopes (Appendix 4-1). All lysimeters were sampled fortnightly from December 15, 2008 through August

24, 2009. After the August 24, 2009 sample, the soil became too dry for the tension lysimeters to collect soil solution samples.

Monitoring Equipment

Tension lysimeters were supplied by PrenartTM (Denmark) and fabricated from quartz and Teflon. I inserted lysimeters at a 60° angle to avoid disturbance to overlying soil. The insertion hole was backfilled with acid washed silica flour. Each lysimeter had a sample area of 33 cm². Soil solution samples were collected approximately 18 h after a vacuum of -70 kPa was applied to each lysimeter.

Zero tension lysimeters were fabricated from 9.5 cm inner diameter polyvinylchloride piping. The piping was sawed in half lengthwise. One half of the pipe was driven into the bottom of the A soil horizon parallel with the soil surface (slope). The zero tension lysimeters had a collection area of 290 cm² that drained to a 1 L amber polyethylene bottle housed in stand pipe below the soil surface. I calculated the mass flux of NH₄-N and NO₃-N from the product of N concentrations and water flux for individual fortnightly samples. These values were averaged across repeated samples to calculate mean N flux over time and summed across repeated samples to calculate cumulative N flux over time. Zero tension lysimeters only collected soil solution during intense or protracted precipitation events. Accordingly, the samples represent soil solution during non-steady state conditions.

Volumetric soil water content sensors (Decagon Devices, Inc. Pullman, WA; EC-5 model sensor) were inserted in the soil profile at the bottom of the A horizon and 60 cm

below the soil surface in the B horizon (Fig 4-3). Soil water content sensors obtained volumetric soil water content by measuring the soil dielectric constant.

Throughfall collectors sampled precipitation below the vegetation canopy. Each collector sampled an area of 176.7cm^2 through a funnel with glass fiber filter that was connected to an amber-colored 1L polyethylene bottle that was buried in the soil.

Laboratory and Field Analyses

Soil texture was determined after sieved (2 mm), oven-dried soil was shaken for 2 h in a 3:1 sodium hexametaphosphate:soil slurry by a wet sieve separation of sand from silt and clay with a $53\text{ }\mu\text{m}$ sieve and subsequent separation of clay from silt by decantation of suspended clay from the wet-sieved clay + silt separate (Kettler & Doran 2001).

Three day net nitrification and ammonification were measured *in situ* in $15 \times 5\text{ cm}$ soil cores (Hart et al. 1994). At all A and B horizon sample points ($N = 24$), two $5 \times 15\text{ cm}$ soil cores were extracted in butyrate liners. Cores were capped at both ends; the top cap was perforated to allow for gas exchange. One core was left in the field to incubate for 3 d and the second core was returned to the lab and extracted for NH_4 and NO_3 within 3 h of sampling with the following procedure: Upon return to the lab, a subsample of homogenized soil ($< 2\text{ mm}$) from each soil core (3 h and 3 d) was extracted for NH_4 and NO_3 by reciprocal shaking for 2 h in a 2 M potassium chloride solution at a m/v ratio of 1:5 (soil:KCl). After shaking, the solution was filtered through a Whatman 1 filter for determination of $\text{NH}_4\text{-N}$ and $\text{NO}_3\text{-N}$. Three day net ammonification and nitrification

were determined by subtracting 3 h NH_4 from 3 d NH_4 and 3 h NO_3 from 3 d NO_3 on a mg N kg^{-1} soil basis. Ammonium-N and NO_3 -N were determined by colorimetric analysis of NH_4 -N on a microplate spectrophotometer (Shand et al. 2008). Ammonium-N was measured directly. Nitrate-N was determined by subtraction of NH_4 -N from a replicate sample in which NO_3 -N was reduced to NH_4 -N with Devarda's alloy and subsequently measured for ambient NH_4 -N plus NH_4 -N that was produced by the reduction of NO_3 -N (Sims et al. 1995). Throughfall and soil solution samples from tension and zero tension lysimeters were analyzed for NH_4 -N and NO_3 -N concentrations with the same colorimetric analysis.

I individually applied 70.4% atom percent enrichment (APE) $^{15}\text{NH}_4\text{Cl}$ and 60.2% APE K^{15}NO_3 to undisturbed 15 x 5 cm soil cores to determine the amount of each species that is transferred into insoluble organic N compounds after 15 minutes and 3 days. Insoluble organic N is defined as the insoluble organic N pool that remains in residual soil after 2 M potassium chloride extraction (Kaye et al. 2002). The amount of ^{15}N tracer addition was based on established isotope methodology showing that low amounts of N that are highly enriched in the heavy isotope can be easily detected in soil pools without disturbing N cycling (Hart et al 1994). At each A and B horizon sample location, five soil cores were collected in butyrate liners, capped and returned to the lab. Upon return to the lab, one soil core was extracted for NH_4 and NO_3 in 2 M KCl using the above procedure to determine ^{15}N natural abundance. Of the remaining four soil cores, two were injected with 70.4% APE $^{15}\text{NH}_4\text{Cl}$ and two were injected with 60.2% APE K^{15}NO_3 using 15 cm 19 gauge through-hole side-port spinal needles (Popper & Sons. Inc., New Hyde Park, NY). Soil cores from the A horizon were injected with 0.75 mg of 70.4%

APE $^{15}\text{NH}_4\text{Cl-N}$ and 0.5 mg of 60.2% APE $\text{K}^{15}\text{NO}_3\text{-N}$ while B horizon soil cores were injected with 0.6 mg of 70.4% APE $^{15}\text{NH}_4\text{Cl-N}$ and 0.4 mg of 60.2% APE $\text{K}^{15}\text{NO}_3\text{-N}$. All N applications were delivered in multiple injections of deionized water that totaled 6 mL of solution per soil core. Fifteen minutes after injection, one $^{15}\text{NH}_4\text{Cl}$ -injected soil core and one K^{15}NO_3 - injected soil core was extracted for NH_4 and NO_3 in 2M KCl using the above procedure. The remaining $^{15}\text{NH}_4\text{Cl}$ -injected and K^{15}NO_3 - injected soil cores were returned to the field after injection, collected after 3d, and then extracted in 2 M KCl using the above procedure. Nitrogen isotope ratios and concentrations were determined on the 2 M KCl extracted soils at the University of California Stable Isotope Facility (Davis, CA) with an elemental analyzer interfaced to an isotope ratio mass spectrometer. This instrument was also used to measure soil organic carbon SOC concentrations. Natural abundance N isotope ratios were also determined at each sample location ($N = 48$) and used to calculate the transfer of mineral ^{15}N tracer applications to insoluble organic N compounds with the following equation:

Mass of $\text{NH}_4\text{-N}$ or $\text{NO}_3\text{-N}$ transferred to the insoluble organic N pool =

$$(^{15}\text{N}_{\text{Sample}} - ^{15}\text{N}_{\text{Ambient}})/\text{AFE}_{\text{Tracer}}$$

where $^{15}\text{N}_{\text{Sample}}$ is the mass of ^{15}N in the sample that received tracer addition, $^{15}\text{N}_{\text{Ambient}}$ is the mass of ^{15}N in the ambient soil, and $\text{AFE}_{\text{Tracer}}$ is the fraction of isotope tracer that was ^{15}N . This method assumes ^{15}N tracer application was equally distributed throughout the soil sample prior to sub-sampling for KCl extraction.

Statistical Analyses

I used paired t-tests to compare 1) soil solution $\text{NH}_4\text{-N}$ vs. $\text{NO}_3\text{-N}$ concentrations 2) $\text{NH}_4\text{-N}$ immobilization into insoluble organic N pools vs. $\text{NO}_3\text{-N}$ immobilization into insoluble organic N pools 3) A vs. B soil horizons and 4) 15 minute immobilization $\text{NH}_4\text{-N}$ and $\text{NO}_3\text{-N}$ vs. 3 day immobilization of $\text{NH}_4\text{-N}$ and $\text{NO}_3\text{-N}$. I used regression analyses to identify relationships between soil solution N concentrations, soil solution N flux, soil solution flux, net N mineralization, 15 minute N immobilization and 3 day mineral N immobilization (dependent variables) and soil texture, total SOC and C/N ratio (independent variables). Stepwise multiple regressions were used to determine if the combined use of sand content, SOC, and C/N ratio improved regression models of 15 minute and 3 day mineral N immobilization. I used analyses of covariance to compare soil solution N concentrations (dependent variable) across topographic location (i.e., ridgetop, hillslope and toeslope; between subjects factor) and soil horizons (A and B horizons). Sand content served as the covariate. SPSS (Illinois, USA) software was used for all statistical analyses.

Results

Soil Properties

I observed large gradients in soil texture, SOC and C/N ratios (Table 4-1). Unlike all other sample locations, the toeslope locations on transects three and four were located in soils that were regularly saturated (Appendix D). Zero tension lysimeters at these

locations collected solution even during times without precipitation, suggesting that deep groundwater, independent from the hillslope, contributed to lysimeter samples at these locations. Accordingly, soil solution data from these locations were eliminated from all analyses due to the high redox activity of NO_3 and NH_4 . All eliminated data are displayed in Appendix D. Soil organic carbon content was positively correlated with sand content in the A horizon only ($r^2 = 0.20$; $p = 0.030$). Similarly, insoluble soil organic N was positively correlated with sand content in the A horizon only ($r^2 = 0.20$; $p = 0.027$). In contrast, C/N ratios were not correlated with sand content or SOC in either the A or B soil horizons. There were no significant relationships between B horizon SOC or insoluble organic N and texture.

Across all transects, with sand content included as a covariate, topographic location and soil horizon accounted for significant variation in soil organic carbon, total insoluble nitrogen, and C/N. However, topographic location and soil horizon did not interact to affect any of these variables (Table 4-2).

Throughfall

I found no significant differences in throughfall volume, NO_3 or NH_4 concentrations in individual or the cumulative sample period (December 15, 2008-August 24, 2009). Mean throughfall $\text{NO}_3\text{-N}$ concentration was 0.51 mg L^{-1} and mean throughfall $\text{NH}_4\text{-N}$ concentration was 0.75 mg l^{-1} .

Table 4-1. Selected soil properties from transect sample locations displayed in Fig. 4-3. * indicates a location where soil solution and throughfall were not collected. %C and %N refer to total soil organic carbon and total soil insoluble nitrogen.

Transect Number	Topographic Location	A Horizon						B Horizon					
		% Sand	% Silt	% Clay	% C	% N	C/N	% Sand	% Silt	% Clay	% C	% N	C/N
1	Ridgetop	54.27	30.82	14.9	1.82	0.07	26.00	67.13	25.48	7.39	0.47	0.03	15.67
1	Hillslope	68.4	17.4	14.2	2.62	0.1	26.20	64.89	25.05	10.06	0.86	0.04	21.50
1*	Toeslope	75.13	16.84	8.02	5.53	0.24	23.04	65.49	23.67	10.84	3.88	0.14	27.71
2	Ridgetop	61.07	27.87	11.07	2.96	0.11	26.91	56.06	31.96	11.98	0.56	0.03	18.67
2	Hillslope	61.38	27.3	11.31	5.44	0.22	24.73	67.77	19.74	12.49	0.62	0.02	31.00
2	Toeslope	68.45	19.08	12.45	5.47	0.32	17.09	68.5	18.8	12.7	0.74	0.02	37.00
3	Ridgetop	54.67	32.27	13.07	2.91	0.14	20.79	61.1	26.1	12.8	1	0.06	16.67
3	Hillslope	65.4	25.73	8.87	2.08	0.09	23.11	65.23	23.2	11.57	0.53	0.03	17.67
3	Toeslope	70.76	18.56	10.68	6.47	0.27	23.96	58.32	26.36	15.31	2.11	0.08	26.38
4	Ridgetop	52.71	37.07	10.22	4.65	0.25	18.60	48.77	36.94	14.29	0.7	0.04	17.50
4	Hillslope	61.4	35.6	3	2.58	0.11	23.45	60.33	26.6	13.07	0.79	0.04	19.75
4	Toeslope	66.91	21.7	11.38	2.98	0.13	22.92	37.61	22.66	39.73	1.26	0.05	25.20
5	Ridgetop	71.53	21.2	7.27	3.47	0.18	19.28	62.39	25.71	11.89	0.97	0.06	16.17
5	Hillslope	78.41	14.26	7.33	2.47	0.13	19.00	67.24	21.61	11.14	0.77	0.05	15.40
5*	Toeslope	77.07	15.73	7.2	6.42	0.27	23.78	82.97	9.58	7.45	1.44	0.06	24.00
6	Ridgetop	75.08	15.77	9.15	4.12	0.22	18.73	80.55	10.39	9.06	0.74	0.04	18.50
6	Hillslope	85.13	7.27	7.6	2.41	0.12	20.08	83.92	8.67	7.4	0.75	0.04	18.75
6	Toeslope	84.2	10.27	5.53	6.22	0.3	20.73	84.25	7.88	7.88	1.78	0.1	17.80
7	Ridgetop	77.72	16.23	6.36	3.08	0.17	18.12	71.69	19.47	8.84	0.66	0.04	16.50
7	Hillslope	91.81	3.06	5.13	6.22	0.31	20.06	91.81	3.99	4.19	0.49	0.02	24.50
7	Toeslope	93.47	0.67	5.87	5.63	0.26	21.65	78.23	12.58	9.19	0.65	0.03	21.67
8	Ridgetop	59.79	25.7	14.51	2.61	0.14	18.64	72.53	14.69	12.79	1.26	0.07	18.00
8	Hillslope	70.13	17.87	12	4.75	0.26	18.27	80.63	10.59	8.79	1.4	0.08	17.50
8	Toeslope	74.43	11.85	13.72	4.24	0.18	23.56	75.98	12.51	11.51	1.3	0.06	21.67

Table 4-2. Mean (standard error) of soil properties across topographic locations and soil horizons. Three independent 3 x 2 analyses of covariance with topographic location and soil horizon main effects and a sand content covariate demonstrated significant effects of topographic location and soil horizon on all three soil properties ($p < 0.05$). There was no significant interaction effect in any of the analyses. Post hoc analyses of topographic location demonstrated the Toeslope location to be significantly different from the Ridgetop and Hillslope locations for all three dependent variables ($p < 0.05$).

Topographic Location	Soil Organic Carbon (g kg^{-1})		Soil Insoluble Nitrogen (g kg^{-1})		C/N Ratio	
	A Horizon	B Horizon	A Horizon	B Horizon	A Horizon	B Horizon
Ridgetop	32.0 (3.1)	8.0 (0.9)	1.6 (0.2)	0.5 (0.1)	20.68 (1.34)	17.20 (0.34)
Hillslope	35.7 (5.8)	7.7 (1.0)	1.7 (0.3)	0.4 (0.1)	21.95 (1.15)	19.74 (0.91)
Toeslope	53.7 (4.2)	16.5 (3.6)	2.5 (0.2)	0.7 (0.1)	23.22 (0.74)	24.24 (1.65)
Total	40.5 (1.5)	10.7 (1.5)	1.9 (0.2)	0.5 (0.1)	21.95 (0.65)	20.39 (0.65)

Soil Solution

In 2008, tension lysimeter soil solution $\text{NH}_4\text{-N}$ and $\text{NO}_3\text{-N}$ concentrations were greater than in 2009. However, comparisons between sample years are complicated by different sample numbers at different points in time (Appendix C). In both sample years mean A horizon tension lysimeter soil solution $\text{NH}_4\text{-N}$ and $\text{NO}_3\text{-N}$ concentrations from each location were positively correlated with sand content across all topographic positions (Fig 4-4; Appendix C). Similarly, mean 2009 zero tension lysimeter $\text{NO}_3\text{-N}$ concentrations were positively correlated with sand content ($r^2 = 0.17$; $p = 0.072$). However mean 2009 zero tension lysimeter $\text{NH}_4\text{-N}$ concentrations were not correlated with soil texture. Neither the mean flux per fortnight sample, precipitation weighted mean flux, nor the total flux of $\text{NH}_4\text{-N}$ or $\text{NO}_3\text{-N}$ (December 15, 2008-August 24, 2009) were correlated with soil texture (data not shown); the cumulative flux of soil solution through the A horizon from December 15, 2008 to August 2009 was negatively correlated with soil texture (Fig 4-5).

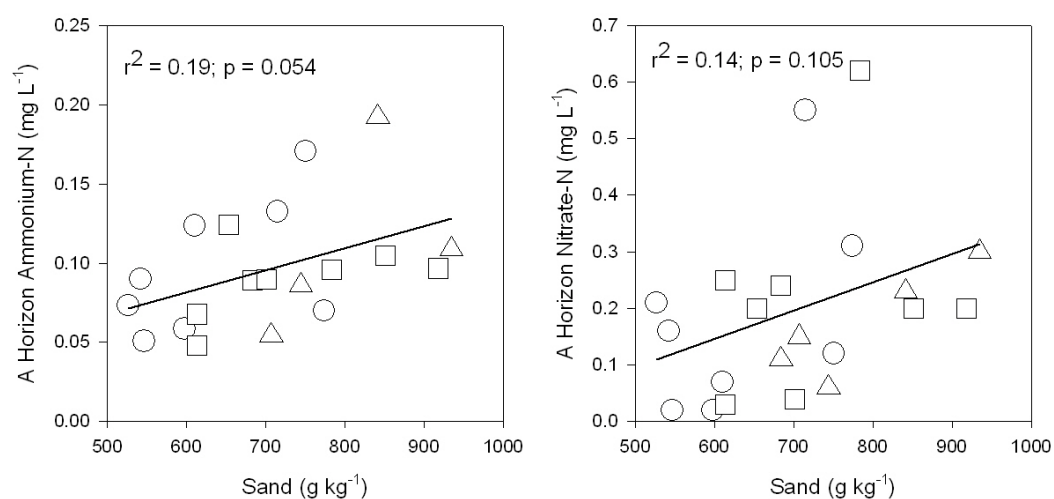


Figure 4-

4: Linear regression between mean 2009 A horizon tension lysimeter soil solution nitrogen concentrations and sand content. Circles indicate ridgetop position, squares indicate hillslope position and triangles indicate toeslope position.

In contrast to the A horizon, B horizon soil solution N concentrations were not correlated with soil texture. On all sample occasions A horizon tension lysimeter soil solution N concentrations were greater than B horizon tension lysimeter N concentrations (paired t-test; $p < 0.0001$; Appendix 4-2). Similarly, soil solution N concentrations were greater in zero tension lysimeters compared to corresponding A horizon tension lysimeters (paired t-test; $N = 22$; $p < 0.0001$). Moreover, for soil solution $\text{NO}_3\text{-N}$, the magnitude of this difference was a positive function of sand content ($r^2 = 0.36$; $p = 0.005$) and saturated hydraulic conductivity (saturated hydraulic conductivity measurements for each A horizon lysimeter location are reported in Jurinko 2009; Fig 4-6).

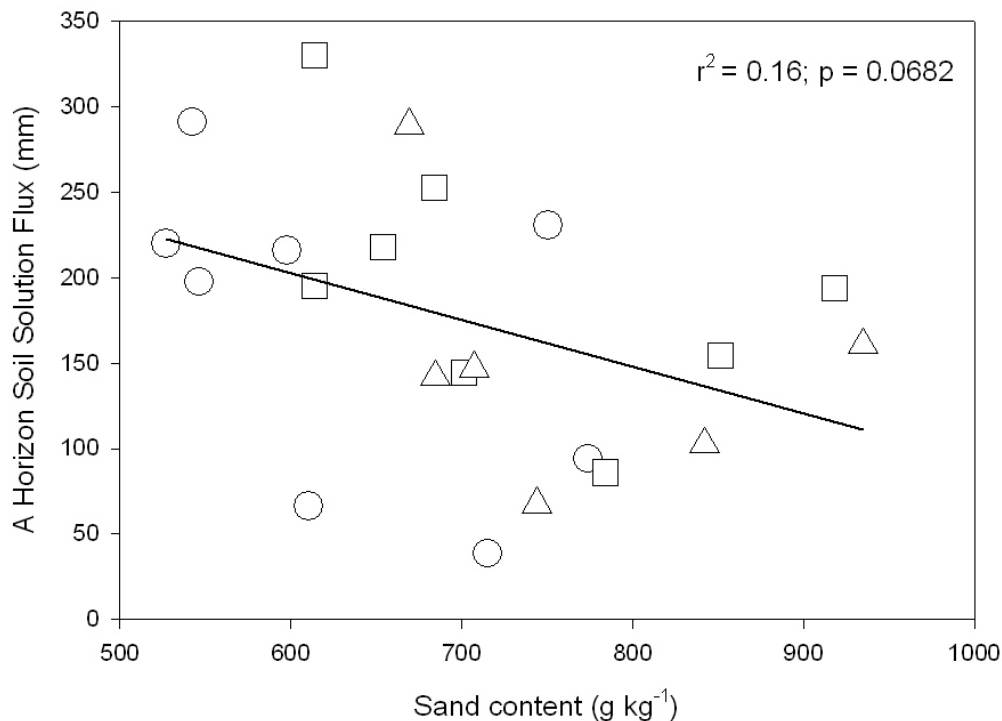


Figure 4-5: Linear regression between cumulative 2009 A horizon soil solution flux across all sample locations ($N = 22$; December 2008- August 2009). Circles indicate ridgetop position, squares indicate hillslope position and triangles indicate toeslope position

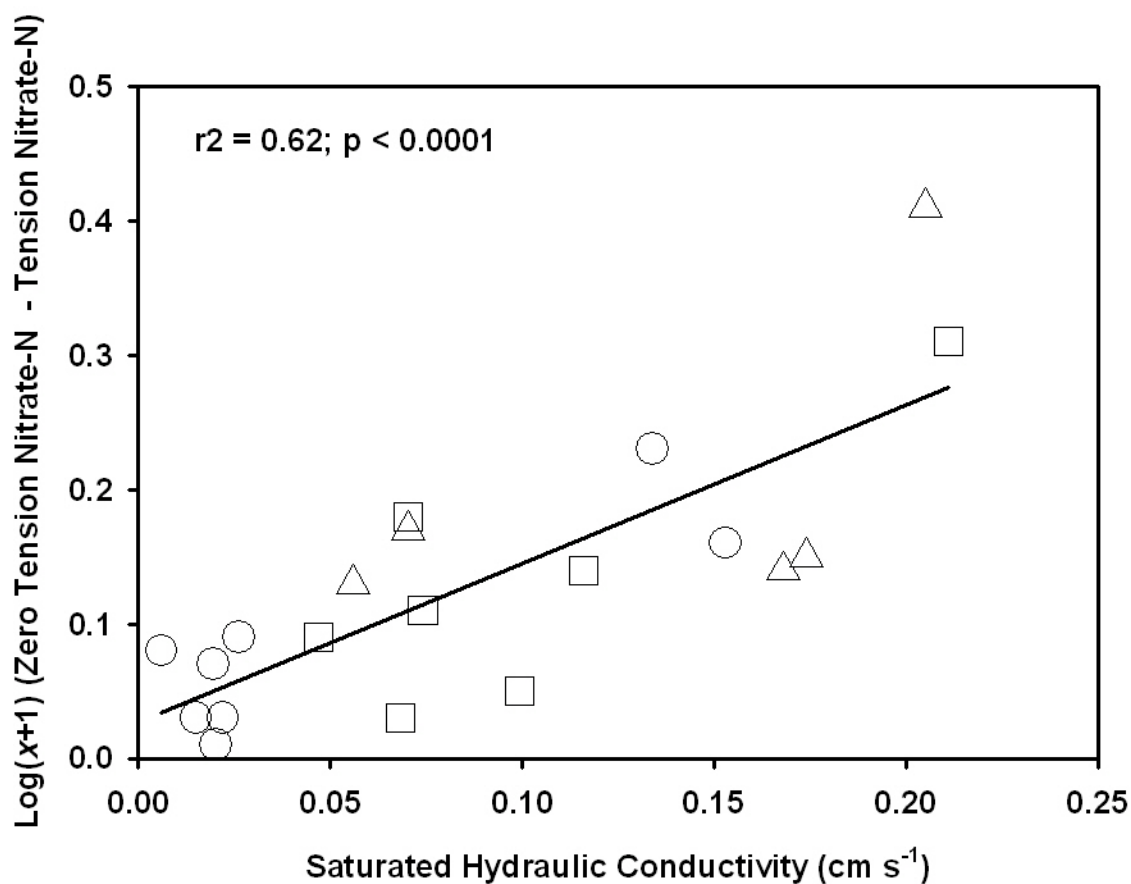


Figure 4-6: Linear regression between the log(x+1) transformed difference between mean 2009 (December 15, 2008-August 24, 2009) zero tension lysimeter nitrate-N concentration and A horizon tension lysimeter nitrate-N (N = 20 pairs) and saturated hydraulic conductivity (Jurinko 2009). Circles indicate ridgetop position, squares indicate hillslope position and triangles indicate toeslope position. Log transformation was necessary due to low y-axis values (Zar 1999).

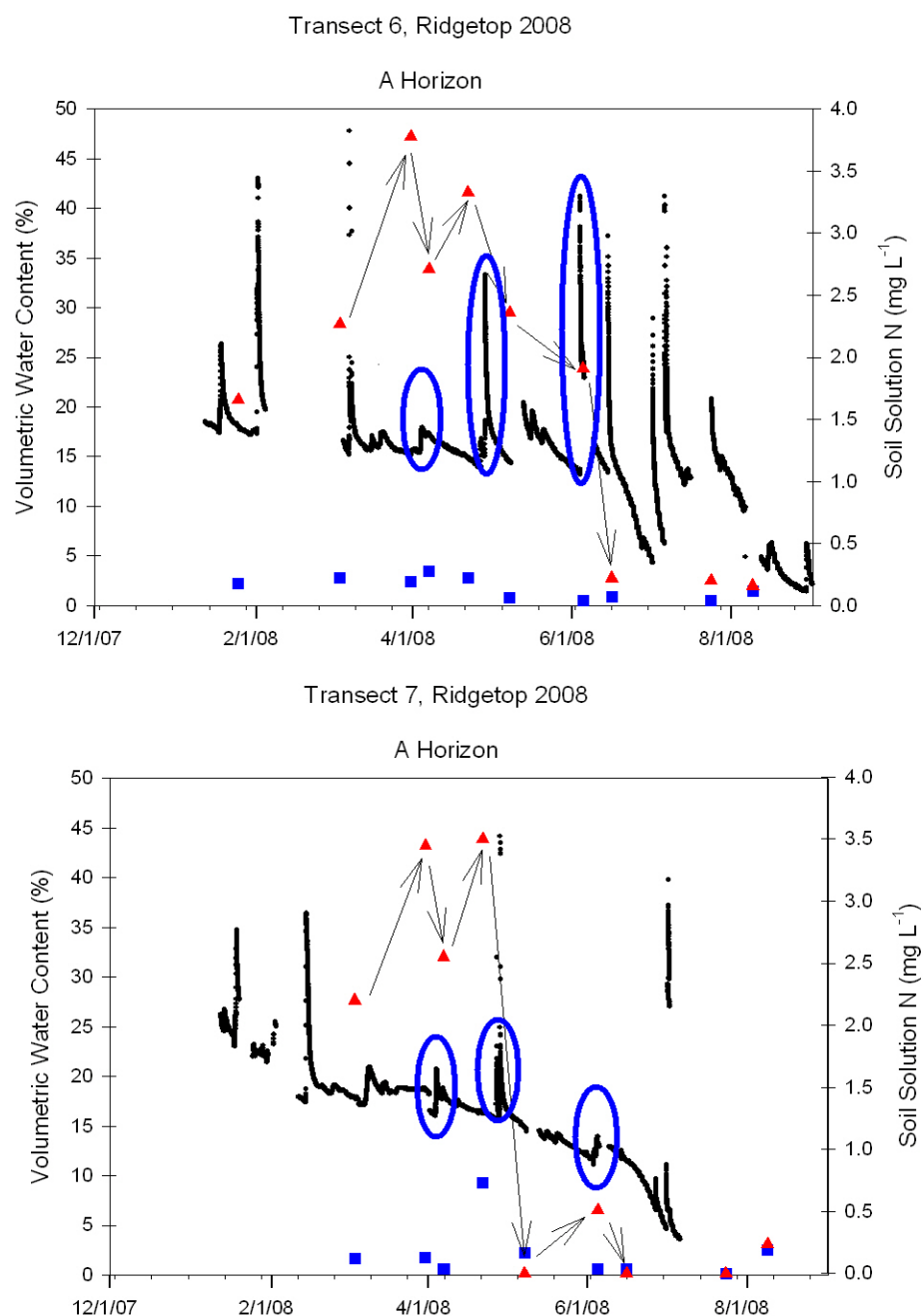


Figure 4-7: Volumetric water content (black lines), tension lysimeter nitrate-nitrogen (red triangles) concentration and tension lysimeter ammonium-nitrogen (blue squares) concentrations from 2008 sandy-soil A horizon replicates. Arrows indicate periods of decreasing soil moisture that are associated with increasing nitrate-nitrogen concentrations. Blue ovals indicate increases in volumetric water content that are associated with a subsequent decrease in soil solution nitrate-nitrogen concentrations.

Across the texture gradient, soil solution collected in tension and zero tension lysimeters at the bottom of the A horizon had lower concentrations of $\text{NH}_4\text{-N}$ than throughfall (Table 4-3). Likewise, soil solution collected in tension lysimeters at the bottom of the A horizon had lower concentrations of $\text{NO}_3\text{-N}$ than throughfall. In contrast, soil solution collected in zero tension lysimeters at the bottom of the A horizon had significantly greater $\text{NO}_3\text{-N}$ concentrations than throughfall at nearly all of the sample locations (paired t-test $N = 20$; $p < 0.001$; Table 4-3). Zero tension lysimeter $\text{NO}_3\text{-N}$ concentrations were lower than throughfall $\text{NO}_3\text{-N}$ concentrations only at the most silty soil locations (i.e., some sample locations on Transects 1, 2 & 3). In tension and zero tension lysimeters, soil solution N concentrations generally increased downslope (Table 4-3).

Table 4-3. Mean (standard error) of throughfall and soil solution nitrogen concentrations from December 15, 2008 through August 24, 2009. Letters within column indicate topographic location was a significant source of variation in analyses of covariance. Different letters within columns indicate significant differences between locations ($p < 0.05$).

	Throughfall		Tension Ammonium-N		Tension Nitrate-N		Zero Tension Ammonium-N	Zero Tension Nitrate-N
	Nitrate-N	Ammonium-N	A Horizon	B Horizon	A Horizon	B Horizon	A Horizon	A Horizon
Ridgetop	-	-	0.01 (0.01)b	0.07 (0.01)	0.18 (0.06)	0.06 (0.01)	0.30 (0.08)b	0.47 (0.10)b
Hillslope	-	-	0.09 (0.01)b	0.06 (0.01)	0.22 (0.06)	0.13 (0.05)	0.27 (0.04)b	0.83 (0.21)b
Toeslope	-	-	0.17 (0.04)a	0.06 (0.01)	0.40 (0.20)	0.22 (0.16)	0.81 (0.37)a	1.34 (0.41)a
Total	0.51 (0.13)	0.75 (0.26)	0.11 (0.03)	0.07 (0.01)	0.23 (0.09)	0.15 (0.06)	0.44 (0.23)	0.79 (0.25)

Soil Volumetric Water Content

Soil volumetric water content was highly variable throughout the textural and topographic gradients (Appendix C). In 2008, I noted a qualitative pattern between A horizon tension lysimeter soil solution $\text{NO}_3\text{-N}$ concentrations and volumetric water content: between March and June of 2008 in sandy-soil sample locations (Transects 6 &

7; see Appendix C) soil solution $\text{NO}_3\text{-N}$ appeared to increase during periods of decreasing volumetric water content and decrease after periods of increasing volumetric water content associated with rainfall (Fig 4-7). However, I did not observe this pattern in 2009. At the four A horizon and four B horizon locations that were sampled in both 2008 and 2009, volumetric water content was greater in 2009 (paired t-test; $N = 8$; $p < 0.0001$). The A horizon volumetric water content was $0.21 \text{ cm}^3 \text{ cm}^{-3}$ in 2008 compared to $0.23 \text{ cm}^3 \text{ cm}^{-3}$ in 2009 while B horizon volumetric water content was $0.21 \text{ cm}^3 \text{ cm}^{-3}$ in 2008 and $0.24 \text{ cm}^3 \text{ cm}^{-3}$ in 2009. Variation in volumetric water content was not correlated with variation in soil solution N.

Net Ammonification and Net Nitrification

Across the ridgetop soil texture gradient in May 2007, there were no relationships between net ammonification or net nitrification and soil texture or SOC in either the A or B soil horizons ($N = 11$ per soil horizon). On this occasion, net immobilization dominated in both soil horizons (data not shown). In April 2008 across both the texture and topographic gradients ($N = 24$ per soil horizon), net ammonification was positively correlated with sand content the A horizon only (Fig 4-8). Net nitrification was not correlated with texture in either the A or B horizons. However, net nitrification was weakly negatively correlated with SOC in the A horizon ($r^2 = 0.12$; $p = 0.090$). I did not identify any variables that were associated with net ammonification or nitrification in the B horizon. Net ammonification and nitrification rates were not significantly different

between soil horizons (paired t-test; $N = 24$; $p > 0.4$). Topographic location had no effect on net ammonification or nitrification.

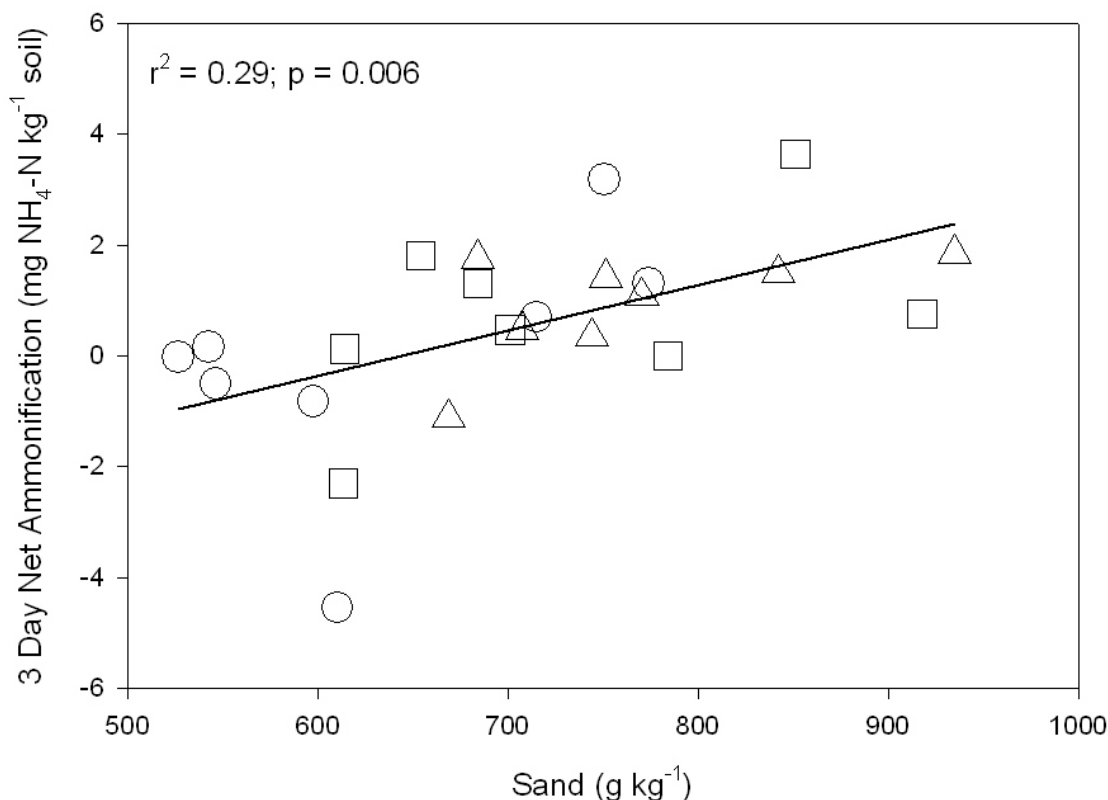


Figure 4-8: Linear regression between 3 day net ammonification and sand content. Circles indicate ridgetop position, squares indicate hillslope position and triangles indicate toeslope position.

Insoluble Organic Nitrogen

The transfer of NH₄-N to insoluble organic N compounds was positively related to sand content in the 15 minute A horizon samples only (Table 4-3). The transfer of NH₄-N or NO₃-N to insoluble organic N compounds was not correlated with soil carbon-to-nitrogen ratio during 15 minute or 3 day incubations. However, the transfer of NH₄-N into insoluble organic nitrogen compounds was correlated with total SOC at 15 minutes

and 3 days while the transfer of $\text{NO}_3\text{-N}$ was correlated with total SOC only at 15 minutes (Fig 4-9; Table 4-4).

Stepwise multiple regression with sand content, SOC concentration and C/N ratio improved univariate models of 15 minute A horizon ammonium transfer to insoluble organic N and 3 day B horizon ammonium transfer to insoluble organic N (data not shown). In these cases, inclusion of C/N ratio in addition to SOC significantly increased the variation described by univariate models. Sand content was excluded from all multivariate models.

Table 4-4. Correlation coefficients (R) and probabilities of Type I errors (p) between the transfer of $^{15}\text{Ammonium-nitrogen}$ and $^{15}\text{Nitrate-nitrogen}$ isotope tracers into insoluble organic nitrogen and sand content (g kg^{-1}), carbon-to-nitrogen ratio, and soil organic carbon (g kg^{-1}).

Dependent Variable	Independent Variables					
	Sand Content		C/N Ratio		Soil Organic Carbon	
Transfer to Soil Insoluble Organic Nitrogen	R	p	R	p	R	p
15 Minute A Horizon Ammonium	+0.41	0.048	-0.17	0.401	+0.78	<0.000
15 Minute B Horizon Ammonium	+0.06	0.793	+0.35	0.090	+0.73	<0.000
15 Minute A Horizon Nitrate	+0.16	0.459	+0.13	0.541	+0.70	<0.000
15 Minute B Horizon Nitrate	+0.01	0.973	+0.32	0.125	+0.70	<0.000
3 Day A Horizon Ammonium	-0.14	0.528	+0.08	0.713	+0.51	0.011
3 Day B Horizon Ammonium	+0.31	0.145	-0.13	0.534	+0.52	0.014
3 Day A Horizon Nitrate	-0.05	0.827	+0.23	0.27	+0.35	0.103
3 Day B Horizon Nitrate	+0.30	0.154	+0.07	0.751	+0.16	0.412

Compared to $\text{NO}_3\text{-N}$, significantly more $\text{NH}_4\text{-N}$ was immobilized into insoluble organic N compounds in both 15 minute and 3 day incubations (paired t-tests; $N=24$; $p < 0.0001$). Similarly, with the exception of 3 day $\text{NH}_4\text{-N}$, more $\text{NH}_4\text{-N}$ and $\text{NO}_3\text{-N}$ were immobilized into insoluble organic N compounds in the A horizon compared to the B horizon in both 15 minute and 3 day incubations (paired t-tests; $N=24$; $p < 0.01$); the 3 day immobilization of $\text{NH}_4\text{-N}$ was not statistically different between A and B horizons

(Fig. 4-9). Finally, 3 day immobilization of both $\text{NH}_4\text{-N}$ and $\text{NO}_3\text{-N}$ was greater than 15 minute immobilization (paired t-tests; $N=24$; $p < 0.0001$).

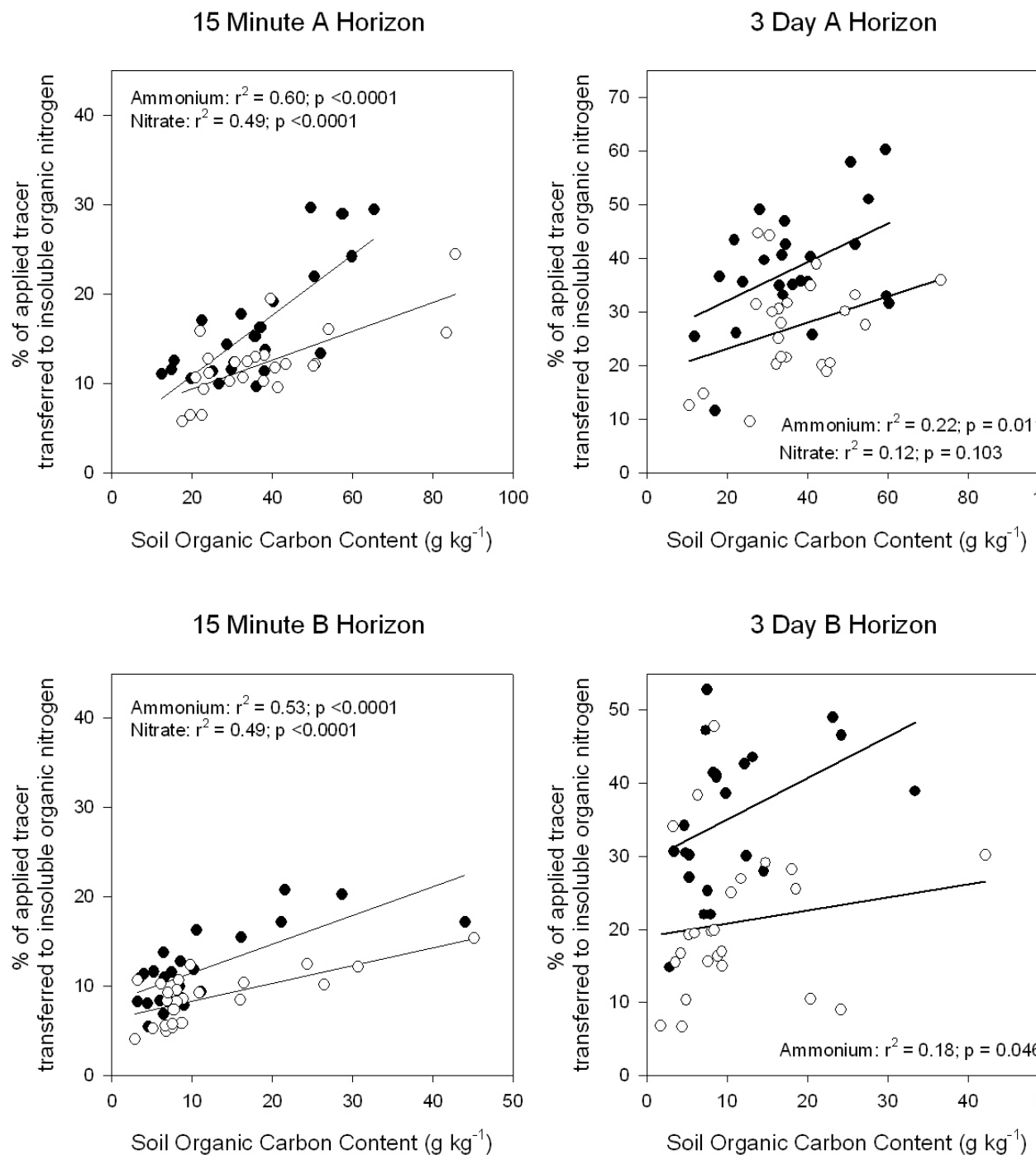


Figure 4-9: Linear regressions between the transfer of ammonium-¹⁵nitrogen (filled circles) and nitrate-¹⁵nitrogen (open circles) isotope tracers to insoluble organic nitrogen compounds and soil organic carbon concentrations.

Discussion

A major goal of terrestrial ecosystem science is to predict the impact of increasing mineral N inputs on recipient and downstream ecosystems. Soil has been identified as the key ecosystem property that controls the ability of ecosystems to retain mineral N inputs. Specifically, C/N ratios and SOC concentrations have been identified as two variables that negatively co-vary with reactive N concentrations, ecosystem reactive N losses, and ecosystem N retention (e.g., Nadelhoffer et al. 1999; Kaye et al. 2002; Barrett et al. 2002; Emmett et al. 1998; Lovett et al. 2002). However, considerable unexplained variation in these relationships has led to the suggestion that soil texture, through its impact on hydrology and biogeochemistry, may play a role in ecosystem nitrogen dynamics (Lovett et al. 2004; Pregitzer et al. 2004; Templer et al. 2005; McGuire & McDonnell 2007).

Within a forested catchment with similar vegetation, but gradients in soil texture, SOC and C/N ratios, I monitored soil solution NH_4 and NO_3 concentrations and flux while measuring net N cycling and immobilization into insoluble organic compounds. My objective was to simultaneously evaluate soil texture, SOC and C/N ratio controls on ecosystem N transformation and transport. At my field site, I found ambiguous evidence for a soil texture-based control on ecosystem N loss and immobilization. Although sand content was positively correlated with soil solution N concentrations and net ammonification (Figs 4-4 & 4-8), the total flux of soil solution was negatively correlated

with sand content (Fig 4-5). Accordingly, there was no correlation between soil solution N flux and texture. Moreover, there was no relationship between mineral N immobilization and soil texture.

Soil Solution Nitrogen

The positive relationship between sand content and SOC as well as the lack of relationship between C/N ratio and either SOC or texture permitted the simultaneous comparison of putative SOC, C/N ratio and texture controls on soil solution N concentrations. Surprisingly, soil solution inorganic N concentrations were positively correlated with sand content but not correlated with SOC or C/N ratio. Across European and North American forested ecosystems, C/N ratio has been shown to be negatively correlated with inorganic N export (Emmett et al. 1998, Lovett et al. 2002). Similarly, 3 day net ammonification was positively correlated with sand content. These data coupled with the lack of a difference in reactive N immobilization across the texture gradient (Table 4-3) suggest that the positive relationship between soil solution N concentrations and sand content (Fig 4-4) is the result of a difference in mineral N production.

The difference between soil solution NO_3 concentrations in zero tension lysimeters compared to corresponding tension lysimeters was positively correlated with sand content and saturated hydraulic conductivity (Fig 4-6). Zero tension lysimeters only collected soil solution during intense or protracted precipitation events that represented saturated soil water flow whereas tension lysimeters sampled relatively immobile soil solution (Lajtha et al. 1999). Because throughfall mineral N concentrations were similar

across the topographic and texture gradients, I attribute this difference to at least two non-exclusive mechanisms: 1) During times of rapid water movement when zero tension lysimeters collect soil solution, the positive relationship between hydraulic conductivity and sand may inhibit N immobilization in sandy soils (McGuire & McDonnell 2007); I measured N immobilization during steady state conditions in soil cores that eliminated the effect of hydrology. 2) Rapid increases in soil water content can increase N mineralization (Franzluebbers et al. 2000). Accordingly, more rapid wetting that would be expected in sandy soils with high hydraulic conductivity may exacerbate the positive relationship between N mineralization and sand content (Fig 4-8) as well as bypass N immobilization sinks in sandy soils. In 2008 I observed increases in soil solution NO_3 concentrations during periods of decreasing volumetric water content in sandy soils only (Fig 4-7; Appendix 4-2). An increase in soil solution NO_3 between precipitation events that is flushed from the soil upon rewetting may also help to explain the pattern identified Figure 4-6 (*sensu* Creed et al. 1996; McGuire & McDonnell 2007). In 2008 I only had four sample locations which did not have zero tension lysimeters, limiting my ability to evaluate the increase in soil solution NO_3 during drying in relation to soil texture.

Ammonium and Nitrate Immobilization

Simultaneous evaluations of soil texture, SOC and C/N ratio do not support a role for soil texture in the prediction of N immobilization. Soil organic carbon concentrations described the most variation in the immobilization of NH_4 and NO_3 to insoluble organic N compounds. In some situations C/N ratios improved univariate models, but the

improvement was modest. However, as mentioned above, it is possible that hydrology may modulate the relationship between N immobilization and soil texture. These data should encourage future analyses of N immobilization that explicitly incorporate hydrology.

The consistent deterioration of relationships between N immobilization and SOC concentrations from 15 minutes to 3 days suggests that N immobilization into insoluble organic compounds over longer periods of time is not directly related to absolute SOC concentrations; SOC quality may also play a role (e.g., Kaye et al. 2002). Nonetheless, the absolute amount of mineral N immobilized into insoluble organic N compounds always increased from 15 minutes to 3 days. These data suggest 15 minute mineral N immobilization is related to absolute SOC concentrations, but longer term immobilization is affected by additional properties such as SOC quality, microbial cycling and mineralogy.

Conclusion

Variation in soil solution N concentrations and net N mineralization in the absence of roots (the most frequently used indicators of ecosystem nitrogen status; Verchot et al. 2001) could not be explained by SOC or C/N ratios but were positively related to sand content. These data, coupled with the lack of relationship between mineral N immobilization and soil texture, suggest that sandy soils are more prone to mineral N losses due to higher production of mineral N rather than reduced immobilization potential during equilibrium hydrological conditions. If a reduction in N

immobilization is an important mechanism promoting higher mineral N concentrations in sandy soils, it appears to occur only during times of rapid soil solution flow.

However, at my site sandy soils did not export more NO₃ than silty soils despite higher NO₃ concentrations because total soil solution flux was negatively correlated with sand content (Fig 4-5). Nonetheless, sandy soils and silty soils may respond differently to potential increases in future mineral nitrogen inputs. The response of these soils to increased nitrogen inputs will be key to predicting potential NO₃ export to surface and ground waters.

Literature Cited

- Aber J., W. McDowell, K. Nadelhoffer, A. Magill, G. Berntson, M. Kamakea, S. McNulty, W. Currie, L. Rustad, and I. Fernandez. 1998. Nitrogen saturation in temperate forest ecosystems. *Bioscience* 48:921-934.
- Barrett, J.E., D.W. Johnson, I.C. Burke. 2002. Abiotic nitrogen uptake in semiarid grassland soils of the U.S. Great Plains. 66:979-987.
- Bohlen, P.J., P.M. Groffman, C.T. Driscoll, T.J. Fahey, T.G. Siccama 2001. Plant-soil-microbial interactions in a northern hardwood forest. *Ecology* 82: 965-978.
- Boyer, E.W., G.M.Hornberger, K.E.Bencala, D.M. Mcknight. 1997. Response characteristics of DOC flushing in an alpine catchment. *Hydrological Processes* 11: 1635 – 1647.

- Carpenter, S., N.F. Caraco, R.W. Howarth, A.N. Sharpley, V.H. Smith. 1998. Nonpoint pollution of surface waters with phosphorus and nitrogen. *Issues in Ecology* 3:1-12.
- Creed, I. F., L. E. Band, N. W. Foster, I. K. Morrison, J. A. Nicolson, R. S. Semkin, and D. S. Jeffries. 1996. Regulation of nitrate-N release from temperate forests: A test of the N flushing hypothesis. *Water Resources Research* 32: 3337-3354.
- Davidson, E., J. Chorover, B. Dail. 2003. A mechanism of abiotic immobilization of nitrate in forest ecosystems: the ferrous wheel hypothesis. *Global Change Biology* 9:228-236.
- Dittman, J.A., C.T. Driscoll, P.M. Groffman, T.J. Fahey. Dynamics of nitrogen and dissolved organic carbon at the Hubbard Brook Experimental Forest. *Ecology* 88:1153-1166..
- Doolittle, J. 2008. USDA NRCS ground penetrating radar report from the Otter Point Creek NOAA NERR.
- Emmett, B.A., D. Boxman, M. Bredemeier, P. Gundersen, O.J. Kjonaas, F. Moldan, P. Schleppi, A. Tietma, R.F. Wright. 1998. Predicting the effects of atmospheric deposition in conifer stands: evidence from the nitrex ecosystem-scale experiments. *Ecosystems* 1:352-360.
- Fitzhugh, R., G. Lovett, and R. Venterea 2003. Biotic and abiotic immobilization of ammonium, nitrite, and nitrate in soils developed under different tree species in the Catskill Mountains, New York, USA. *Global Change Biology* 9: 1591-1601.

- Galloway, J., J. Aber, J. Erisman S. Seitzinger, R. Howarth, E. Cowling, and J. Cosby. 2003. The nitrogen cascade. *Bioscience* 53:341-356.
- Gaskin, J. W., J. W. Dowd, W. L. Nutter and W. T. Swank. 1989. Vertical and Lateral Components of Soil Nutrient Flux in a Hillslope. *Journal of Environmental Quality* 18:403-410. .
- Hassink, J. 1997. The capacity of soils to preserve organic C and N by their association with clay and silt particles. *Plant and Soil* 191:77-87.
- Hättenschwiler, S. and P.M. Vitousek 2000. The role of polyphenols in terrestrial ecosystem nutrient cycling. *Trends in Ecology and Evolution* 15:238-244.
- Hart, S.C., J.M. Stark, E.A. Davidson, and M.K. Firestone. 1994. Nitrogen Mineralization, Immobilization, and Nitrification. pp. 985-1018 In *Methods of Soil Analysis*, Part 2 - Microbiological and Biochemical Properties - SSSA Book Series, no. 5, Madison, WI.
- Hill, A.R., W.A. Kemp, J.M. Buttle, D. Goodyear. 1999. Nitrogen chemistry of subsurface storm runoff on forested Canadian Shield hillslopes. *Water Resources Research* 35: 811 –821.
- Hornberger, G.M., K.E. Bencala, D.M. Mcknight. 1994. Hydrological controls on dissolved organic carbon during snowmelt in the snake river near Montezuma, CO. *Biogeochemistry* 25 147 – 165.
- Jurinko, K. 2009. Developing Saturated Hydraulic Conductivity Pedotransfer Functions within a Small Pedologically and Topographically Diverse Chesapeake Bay Catchment. B.S. Thesis, Geohydrology. The Pennsylvania State University.

- Kaye, J.P., and S.C. Hart. 1997. Competition for nitrogen between plants and soil microorganisms. *Trends in Ecology and Evolution* 12: 139-143.
- Kaye, J.P., J.E. Barrett, and I.C. Burke. 2002. Stable carbon and nitrogen pools in grassland soils of variable texture and carbon content. *Ecosystems* 5: 461-471.
- Lajtha, K. W.M. Jarrell, D.W. Johnson, P. Sollins 1999. Collection of soil solution. *Standard Soil Methods for Long Term Ecological Research.* (ed) Robertson GP et al. Oxford.
- Lovett G.M., Weathers, K.C., Sobczak, W.V. 2000. Nitrogen saturation and retention in forested watersheds of the Catskill Mountains, New York. *Ecological Applications* 10: 73-84.
- Lovett, G.M., K.C. Weathers, M.A. Arthur. 2002. Control of nitrogen loss from forested watersheds by soil carbon:nitrogen ratio and tree species composition. *Ecosystems* 5:712-718.
- Lovett, G.M., K.C. Weathers, M.A. Arthur, J.C. Schultz. 2004. Nitrogen cycling in a northern hardwood forest: Do species matter? *Biogeochemistry* 67:289-308.
- McGuire, K. J. and J. J. McDonnell. 2007. Stable isotope tracers in watershed hydrology. In: Michener, R. and Lajtha, K. *Stable isotopes in ecology and environmental science.* 2nd edition. Blackwell, Malden, MA.
- Nadelhoffer, K., B. Emmett, P. Gundersen, O. Kjonaas, C. Koopmans, P. Schleppi, A. Tietema, and R. Wright. 1999. Nitrogen deposition makes a minor contribution to carbon sequestration in temperate forests. *Nature* 398: 145-148.
- Ocampo, C. J., C. E. Oldham, M. Sivapalan and J. V. Turner. 2006. Hydrological versus biogeochemical controls on catchment nitrate export: a test of the flushing mechanism *Hydrological Processes* 20: 4269 -4286.

- Pastor, J., J.D. Aber, C.A. McClaugherty, J.M. Melillo. 1984. Aboveground production and N and P cycling along a nitrogen mineralization gradient on Blackhawk Island, Wisconsin. *Ecology* 65:256-268.
- Pregitzer, K.S., D.R. Zak, A.J. Burton, J.A. Ashby, N.W. MacDonald. 2004. Chronic nitrate additions dramatically increase the export of carbon and nitrogen from northern hardwood ecosystems. *Biogeochemistry* 68:179-197.
- Schimel, D.S., B.H. Braswell, E.A. Holland, R. McKeown, D.S. Ojima, T.H. Painter, W.J. Parton, and A.R. Townsend. Climatic, edaphic, and biotic controls over storage and turnover of carbon in soils. 1994. *Global Biogeochemical Cycles* 8:279-293.
- Shand CA, Williams BL, Coutts G. 2008. Determination of N-species in soil extracts using microplate techniques. *Talanta* 74:648-654.
- Sims GK, Ellsworth TR, Mulvaney RL. 1995. Microscale determination of inorganic nitrogen in water and soil extracts. *Communications in Soil Science and Plant Analysis* 26:303-316.
- Smil V. 2004. *Enriching the Earth: Fritz Haber, Carl Bosch and the Transformation of World Food Production*. MIT Press, Boston.
- Stark JM, and Hart SC. 1996. Diffusion technique for preparing salt solutions, Kjeldahl digests, and persulfate digests for nitrogen-15 analysis. *Soil Science Society of America Journal* 60:1846-1855.
- Stevenson, F.J. 1994. *Humus chemistry: genesis, composition and reactions*. 2nd edition. John Wiley and Sons, NY.

- Templer, PH, G Lovett, K Weathers, S Findlay, and T Dawson. 2005. Influence of tree species on forest nitrogen retention in the Catskill Mountains, New York, USA. *Ecosystems* 8:1-16.
- van Verseveld, W.J., J.J. McDonnell, K. Lajtha. 2008. A mechanistic assessment of nutrient flushing at the catchment scale. *Journal of Hydrology* 358:268-287.
- Verchot, L.V., Z Holmes, L. Mulon, P.M. Groffman, G.M. Lovett. 2001. Gross vs. net rates of N mineralization and nitrification as indicators of functional differences between forest types. *Soil Biology & Biochemistry* 33:1889-1901.

Chapter 5

Conclusions

The three empirical data chapters in this document have focused on uniting soil hydrology and biogeochemistry at the pedon scale. Building on conceptual models of soil water flow and nutrient cycling from the hydrological and biogeochemical literatures, I sought to examine linkages between these soil hydrology and biogeochemistry. Biogeochemists have used a “black box” approach to understanding ecosystem N dynamics (Likens & Bormann 1994). This approach measures biogeochemical inputs and outputs while searching for the mechanisms that drive internal cycling (transformation). At the pedon scale, I incorporated hydropedology variables into this approach.

Chapter 2, “Global within-site variance in soil solution nitrogen and hydraulic conductivity are correlated with clay content”, described how soil structure, as modified by clay content, can affect the spatial variability of soil solution N transport. This work empirically verified a conceptual model of soil hydrology (Jarvis 2007) while incorporating dissolved nitrogen dynamics. My data suggest hydrology, biogeochemistry and disturbance interact to affect spatial variation of soil solution nitrogen.

Chapter 3, “Hydrological and biogeochemical controls on the timing and magnitude of nitrous oxide flux across an agricultural landscape”, examined how the hydrological status of the “black box” (Fig 5-1) affects soil flux of nitrous oxide. My data demonstrated that volumetric water content was not a consistent predictor of nitrous

oxide flux, but the thermodynamically based property, matric potential, was a consistent predictor of nitrous oxide flux across differing soils. Although the use of matric potential to predict N gas production is novel, matric potential has long been used to predict water movement through the soil. These data extend the use of matric potential from predicting water flow to predicting gaseous N flux. Future work should incorporate these biogeochemical responses to matric potential.

Chapter 4, “Nitrogen transport and transformation along gradients of topography and soil texture”, identified patterns between mineral nitrogen concentrations, production and immobilization in relation to soil texture, soil organic carbon, and C/N ratios. Data from this chapter demonstrate differing controls on nitrogen production, immobilization and transport. Soil solution nitrogen concentrations appear to be controlled by mineralization rather than immobilization. Finally, high saturated hydraulic conductivity appears to promote increased soil solution nitrate concentrations during dynamic soil water flow.

Explicit incorporation of hydropedology and biogeochemistry can aid in determining biogeochemical transport and transformation. My work supports the current paradigm that dynamic periods of soil hydrology disproportionately affect large amounts of biogeochemical cycling (McClain et al. 2003). My work expands upon this by demonstrating that in addition to soil hydrology’s affect on biogeochemical transport and transformation, soil properties also affect how biogeochemical transport and transformation respond to similar fluctuations in hydrology.

Future work coupling hydropedology and biogeochemistry should focus on interactions between hydrology, organic nitrogen and organic carbon. Little insight is

available to suggest how cycling of dissolved organic carbon and dissolved organic nitrogen contribute to ecosystem outputs of nitrogen in gaseous and, in particular, dissolved species. Although the importance of insoluble carbon and insoluble nitrogen stability have gained attention in recent years (e.g. Kaye et al. 2002), relatively few data are available to evaluate the stability of dissolved organic nitrogen. Hydropedology is likely to play a strong role affecting the cycling of dissolved organic nitrogen as it moves along flowpaths through the soil and into ground and surface waters.

Literature Cited

- Fisher SG, Sponseller RA, Heffernan JB. 2004. Horizons in biogeochemistry: flowpaths to progress. *Ecology* 85:2369-2379.
- Lohse KA, Brooks PD, McIntosh JC, Meixner T, Huxman TE. 2009. Interactions between biogeochemistry and hydrologic systems. *Annual Review of Environment and Resources*. In press.
- McClain ME, Boyer EW, Dent CL, Gergel SE, Grimm NB, Groffman PM, Hart SC, Harvey JW, Johnston CA, Mayorga E, McDowell WH, Pinay G. 2003. Biogeochemical hot spots and hot moments at the interface of terrestrial and aquatic ecosystems. *Ecosystems* 6: 301-312.
- Wagener, S. M., Oswood M.W., Schimel J.P. 1998. Rivers and soils: parallels in carbon and nutrient processing. *BioScience* 48:104–108.

Appendix A

Chapter 2 raw data for analyses and literature cited.

Appendix A. Raw Data

Nitrate

Source	Location	Texture Determination	%Sand	%Silt	%Clay	CV (%)	Sampling Method	Number of Lysimeters per Replicate	Replicates	Total Sample Times	Depth	Dominant Vegetation	Time Since Major Disturbance (i.e. Fire or Harvest) or Ecosystem Establishment
Adamson (1998)	United Kingdom	Mean Text. Class (Peat)	Peat	Peat	Peat	36.64	T	1	6	78	10 & 50 cm mean	Heath	41
Bohlen et al. (2004)	NY, USA	Author Contacted/ WSS	32.1	55.9	12	83.20	O&T Mean	4	3	27	15 & 40 cm mean	Hardwood-Deciduous	>100
Borken et al. (2004)	Germany	Borken & Beese (2002)	14	58	28	34.6	T	4	3	12	10cm	Conifer	115
Borken et al. (2004)	Germany	Borken & Beese (2002)	39	46	15	50.86	T	4	3	13	10cm	Conifer	103
Brenner et al. (2006)	AK, USA	WSS	15.05	77	8	49.45	T	5, 4	3	20	12 & 40 cm mean	Hardwood-Deciduous	>100
Brenner et al. (2006)	AK, USA	WSS	15.05	77	8	81.01	T	5, 4	3	20	12 & 40 cm mean	Conifer	>200
De Schrijver et al. (2008)	Belgium	Author contacted	>90	5-9	<5	42.58	T	3	4	12	100 cm	Hardwood-Deciduous	29
De Schrijver et al. (2008)	Belgium	Author contacted	>90	5-9	<5	45.50	T	3	2	12	100 cm	Conifer	61
De Schrijver et al. (2008)	Belgium	Author contacted	>90	5-9	<5	53.76	T	3	2	12	100 cm	Conifer	61
De Schrijver et al. (2008)	Belgium	Author contacted	>90	5-9	<5	76.09	T	3	2	12	25cm	Heath	>229
De Schrijver et al. (2008)	Belgium	Author contacted	>90	5-9	<5	38.46	T	3	2	12	25cm	Heath	>229
Dijkstra et al. (2007)	MN, USA	Author contacted	94	2.5	3.5	86.16	T	1	12	20	100cm	Grassland	6
Dittman et al. (2007)	NY, USA	Mean Text. Class (Sandy Loam)	65	25	10	72.45	O	1	2	145	22.5cm, 44.5cm mean	Conifer	73
Dittman et al. (2007)	NY, USA	Mean Text. Class (Sandy Loam)	65	25	10	85.96	O	1	3	145	22.5cm, 44.5cm mean	Hardwood-Deciduous	73
Dittman et al. (2007)	NY, USA	Mean Text. Class (Sandy Loam)	65	25	10	86.31	O	1	3	145	22.5cm, 44.5cm mean	Hardwood-Deciduous	73
Fang et al. (2008)*	Zhaoqing, China	Author contacted	36.8	29.4	33.8	34.12	O	2	3	24	20cm	Evergreen (young growth)	~70
Fang et al. (2008)*	Zhaoqing, China	Author contacted	22.1	34.5	43.4	31.26	O	2	3	24	20cm	Evergreen (old growth)	>400
Fisk et al. (2002)*	MI, USA	Reported	63	32	4	84.57	T	8	3	30	100cm	Hardwood-Deciduous (old growth)	200-300
Fisk et al. (2002)*	MI, USA	Reported	70	25	5	95.78	T	8	3	30	100cm	Hardwood-Deciduous	60-80
Hagedorn et al. (2001)†	Switzerland	Reported	5	46	49	34.38	T	1	5	>20	5cm	Deciduous (young growth)	250
Holloway and Dahlgren (2001)	CA, USA	Mean Text. Class (Sandy Loam)	65	25	10	48.35	C	1	3	12	30-60cm	Conifer	na
Holloway and Dahlgren (2001)	CA, USA	Mean Text. Class (Silt Loam)	25	67.5	13.75	73.85	C	1	3	12	30-60cm	Savanna-Shrub	na
Hope (2009)*	BC, Canada	Reported	64.67	30.97	4.27	42.94	T	6	3	~24	50-60cm	Conifer	>100
Huygens et al. (2008)	Chile	Huygens et al. (2007)	71	23	6	40.64	T	1	4	na	10, 50, 100 cm mean	Hardwood-Evergreen	325
Johnson et al. (2001)	NV, USA	Author Contacted/ Mean Text. Class (Sand)	92.5	7.5	5	59.16	T	1	6	4	15 and 30 mean	Conifer	>80
Jones and Willett (2006)	United Kingdom	Author Contacted	19	69	12	48.19	C	1	6	na	A horizon	Hardwood-Deciduous	"mature"
Jones and Willett (2006)	United Kingdom	Author Contacted	44	36	20	19.34	C	1	6	na	A horizon	Hardwood-Deciduous	"mixed" age
Lajtha et al. (1995)	MA, USA	Author Contacted/ Seely & Lajtha 1997	90	10	<1	20.12	O	4	2	>10	50cm	Grassland	4
Lajtha et al. (1995)	MA, USA	Author Contacted/ Seely & Lajtha 1997	90	10	<1	28.28	O	4	2	>10	50cm	Savanna-Shrub	21
Lajtha et al. (1995)*	MA, USA	Author Contacted/ Seely & Lajtha 1997	90	10	<1	43.07	O	4	2	>10	50cm	Mixed Hardwood-Deciduous (young growth)	36
Lajtha et al. (1995)	MA, USA	Author Contacted/ Seely & Lajtha 1997	90	10	<1	53.04	O	4	2	>10	50cm	Conifer	37
Lajtha et al. (1995)	MA, USA	Author Contacted/ Seely & Lajtha 1997	90	10	<1	19.74	O	4	2	>10	50cm	Mixed Hardwood-Deciduous	44
Lajtha et al. (1995)	MA, USA	Author Contacted/ Seely & Lajtha 1997	90	10	<1	66.60	O	4	2	>10	50cm	Hardwood-Deciduous	80
Lajtha et al. (1995)	MA, USA	Author Contacted/ Seely & Lajtha 1997	90	10	<1	46.61	O	4	2	>10	50cm	Hardwood-Deciduous	132
Lajtha et al. (1995)*	MA, USA	Author Contacted/ Seely & Lajtha 1997	90	10	<1	37.42	O	4	2	>10	50cm	Mixed Hardwood-Deciduous (old growth)	140
Lajtha et al. (1995)	MA, USA	Author Contacted/ Seely & Lajtha 1997	90	10	<1	13.78	O	4	2	>10	50cm	Hardwood-Deciduous	197
Lajtha et al. (1995)	MA, USA	Author Contacted/ Seely & Lajtha 1997	90	10	<1	28.46	O	4	2	>10	50cm	Hardwood-Deciduous	226

Lajtha et al. (2005)	OR, USA	Reported	na	na	13	69.28	T	5	3	na	30 & 100 cm mean	Conifer Hardwood-Evergreen (300 year old soil)	"old growth"
Lohse and Matson (2005)†	HA, USA	WSS	31.5	31	37.5	52.29	T	2	4	>20	47cm	Hardwood-Evergreen (4.1my old soil)	no known harvest
Lohse and Matson (2005)†	HA, USA	WSS	48.6	34.1	17.3	35.50	T	2	4	>20	28cm mean	Conifer	no known harvest
Marques and Ranger (1997)*	France	Reported	38.3	50.67	11.6	71.88	O	1	4	32	15, 30, 60 mean	Conifer	20
Marques and Ranger (1997)	France	Reported	45.25	38.73	16.025	83.25	O	1	4	32	15, 30, 60 mean	Conifer	40
Marques and Ranger (1997)*	France	Reported	44.33	35.08	18.05	68.35	O	1	4	32	15, 30, 60, mean	Conifer	60
McLaughlin and Phillips (2006)*	ME, USA	Author Contacted/ Mean Text. Class (Loamy Sand)	80	15	7.5	75.00	T	2	4	21	25 cm & 50cm mean	Conifer (old growth)	~75
McLaughlin and Phillips (2006)*	ME, USA	Author Contacted/ Mean Text. Class (Loamy Sand)	80	15	7.5	101.54	T	2	8	21	25 cm & 50cm mean	Conifer (young growth)	15
Mitchell et al. (2001)	NY, USA	WSS/ Mitchell et al. (2003)	37.5	38.75	17.5	47.64	T	3-4	3	>10	15cm & 50cm mean	Hardwood-Deciduous	33
Mitchell et al. (2001)	NY, USA	WSS/ Mitchell et al. (2003)	92.5	7.5	5	36.79	T	3-4	3	>10	15cm & 50cm mean	Hardwood-Deciduous	24
Mitchell et al. (2001)	NY, USA	WSS/ Mitchell et al. (2003)	65	25	10	60.92	T	3-4	3	>10	15cm & 50cm mean	Hardwood-Deciduous	70
Mobley, Richter et al. (Unpublished)	SC, USA	Richter et al. (1994)	67.6	17	15.4	56.25	O	12	1	19	7.5cm	Hardwood-Deciduous	
Murphy et al. (2006)*	NV, USA	Author Contacted/ Mean Text. Class (Loam)	37.5	38.75	17.5	49.05	T	1	4	3 years	30cm 30cm & 100cm mean	Conifer Hardwood-Evergreen	>80
Neill et al. (2006)*	Brazil	Reported	na	na	30.75	31.09	T	1	5	>20	20, 40, 100cm	Hardwood-Deciduous	na
Rothe et al. (2002)	Germany	Kreutzer and Weiss (1998)	29.02	47.01	18.45	45.33	T	1	10	48	20, 40, 100cm	Conifer Hardwood-Evergreen	90
Rothe et al. (2002)	Germany	Weiss (1998)	29.02	47.01	18.45	94.33	T	1	10	48	10cm & 60cm mean	Conifer Hardwood-Evergreen	85
Schroth et al. (2000)	Brazil	Reported	na	na	80	25.30	T	1	6	13	20, 40, 75, 150, 250 350 cm mean	Hardwood-Evergreen	"primary growth"
Schwendenmann and Veldkamp (2005)	Costa Rica	Reported	na	na	75.86	0.16	T	4	4	>20	50cm	Hardwood-Evergreen	na
Silva et al. (2005)	OK, USA	Reported	50	27.5	22.5	16.67	T	2	2	23	50cm	Grassland	>50
Silva et al. (2005)	OK, USA	Reported	45	35.5	17.5	19.35	T	2	2	23	50cm	Hardwood-Deciduous	>50
Silva et al. (2005)	OK, USA	Reported	80	10	10	45.45	T	2	2	23	50cm	Grassland	>50

Silva et al. (2005)	OK, USA	Reported	87.5	7.5	5	24.12	T	2	2	23	50cm	Hardwood-Deciduous	>50
Strahm et al. (2005)*	WA, USA	Author contacted	16.42	44.72	38.86	33.16	T	1	4	>10	100 cm	Conifer	47
Zak et al. (2004)	MI, USA	Author contacted	84	13	3	8.62	T	4	3	22	75cm	Hardwood-Deciduous	88

Sampling method abbreviations: T = tensions lysimeters, O = Zero tension lysimeters and C = centrifuge

Texture Determination Abbreviation: WSS = Web Soil Survey (see literature cited)

na = not available

* = report used in young vs. old forest paired comparison; Hope (2009), Murphy et al. (2006), Neill et al. (2006) and Strahm et al. (2005) paired sites were harvested immediately prior to data collection and thus not included in clay-CV regression.

† = report used in paired N addition comparison

Dissolved Organic Nitrogen Raw Data

Source	Location	Texture Determination	%Sand	%Silt	%Clay	CV (%)	Sampling Method	Number of Replicate Lysimeters per Depth	Replicates	Sample Times	Lysimeter Depth	Dominant Vegetation	Time Since Major Disturbance (i.e. Fire or Harvest) or Ecosystem Establishment
Adamson et al. (1998)	United Kingdom	Mean Text. Class (Peat)	Peat	Peat	Peat	5.46	T	1	6	26	10 & 50 cm mean	Heath	na
Asano et al. (2006)	OR, USA	WSS	27.65	52.55	19.80	58.76	T	1	19	15	50cm	Conifer	~150
Borken et al. (2004)	Germany	Borken & Beese (2002)	27	54	19	32.35	T	4	3	10	10cm	Hardwood-Deciduous	20
Borken et al. (2004)	Germany	Borken & Beese (2002)	14	58	28	24.72	T	4	3	6	10cm	Conifer	19
Borken et al. (2004)	Germany	Borken & Beese (2002)	39	46	15	54.7	T	4	3	12	10cm	Conifer	25
Borken et al. (2004)	Germany	Unterlüß, Borken & Beese (2002)	77	16	7	24.73	T	4	3	8	10cm	Hardwood-Deciduous	31
Borken et al. (2004)	Germany	Unterlüß, Borken & Beese (2002)	74	23	3	34.1	T	4	3	8	10cm	Conifer	27
Borken et al. (2004)	Germany	Unterlüß, Borken & Beese (2002)	81	16	3	20.18	T	4	3	8	10cm	Conifer	33
Brenner et al. (2006)	AK, USA	WSS	15.05	77.00	8.00	19.50	T	5,4	3	20	13 & 40 cm mean	Hardwood-Deciduous	>100
Brenner et al. (2006)	AK, USA	WSS	15.05	77.00	8.00	14.63	T	5,4	3	20	14 & 40 cm mean	Conifer	>200
Currie et al. (1996)†	MA, USA	Author Contacted	68.00	16.70	12.00	80.27	T	5	1	14	60cm	Conifer	67
Currie et al. (1996)†	MA, USA	WSS/ Author Contacted	68.00	16.70	12.00	81.63	T	5	1	14	60cm	Hardwood-Deciduous	50
Dijkstra et al. (2007)	MN, USA	Author contacted	94.00	2.50	3.50	57.4	T	1	12	20	60cm	Grassland	6

Dittman et al. (2007)	NY, USA	Mean Text. Class (Sandy Loam)	65.00	25.00	10.00	49.98	O	1	2	145	22.5 & 44.5cm mean	Conifer	73
Dittman et al. (2007)	NY, USA	Mean Text. Class (Sandy Loam)	65.00	25.00	10.00	57.88	O	1	3	145	22.5 & 44.5cm mean	Hardwood-Deciduous	73
Dittman et al. (2007)	NY, USA	Mean Text. Class (Sandy Loam)	65.00	25.00	10.00	65.72	O	1	3	145	22.5cm, 44.5cm mean	Hardwood-Deciduous	73
Fang et al. (2008)*	Zhaoqing, China	Author contacted	36.80	29.40	33.80	53.29	O	2	3	24	20cm	Evergreen (young growth)	~70
Fang et al. (2008)*	Zhaoqing, China	Author contacted	22.10	34.50	43.40	39.97	O	2	3	24	20cm	Hardwood-Evergreen (old growth)	>400
Fisk et al. (2002)*	MI, USA	Reported	63.00	32.00	4.00	37.44	T	8	3	30	30	Hardwood-Deciduous (old growth)	200-300
Fisk et al. (2002)*	MI, USA	Reported	70.00	25.00	5.00	48.82	T	8	3	30	30	Hardwood-Deciduous (young growth)	60-80
Hagedorn et al. (2001)†	Switzerland	Reported	5.00	46.00	49.00	27.50	T	1	5	>20	5cm	Conifer	250
Huygens et al. (2008)	Chile	Huygens et al. (2007)	71.00	23.00	6.00	43.32	T	1	4	na	10, 50, 100 cm mean	Hardwood-Evergreen	325
Jones and Willett (2006)	United Kingdom	Author contacted	19.00	69.00	12.00	85.40	C	1	6	na	A horizon	Hardwood-Deciduous	"mature"
Jones and Willett (2006)	United Kingdom	Author contacted	44.00	36.00	20.00	38.10	C	1	6	na	A horizon	Hardwood-Deciduous	"mixed" age
Kaiser and Guggenberger (2005)	Germany	Reported	na	na	17.00	44.06	O&T Mean	8	3	2	25-30cm & 90cm mean	Hardwood-Deciduous	90
Lillerfein et al. (2004)	CA, USA	Dickson & Crocker (1953)	40.30	57.59	2.11	43.77	T	1	5	8	10, 40, 150 cm mean	Conifer	77
Lillerfein et al. (2004)	CA, USA	Dickson & Crocker (1953)	42.10	55.76	2.14	38.58	T	1	6	8	150 cm	Conifer	255
Lillerfein et al. (2004)	CA, USA	Dickson & Crocker (1953)	45.70	50.36	3.94	41.62	T	1	5	8	16, 40, 150 cm mean	Conifer	616
Lillerfein et al. (2004)	CA, USA	Dickson & Crocker (1953)	44.60	53.40	2.00	35.23	T	1	5	8	20, 40, 150 cm mean	Conifer	1200
Mobley, Richter et al. (Unpublished)	SC, USA	Richter et al. (1994)	67.60	17.00	15.40	37.33	O		12	19	7.5cm	Hardwood-Deciduous	na
Park and Matzner (2003)	Germany	Eusterhues et al. (2005)	na	na	9.40	8.33	T	1	3	46	20cm	Hardwood-Deciduous	130
Qualls and Richardson (2003)	FL, USA	Mean Text. Class (Peat)	Peat	Peat	Peat	29.50	O	1	>10	3	12.5 & 60 cm mean	Grassland	na
Schroth et al. (2002)	Brazil	Reported	na	na	80.00	35.58	T	1	6	13	10 & 60cm mean	Evergreen	"primary growth"
Schrumpf et al. (2005)*	Tanzania	Author Contacted	16.00	19.88	64.10	37.70	T	3	3	>50	15, 30, 100 cm mean	Hardwood-Evergreen	"mature" >60
Schwendenmann and Veldkamp (2005)	Costa Rica	Reported	na	na	71.38	28.61	T	4	4	>20	20, 40, 75, 150, 250 350 cm mean	Hardwood-Evergreen	na
Strahm et al. (2005)*	WA, USA	Author contacted	16.42	44.72	38.86	27.28	T	1	4	>10	100 cm	Conifer	47
Zak et al. (2004)	MI, USA	Author contacted	84.00	13.00	3.00	9.30	T	4	3	22	75cm	Hardwood-Deciduous	88

Appendix 1. Sampling method abbreviations: T = tensions lysimeters, O = Zero tension lysimeters and C = centrifuge.

Texture Determination Abbreviation: WSS = Web Soil Survey (see literature cited)

na = not available

* = report used in young vs. old forest paired comparison; Schrumpf et al. (2005) and Strahm et al. (2005) paired sites were harvested immediately prior to data collection and thus not included in clay-CV regression

† = report used in paired N addition comparison

Saturated Hydraulic Conductivity Data

Source	Location	Clay Determination	%Sand	%Silt	%Clay	CV (%)	Sampling Method	N	Sampling Location
Buczko et al. (2006)	Germany	Reported	93.70	3.10	3.20	13.39	Ring Infiltrometer	30	Field
Buczko et al. (2006)	Germany	Reported	92.80	3.40	3.80	7.96	Ring Infiltrometer	33	Field
Buczko et al. (2006)	Germany	Reported	91.70	5.40	2.90	9.85	Ring Infiltrometer	33	Field
Buczko et al. (2006)	Germany	Reported	89.00	6.20	4.80	11.33	Ring Infiltrometer	28	Field
Grace et al. (2006)	NC, USA	Mean Texture Class (Clay loam)	32.50	34.25	33.45	42.86	Constant head	11	Lab
Jansson and Johansson (1996)	Switzerland	Reported	17.70	70.40	8.80	100.85	Permeater	0-5	Lab
Johnson et al. (2006)	Brazil	Author Contacted	na	na	32.40	41.32	Infiltrometer	4	Field
Johnson et al. (2006)	Brazil	Author Contacted	na	na	36.40	56.51	Infiltrometer	4	Field
Julia et al. (2004)	Spain	Reported	20.50	31.10	20.50	73.17	Various	120	Various
Julia et al. (2004)	Spain	Reported	5.00	7.00	5.00	101.42	Various	38	Various
Julia et al. (2004)	Spain	Reported	27.00	33.20	27.00	41.67	Various	472	Various
Julia et al. (2004)	Spain	Reported	19.70	30.30	19.70	94.34	Various	200	Various
Julia et al. (2004)	Spain	Reported	24.70	26.80	24.70	51.55	Various	163	Various
Julia et al. (2004)	Spain	Reported	25.20	26.20	25.20	71.94	Various	46	Various
Julia et al. (2004)	Spain	Reported	15.50	27.70	15.50	96.15	Various	182	Various
Julia et al. (2004)	Spain	Reported	20.80	32.00	20.80	79.37	Various	141	Various
Julia et al. (2004)	Spain	Reported	17.70	23.90	17.70	104.53	Various	30	Various
Julia et al. (2004)	Spain	Reported	38.20	25.70	38.20	66.67	Various	98	Various
Julia et al. (2004)	Spain	Reported	35.70	21.50	35.70	58.82	Various	288	Various
Julia et al. (2004)	Spain	Reported	25.00	21.10	25.00	47.62	Various	78	Various
Julia et al. (2004)	Spain	Reported	24.20	21.60	24.20	63.03	Various	408	Various
Julia et al. (2004)	Spain	Reported	15.40	26.60	15.40	111.11	Various	145	Various

Julia et al. (2004)	Spain	Reported	25.00	35.60	25.00	31.06	Various	225	Various
Julia et al. (2004)	Spain	Reported	18.10	30.90	18.10	69.12	Various	39	Various
Julia et al. (2004)	Spain	Reported	19.70	28.10	19.70	98.43	Various	79	Various
Julia et al. (2004)	Spain	Reported	25.40	29.20	25.40	47.85	Various	49	Various
Julia et al. (2004)	Spain	Reported	28.50	37.40	28.50	16.13	Various	37	Various
Li et al. (2007)	China	Mean Sand	92.50	7.50	5.00	35.57	Permeater	4	Field
Li et al. (2007)	China	Mean Texture Class (Loamy Sand)	80.00	15.00	7.50	5.48	Permeater	3	Field
Li et al. (2007)	China	Mean Texture Class (Sandy Loam)	65.00	25.00	10.00	113.95	Permeater	12	Field
Li et al. (2007)	China	Mean Texture Class (Silty Loam)	25.00	67.50	13.75	78.58	Permeater	13	Field
Li et al. (2007)	China	Mean Texture Class (Silty Clay Loam)	10.00	66.25	36.25	50.58	Permeater	3	Field
Malmir (1996)	Malaysia	Clay Mean	22.50	30.00	70.00	70.23	Infiltrometer	10	Field
Malmir (1996)	Malaysia	Sand Mean	92.50	7.50	5.00	33.33	Infiltrometer	10	Field
Neirynck et al. (2000)	Belgium	Reported	10.50	74.00	15.50	72.99	Not available	5-10	Lab
Perkins et al. 2007	GA, USA	Mean Texture Class (Loamy sand)	80.00	15.00	7.50	78.00	Ring Infiltrometer	24	Field
Ramos et al. (2007)	Spain	Reported	70.40	23.10	6.50	33.00	Infiltrometer	6	Field
Schack-Kirchner et al. (2007)	Brazil	Reported	7.00	22.00	71.00	40.89	Falling head	6	Lab
Sheridan et al. (2007)	Australia	Mean Texture Class (Sandy clay & Clay)	30.00	24.00	30.00	66.89	Ring Infiltrometer	27	Field
Xu et al. (2002)	SC, USA	Author Contacted	65.00	25.00	10.00	102.53	Not available	6	Lab
Young et al. (2004)	NV, USA	Reported	95.00	3.00	2.00	28.57	Infiltrometer	na	Field
Young et al. (2004)	NV, USA	Reported	85.00	12.00	3.00	78.75	Infiltrometer	na	Field
Young et al. (2004)	NV, USA	Reported	70.00	24.00	6.00	13.64	Infiltrometer	na	Field
Young et al. (2004)	NV, USA	Reported	47.00	25.00	28.00	42.84	Infiltrometer	na	Field
Young et al. (2004)	NV, USA	Reported	53.00	22.00	25.00	41.67	Infiltrometer	na	Field
Ziegler et al. (2006)	Malaysia	Reported	34.00	27.50	38.50	70.00	Amoozemeter	10	Field

na = not available

Literature Cited

- Adamson JK, Scott WA, Rowland AP. 1998. The dynamics of dissolved nitrogen in a blanket peat dominated catchment. *Environmental Pollution* 99:69-77.
- Andry H, Yamamoto T, Irie T, Moritani S, Inoue M, Fujiyama H. 2009. Water retention, hydraulic conductivity of hydrophilic polymers in sandy soil as affected by temperature and water quality. *Journal of Hydrology* 373: 177-183.
- Asano Y, Compton JE, Church MR. 2006. Hydrologic flowpaths influence inorganic and organic nutrient leaching in a forest soil. *Biogeochemistry* 81:191-204.
- Bagarello V, Sferlazza S, Sgroi A. 2009. Comparing two methods of analysis of single-ring infiltrometer data for a sandy-loam soil. *Geoderma* 149: 415-420.
- Bayramin I, Basaran M, Erpul G, Dolarslan M, Canga MR. 2009. Comparison of soil organic carbon content, hydraulic conductivity, and particle size fractions

between a grassland and a nearby black pine plantation of 40 years in two surface depths. *Environmental Geology* 56: 1563-1575.

Bohlen PJ, Pelletier, DM, Groffman, PM, Fahey, TJ, Fisk, MC. 2004. Influence of earthworm invasion on redistribution and retention of soil carbon and nitrogen in northern temperate forests. *Ecosystems* 7: 13-27.

Bormann H, Klaassen K. 2008. Seasonal and land use dependent variability of soil hydraulic and soil hydrological properties of two Northern German soils. *Geoderma* 145: 295-302.

Brenner RE, Boone RD, Jones JB, Lajtha K, Ruess RW. 2006. Successional and physical controls on the retention of nitrogen in an undisturbed boreal forest ecosystem. *Oecologia* 148:602-611.

Buczko U, Bens O, Huttle RF. 2006. Water infiltration and hydrophobicity in forest soils of a pine-beech transformation chronosequence. *Journal of Hydrology* 331:383-395.

Caldwell TG, Young MH, Zhu J, McDonald EV. 2008. Spatial structure of hydraulic properties from canopy to interspace in the Mojave Desert. *Geophysical Research Letters* doi:10.1029/2008GL035095

Chandler KR, Chappell NA. 2008. Influence of individual oak (*Quercus rober*) trees on saturated hydraulic conductivity. *Forest Ecology and Management* 256: 1222-1229.

Currie WS, Aber JD, McDowell WH, Boone RD, Magill AH. 1996. Vertical transport of dissolved organic C and N under long-term N amendments in pine and hardwood forests. *Biogeochemistry* 35:471-505.

- De Schrijver A, Staelens J, Wuyts K, Van Hoydonck G, Janssen N, Mertens J, Gielis L, Geudens G, Augusto L, Verheyen K. 2008. Effect of vegetation type on throughfall deposition and seepage flux. *Environmental Pollution* 153:295-303.
- Dijkstra FA, West JB, Hobbie SE, Trost JB, Reich PB. 2007. Dissolved inorganic and organic N leaching from a grassland field experiment: interactive effects of plant species richness, atmospheric [CO₂] and N fertilization. *Ecology* 88:490-500.
- Dittman JA, Driscoll CT, Groffman PM, Fahey TJ. 2007. Dynamics of nitrogen and dissolved organic carbon at the Hubbard Brook Experimental Forest. *Ecology* 88:1153-1166.
- Fang YT, Gundersen P, Mo JM, Zhu, WX. 2008. Input and output of dissolved organic and inorganic nitrogen in subtropical forests of South China under high air pollution. *Biogeosciences* 5:339-352.
- Fisk MC, Zak DR, Crow TR. 2002. Nitrogen storage and cycling in old- and second-growth northern hardwood forests. *Ecology* 83:73-87.
- Grace, JM III, Skaggs RW, Cassel, DK. 2006. Soil physical changes associated with forest harvesting operations on an organic soil. *Soil Science Society of America Journal* 70:503-509.
- Hagedorn F, Bucher JB, Schleppi P. 2001. Contrasting dynamics of dissolved inorganic and organic nitrogen in soil and surface waters of a forested catchments with Gleysols. *Geoderma* 100:173-192.
- Holloway JM, Dahlgren RA. 2001. Seasonal and even-scale variations in solute chemistry for four Sierra Nevada catchments. *Journal of Hydrology* 250:106-121.

- Hope, GD. 2009. Clearcut harvesting effects on soil and creek inorganic nitrogen in high elevation forests of southern interior British Columbia. *Canadian Journal of Soil Science* 89:35-44.
- Hu W, Shao MA, Wang QJ, Fan J, Reichardt K. Spatial variability of soil hydraulic properties on steep slope in the loess plateau of China. *Scientia Agricola* 65:268-276.
- Huygens D, Boeckx P, Templer P, Paulino L, van Cleemput O, Oyarzun C, Muller C, Godoy R. 2008. Mechanisms for retention of bioavailable nitrogen in volcanic rainforest soils. *Nature Geoscience* 1:543-548.
- Jansson KJ, Johansson J. 1998. Soil changes after traffic with a tracked and a wheeled forest machine: a case study on a silt loam in Sweden. *Forestry* 71:57-66.
- Johnson DW, Susfalk RB, Dahlgren DA, Caldwell TG, Miller WW. 2001. Nutrient fluxes in a snow-dominated, semi-arid forest: Spatial and temporal patterns. *Biogeochemistry* 55:219-245.
- Johnson MS, Lehmann J, Guimaraes Couto E, Novaes Filho JP, Riha SJ. 2006. DOC and DIC in flowpaths of Amazonian headwater catchments with hydrologically contrasting soils. *Biogeochemistry* 81:45-57.
- Jones DL, Willett VB. 2006. Experimental evaluation of methods to quantify dissolved organic nitrogen (DON) and dissolved organic carbon (DOC) in soil. *Soil Biology & Biochemistry* 38:991-999.
- Kaiser K, Guggenberger G. 2005. Storm flow flushing in a structured soil changes the composition of dissolved organic matter leached into the subsoil. *Geoderma* 127:177-187.

- Lajtha K, Seely B, Valiela I. 1995. Retention and leaching losses of atmospherically-derived nitrogen in the aggrading coastal watershed of Waquoit Bay, MA. *Biogeochemistry* 28:33-54.
- Lajtha K, Crow S, Yano Y, Kaushal SS, Sulzman SW, Sollins P, Spears JDH. 2005. Detrital controls on soil solution N and dissolved organic matter in soils: a field experiment. *Biogeochemistry* 76:261-281.
- Li Y, Chen D, White RE, Zhu A, Zhang J. 2007. Estimating soil hydraulic properties of Fengqiu County soils in the North China Plain using pedo-transfer functions. *Geoderma* 138:261-271.
- Lilienfein J, Qualls RG, Uselman SM, Bridgham SD. 2004. Adsorption of dissolved organic carbon and nitrogen in soils of a weathering chronosequence. *Soil Science Society of America Journal* 68:292-305.
- Lilly, A, Nemes A, Rawls WJ, Pachepsky YA. 2008. Probabilistic approach to the identification of input variables to estimate hydraulic conductivity. *Soil Science Society of America Journal* 72:16-24.
- Lohse KA, Matson PA. 2005. Consequences of nitrogen additions for soil processes and soil solution losses from wet tropical forests. *Ecological Applications* 15:1629-1648.
- Lundmark A, Jansson P. 2009. Generic soil descriptions for modelling water and chloride dynamics in the unsaturated zone based on Swedish soils. *Geoderma* 150:85-98.

- Malmer A. 1996. Hydrological effects and nutrient losses of forest plantation establishment on tropical rainforest land in Sabah, Malaysia. *Journal of Hydrology* 174:129-148.
- Manderscheid B, Matzner E. 1995. Spatial and temporal variation of soil solution chemistry and ion fluxes through the soil in a mature Norway Spruce (*Picea abies* (L.) Karst.) stand. *Biogeochemistry* 30:99-114.
- Marques R, and Ranger J. 1997. Nutrient dynamics in a chronosequence of Douglas-fir (*Pseudotsuga menziesii* (Mirb.) Franco) stands on the Beaujolais Mounts (France). 1: Qualitative approach. *Forest Ecology and Management* 91:255-277.
- McLaughlin JW, Phillips SA. 2006. Soil carbon, nitrogen and base cation cycling 17 years after whole tree harvesting in a low-elevation red spruce (*Picea rubens*)-balsam fir (*Abies balsamea*) forested watershed in central Maine, USA. *Forest Ecology and Management* 222:234-253.
- Mitchell MJ, Driscoll CT, Owen JS, Schafer D, Michener R, Raynal DJ. 2001. Nitrogen biogeochemistry of three hardwood ecosystems in the Adirondack region of New York. *Biogeochemistry* 56:93-133.
- Murphy JD, Johnson DW, Miller WW, Walker RF, Blank RR. 2006. Prescribed fire effects on forest floor and soil nutrients in a Sierra Nevada forest. *Soil Science* 171:181-199.
- Neill C, Piccolo MC, Cerri CC, Stedler PA, Melillo JM. 2006. Soil solution nitrogen losses during clearing of lowland Amazon forest for pasture. *Plant and Soil* 281:233-245.

- Neirynck J, Mirtcheva S, Sioen G, Lust N. 2000. Impact of *Tilia platyphyllos* Scop., *Fraxinus excelsior* L., *Acer pseudoplatanus* L., *Quercus robur* L., and *Fagus sylvatica* L. on earthworm biomass and physico-chemical properties of a loamy soil. *Forest Ecology and Management* 133:275-286.
- Park JH, Matzner E. 2003. Controls on the release of dissolved organic carbon and nitrogen from a deciduous forest floor investigated by manipulations of aboveground litter inputs and water flux. *Biogeochemistry* 66:265-286.
- Perkins, DB, Haws NW, Jawitz JW, Das BS, Rao PSC. 2007. Soil hydraulic properties as ecological indicators in forested watersheds impacted by mechanized military training. *Ecological Indicators* 7:589-597.
- Qualls RG, Richardson CJ. 2003. Factors controlling concentration, export, and decomposition of dissolved organic nutrients in the Everglades of Florida. *Biogeochemistry* 62:197-229.
- Ramos MC, Cots-Folch R, Martinez-Casanovas JA. 2007. Effects of land terracing on soil properties in the Priorat region in northeastern Spain: A multivariate analysis. *Geoderma* 142:251-261.
- Rothe A, Huber C, Kreutzer K, Weis W. 2002. Deposition and soil leaching in stands of Norway spruce and European Beech: Results from the Hogwald research in comparison with other European case studies. *Plant and Soil* 240:33-45.
- Santra P, Das BS. 2008. Pedotransfer functions for soil hydraulic properties developed from a hilly watershed of Eastern India. *Geoderma* 146: 439-448.
- Schack-Kirchner H, Fenner PT, Hildebrand EE. 2007. Different responses in bulk density and saturated hydraulic conductivity to soil deformation by logging

machinery on a Ferralsol under native forest. *Soil Use and Management* 23:286-293.

Schroth G, Seixas R, Da Silva LF, Teixeira WG, Zech W. 2000. Nutrient Concentrations and acidity in ferralitic soil under perennial cropping, fallow and primary forest in central Amazonia. *European Journal of Soil Science* 51:219-231.

Schrumpf, M, Zech W, Lehmann J, Lyaruu HVC. 2006. TOC, TON, TOS and TOP in rainfall, throughfall, litter percolate and soil solution of a montane rainforest succession at Mt. Kilimanjaro, Tanzania. *Biogeochemistry* 78:361-387.

Schwendenmann L, Veldkamp E. 2005. The role of dissolved organic carbon, dissolved organic nitrogen and dissolved inorganic nitrogen in a tropical wet forest ecosystem. *Ecosystems* 8:339-351.

Sheridan GJ, Lane PNJ, Noske PJ. 2007. Quantification of hillslope runoff and erosion processes before and after wildfire in a wet *Eucalyptus* forest. *Journal of Hydrology* 343:12-48.

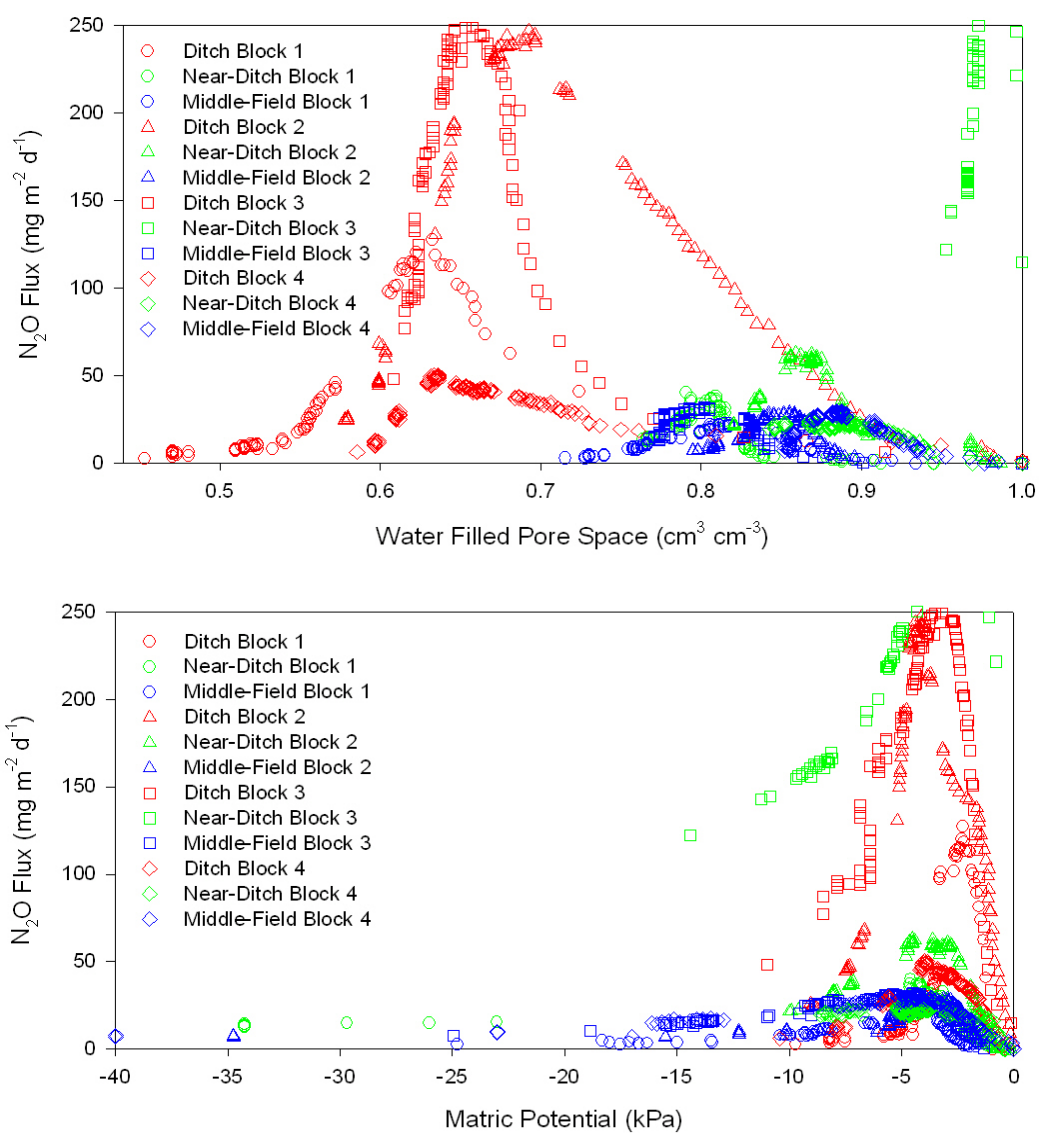
Silva RG, Holub SM, Jorgensen EE, Ashanuzzaman ANM. 2005. Indicators of nitrate leaching loss under different land use of clayey and sandy soils in southeastern Oklahoma. *Agriculture, Ecosystems and Environment* 109:346-359.

Strahm BD, Harrison RB, Terry TA, Flaming BL, Licata CW, Petersen KS. 2005. Soil solution nitrogen concentrations and leaching rates as influenced by organic matter retention on a highly productive Douglas-fir site. *Forest Ecology and Management* 218:74-88.

- Verbist K, Batens J, Cornelis WM, Gabriels D, Torres C, Soto G. 2009. Hydraulic conductivity as influenced by stoniness in degraded drylands of Chile. *Soil Science Society of America Journal* 73:471-484.
- Xu YJ, Burger JA, Aust WM, Patterson SC, Miwa M, Preston DP. 2002. Changes in surface water table depth and soil physical properties after harvest and establishment of loblolly pine (*Pinus taeda* L.) in Atlantic coastal plain wetlands of South Carolina. *Soil & Tillage Research* 63:109-121.
- Young MH, McDonald EV, Caldwell TG, Benner SG, Meadows DG. 2004. Hydraulic properties of a desert soil chronosequence in the Mojave Desert, USA. *Vadose Zone Journal* 3:956-953.
- Zak DR, Pregitzer KS, Holmes WE, Burton AJ, Zogg GP. 2004. Anthropogenic N deposition and the fate of $^{15}\text{NO}_3^-$ in a northern hardwood ecosystem. *Biogeochemistry* 69:143-157.
- Ziegler AD, Negishi JN, Sidle RC, Noguchi S, Nik, AR. 2006. Impacts of logging disturbance on hillslope saturated hydraulic conductivity in a tropical forest in Peninsular Malaysia. *Catena* 67:89-104.

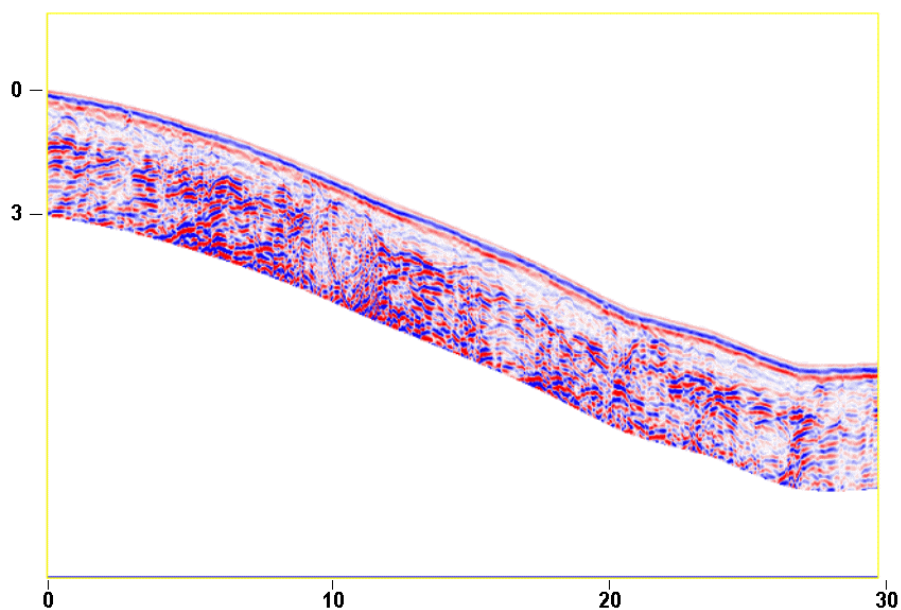
Appendix B

Nitrous oxide flux as a function of water filled pore space and matric potential for all 12 replicate soil columns. Note the x-axes encompass the full range of recorded WFPS and matric potential during the 96h experiment.

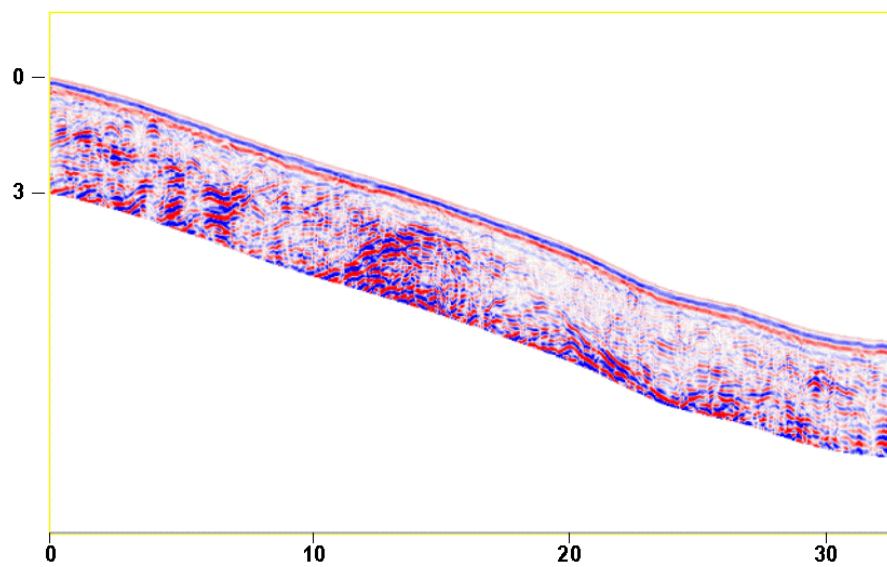


Appendix C

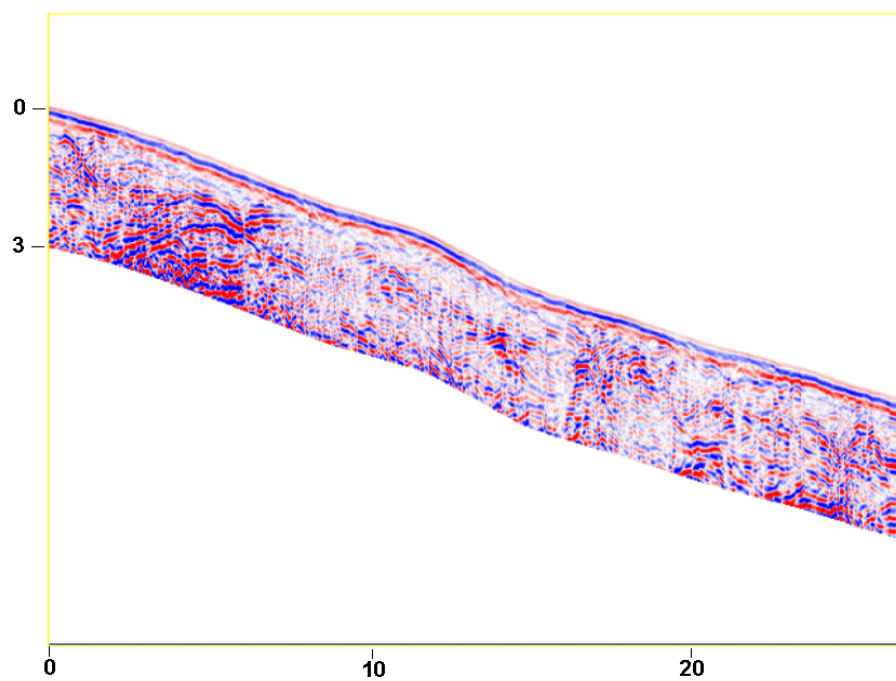
Ground penetrating radar (GPR) images collected for seven of the eight transects depicted in Figure 4-3. The third transect from the North in Figure 4-3 was omitted due to its steep slope. All remaining seven transects are ordered below from North to South (see Fig 4-3). The x and y axes display vertical depth and horizontal distance, respectively, in meters. The increase in color intensity at $\approx 1\text{m}$ corresponds to a density change that is coincident with the presence of a lithified paleosol. The blue and red banding at the soil surface indicate changes in density associated with the GPR-air interface and the air-soil surface interface. Images were corrected to display actual slope.



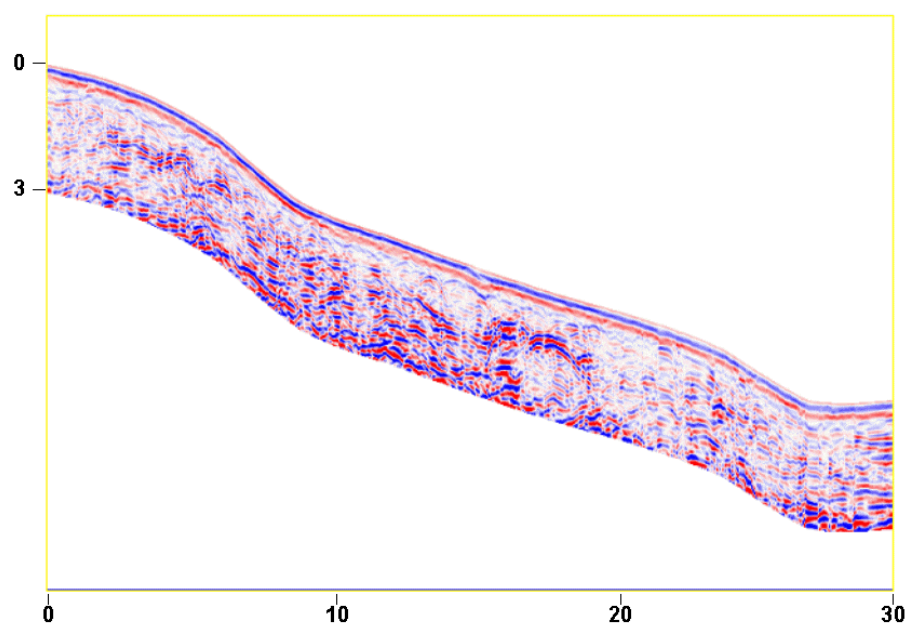
Above: Transect 1. Axis units are in meters. Image was corrected to true slope.



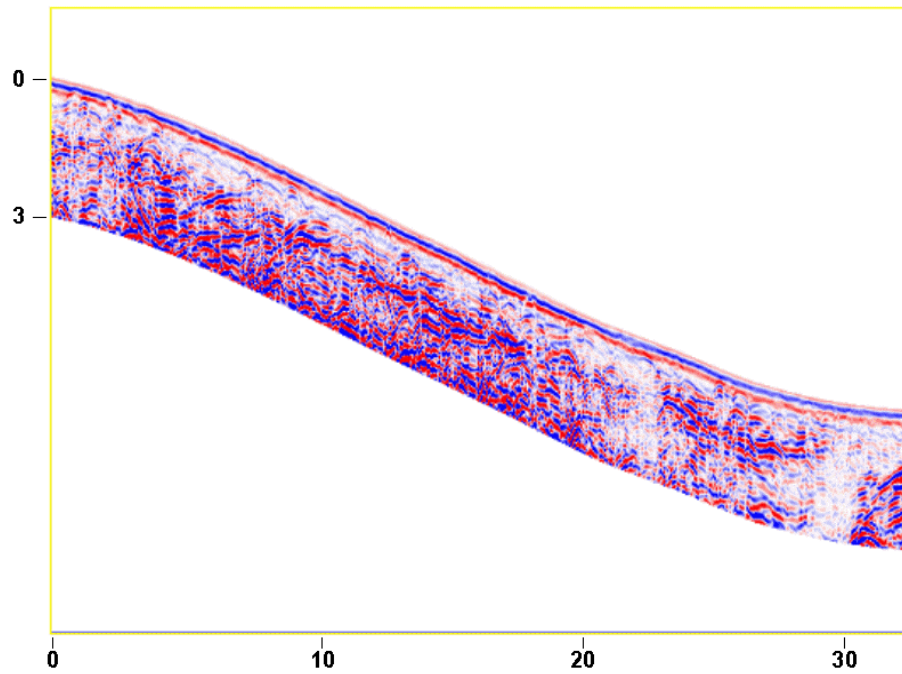
Above: Transect 2. Axis units are in meters. Image was corrected to true slope.



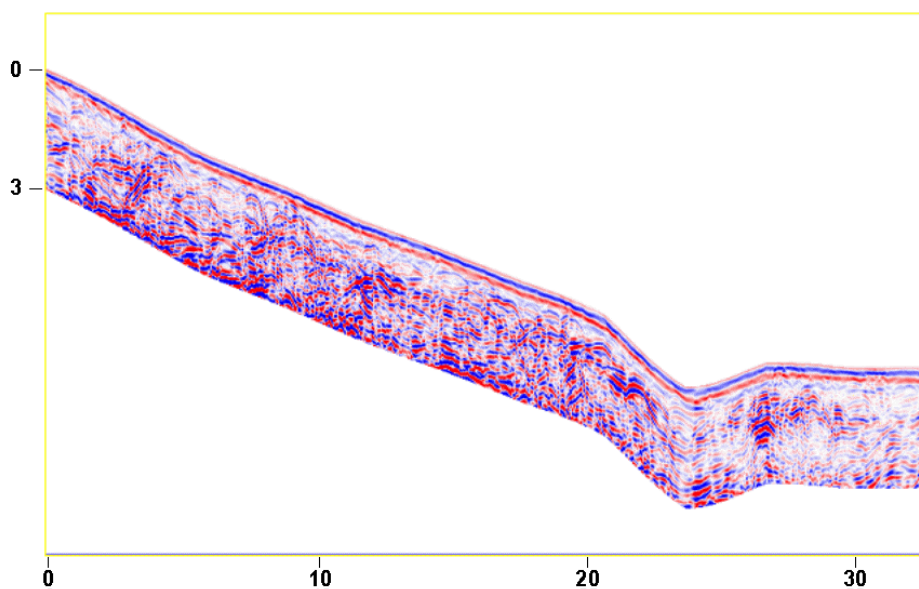
Above: Transect 4. Axis units are in meters. Image was corrected to true slope.



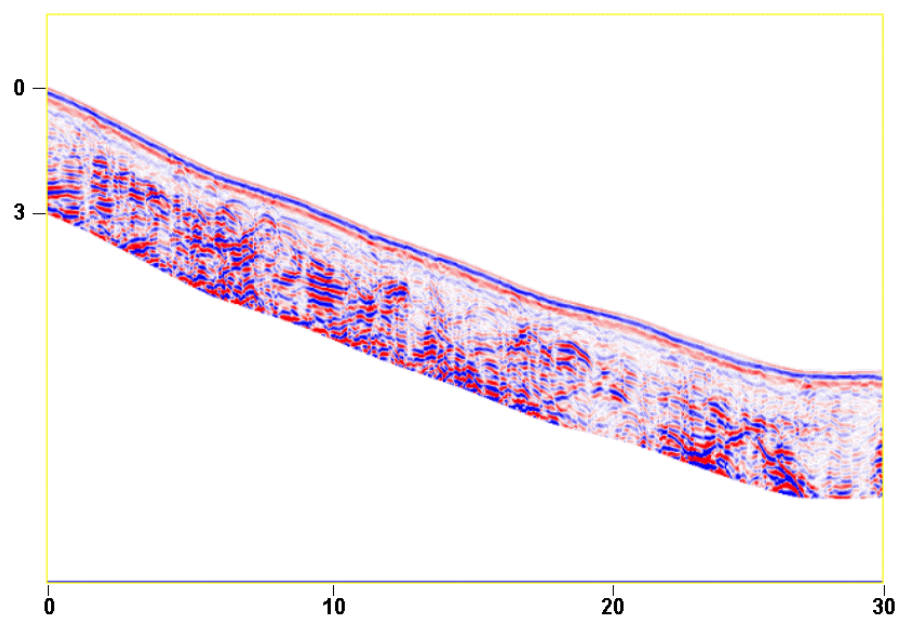
Above: Transect 5. Axis units are in meters. Image was corrected to true slope.



Above: Transect 6. Axis units are in meters. Image was corrected to true slope.



Above: Transect 7. Axis units are in meters. Image was corrected to true slope.



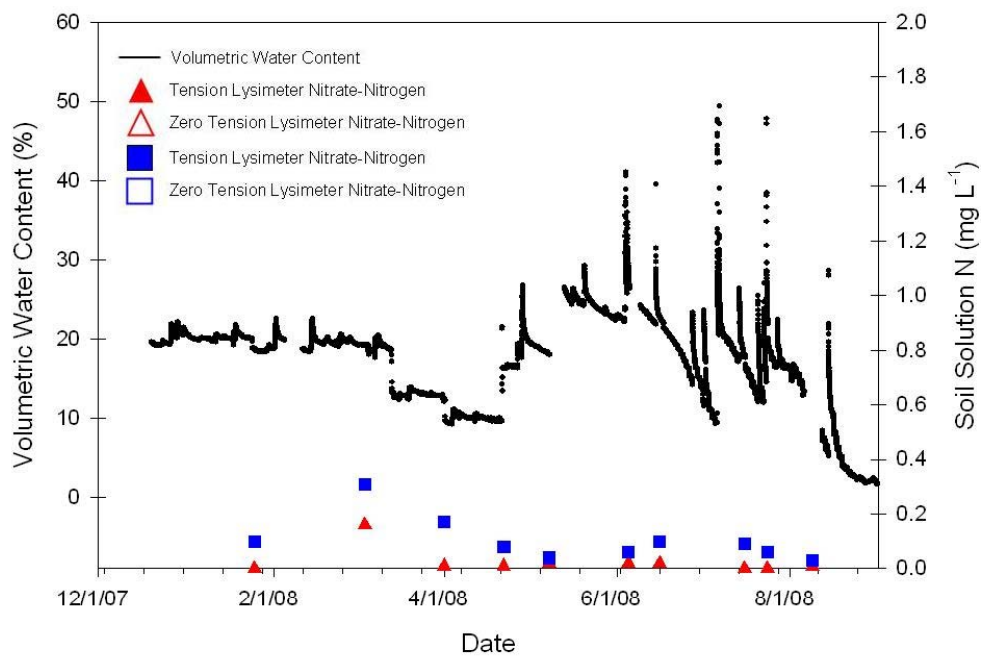
Above: Transect 8. Axis units are in meters. Image was corrected to true slope.

Appendix D

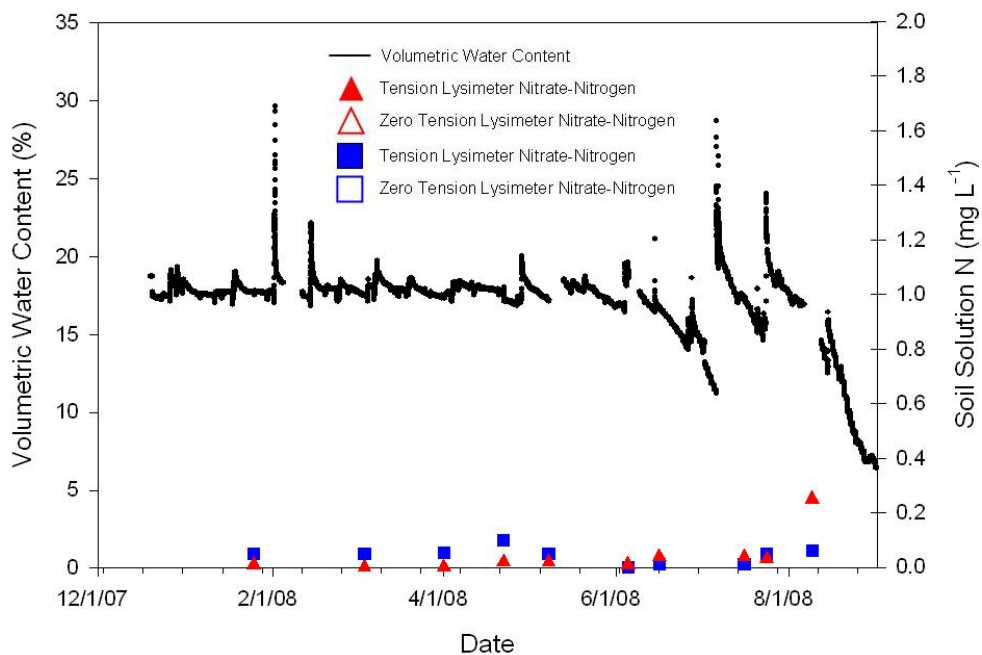
Volumetric water content and soil solution ammonium-nitrogen and nitrate-nitrogen concentrations in the bottom of the A soil horizon and B horizon. All 22 A horizon and 22 B horizon sample locations are displayed. Note that B horizon volumetric water content was obtained at 60 cm below the soil surface and B horizon soil solution was collected at ≈ 100 cm below the soil surface. Volumetric water content is indicated by the black line. Solid red triangles indicate tension lysimeter nitrate-nitrogen concentrations. Solid blue squares indicate tension lysimeter ammonium-nitrogen concentrations. Open red triangles indicate zero tension lysimeter nitrate-nitrogen concentrations. Open blue squares indicate zero tension lysimeter ammonium-nitrogen concentrations. See Table 4-1 for corresponding soil properties at each sample location.

Transect 1, Ridgetop 2008

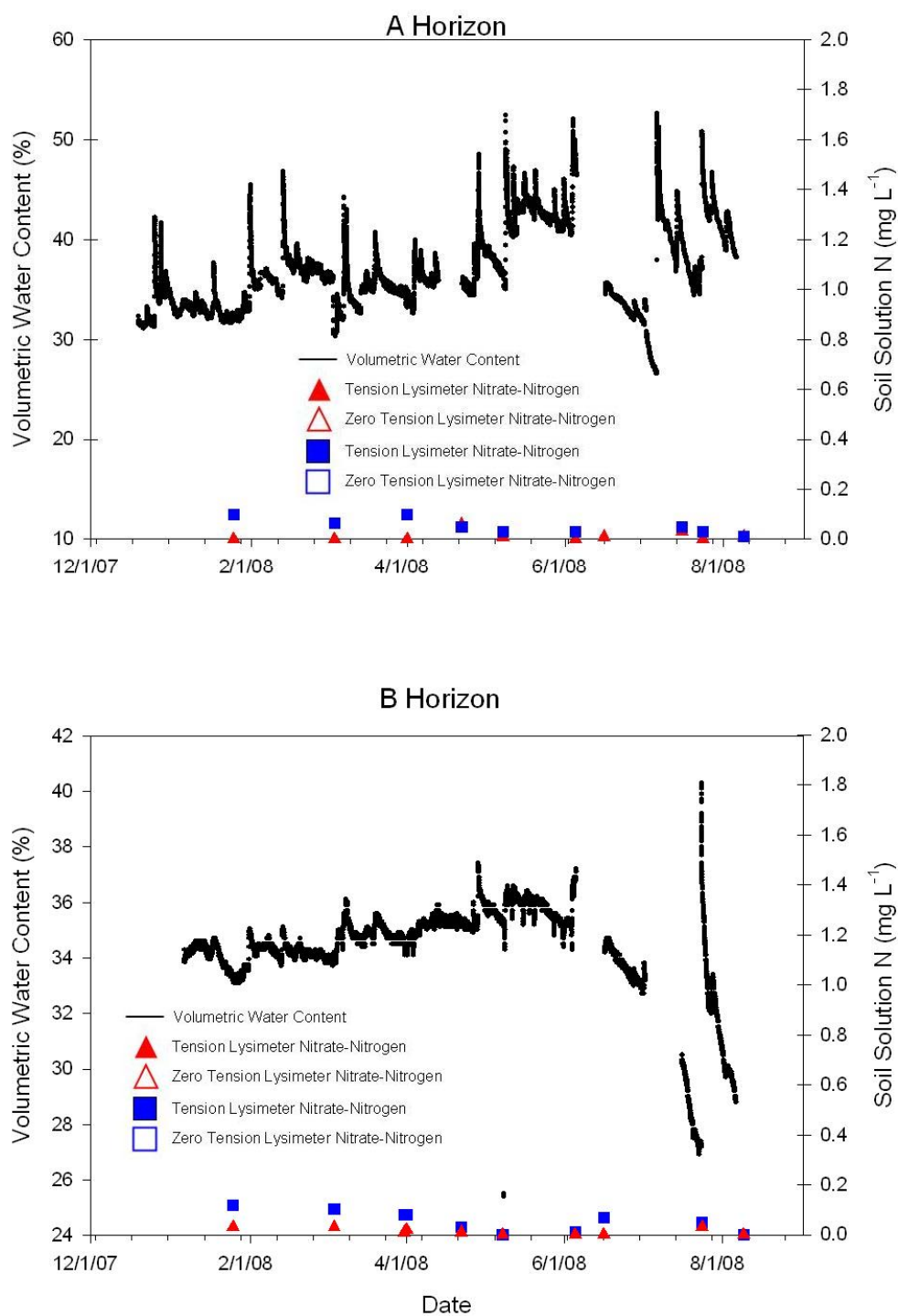
A Horizon



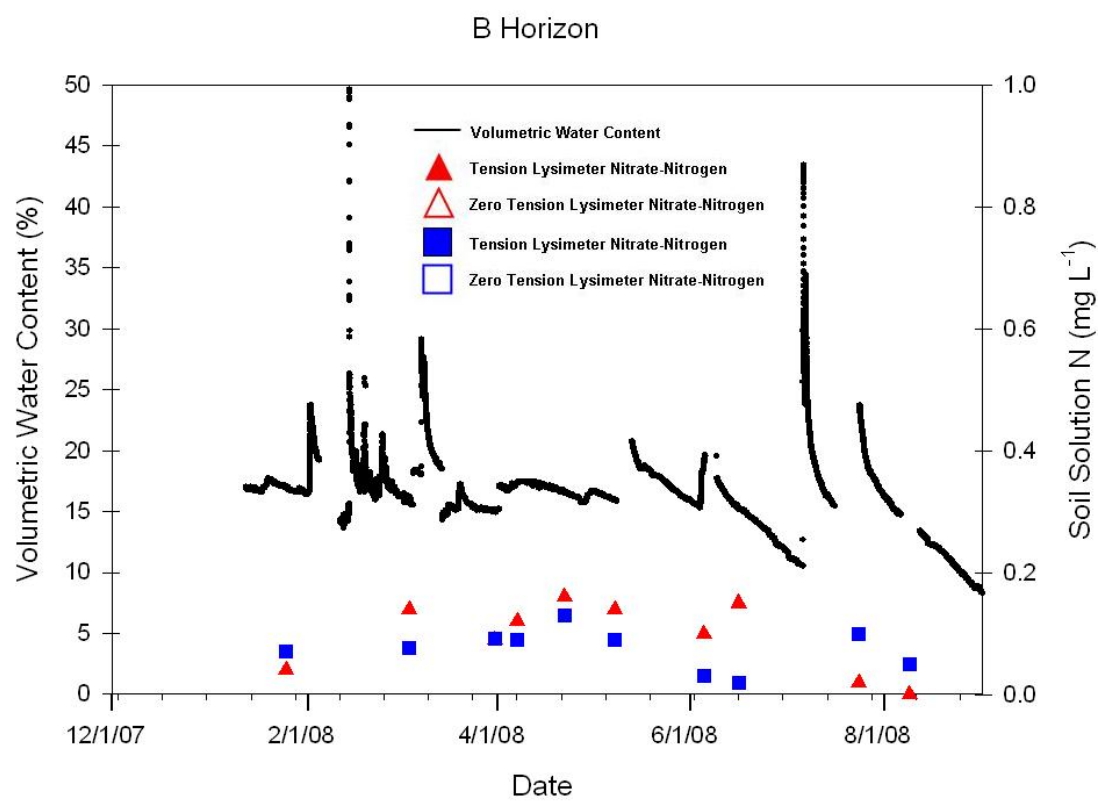
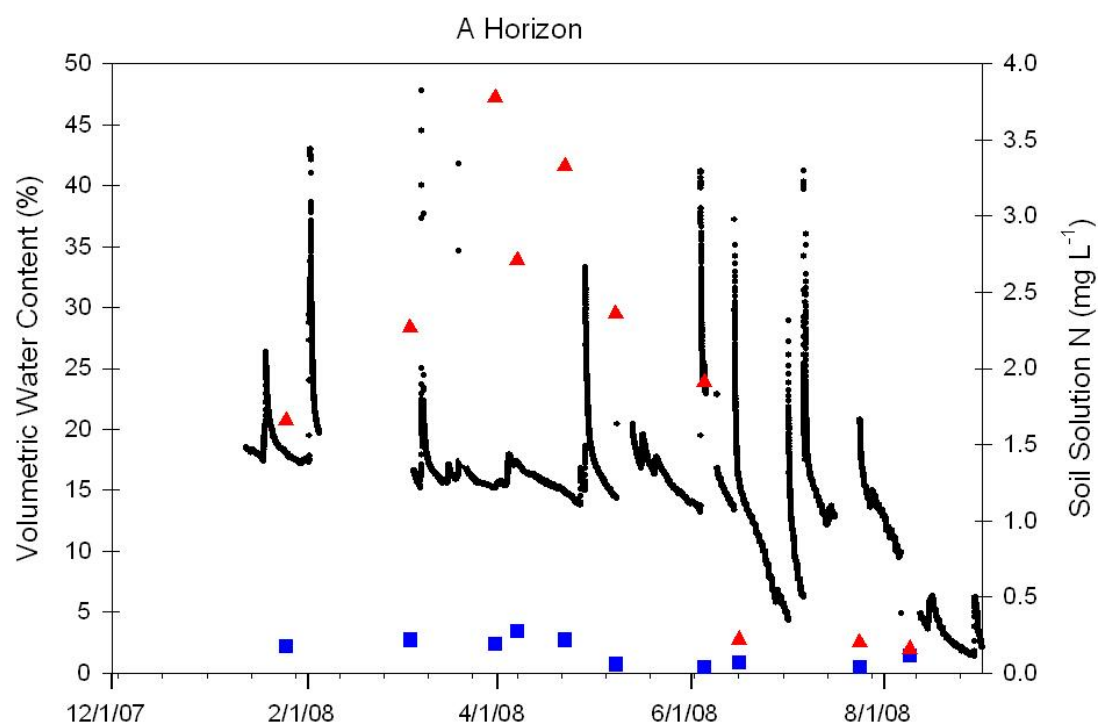
B Horizon



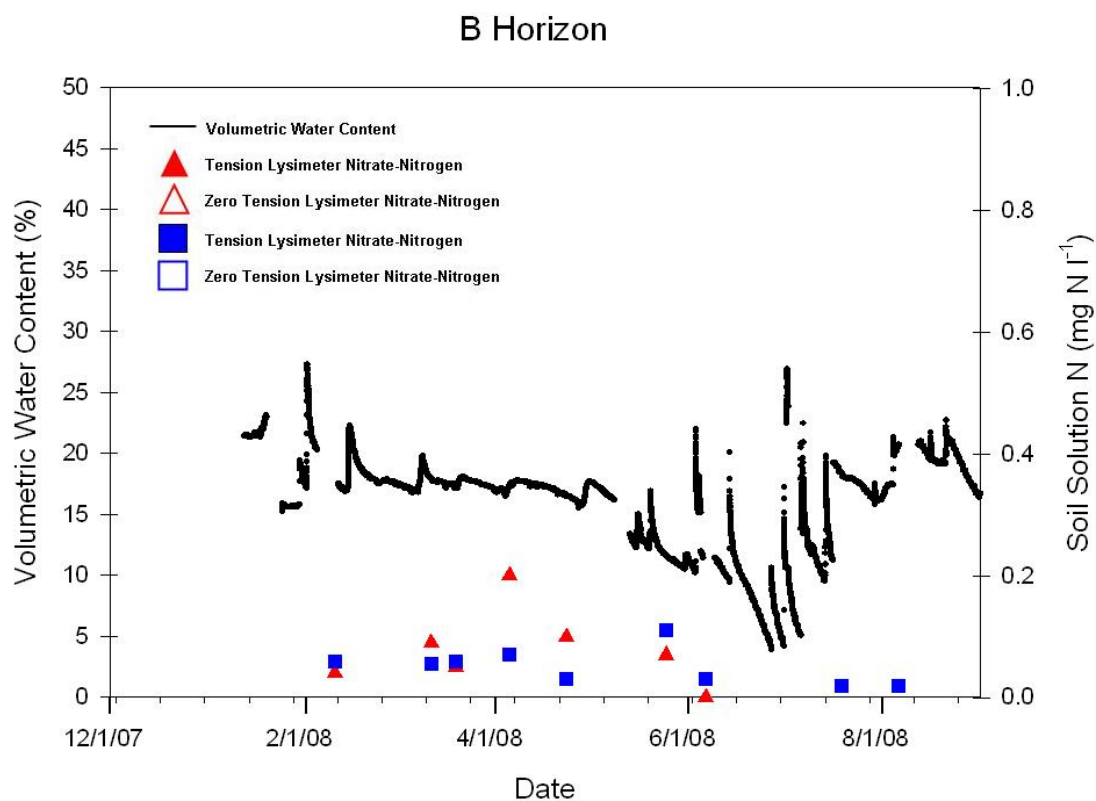
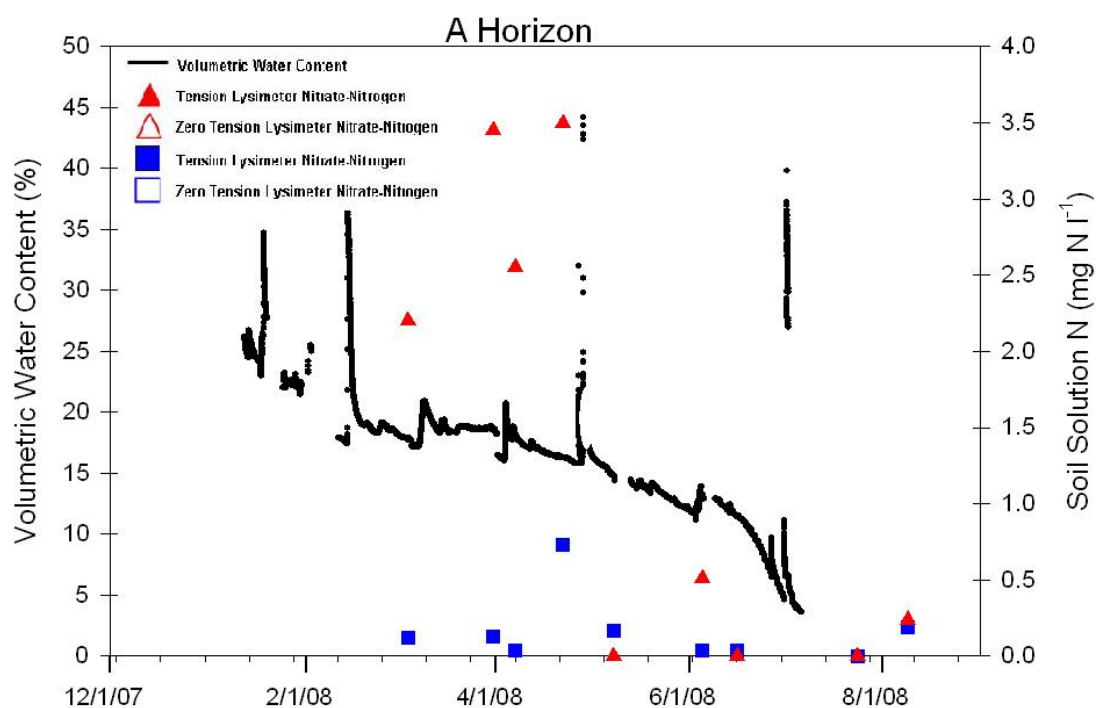
Transect 4, Ridgetop 2008



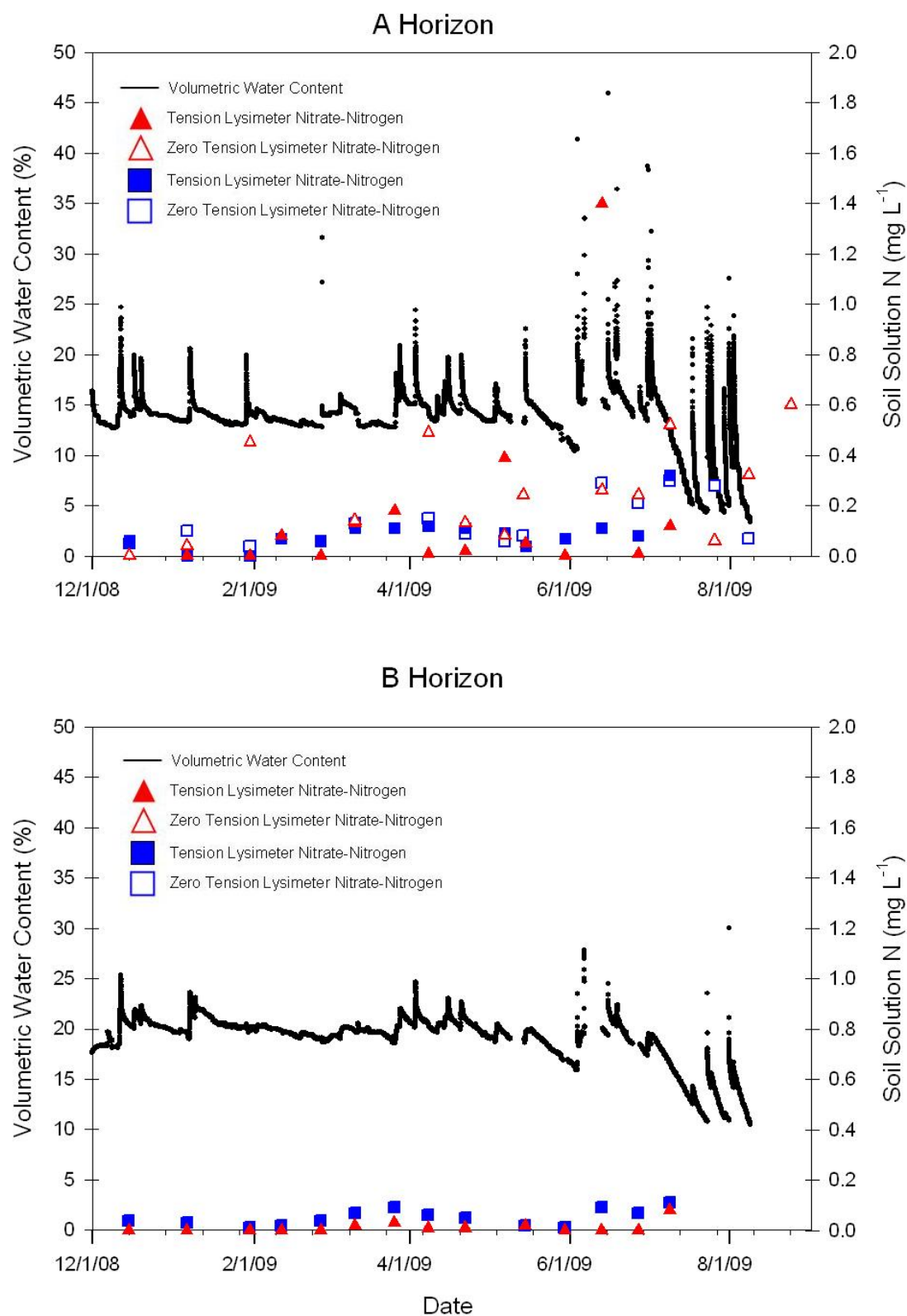
Transect 6, Ridgetop 2008



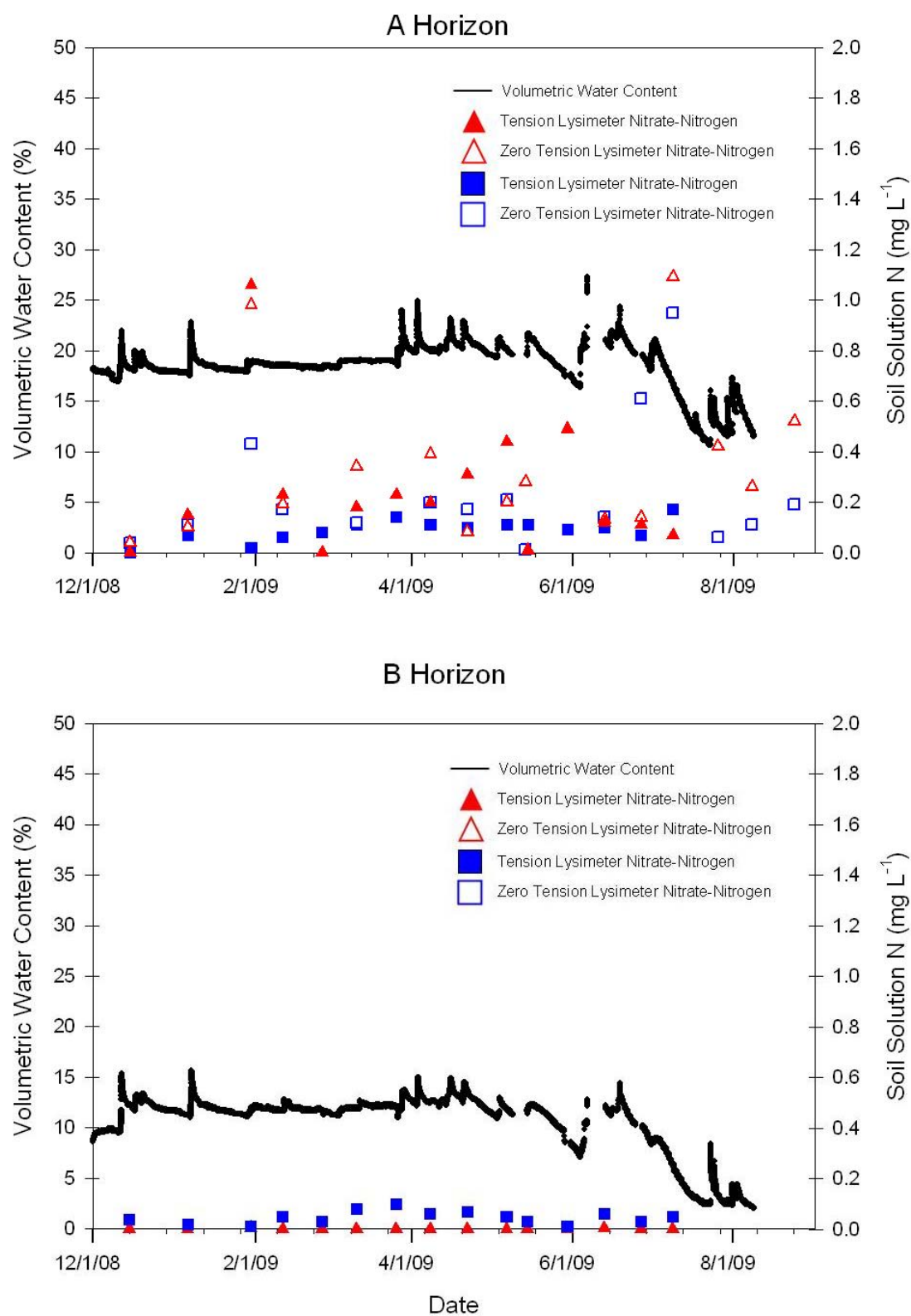
Transect 7, Ridgetop 2008



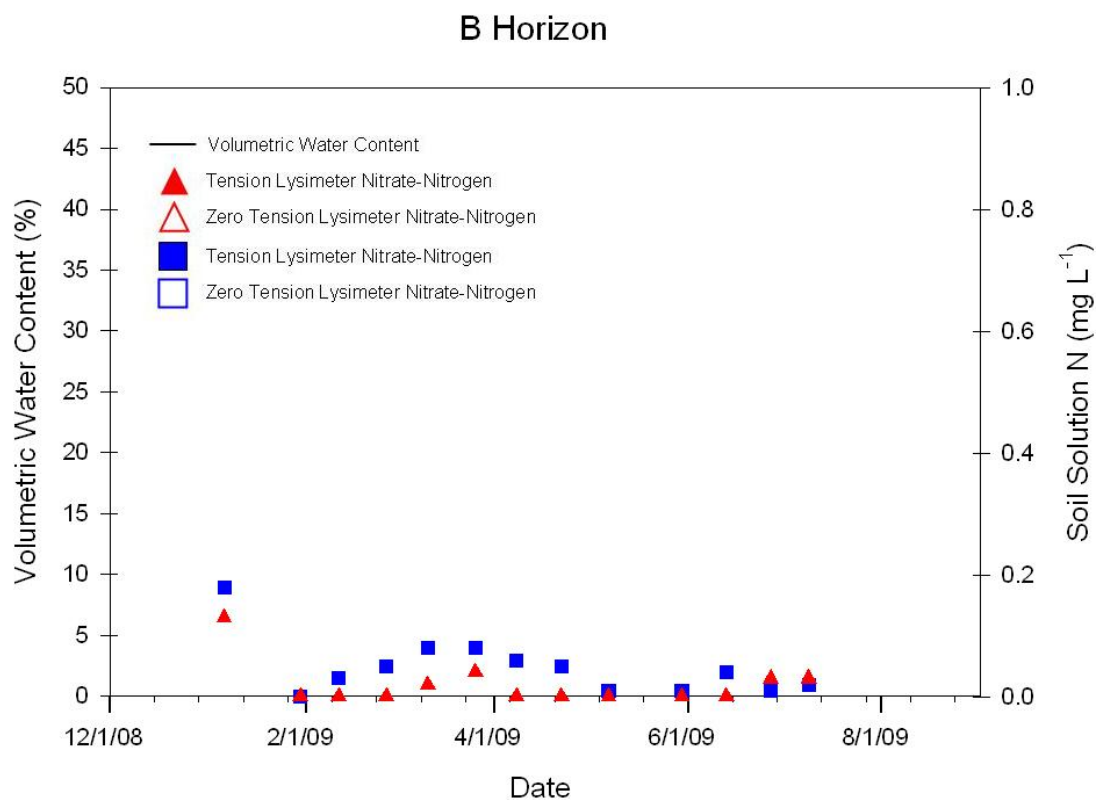
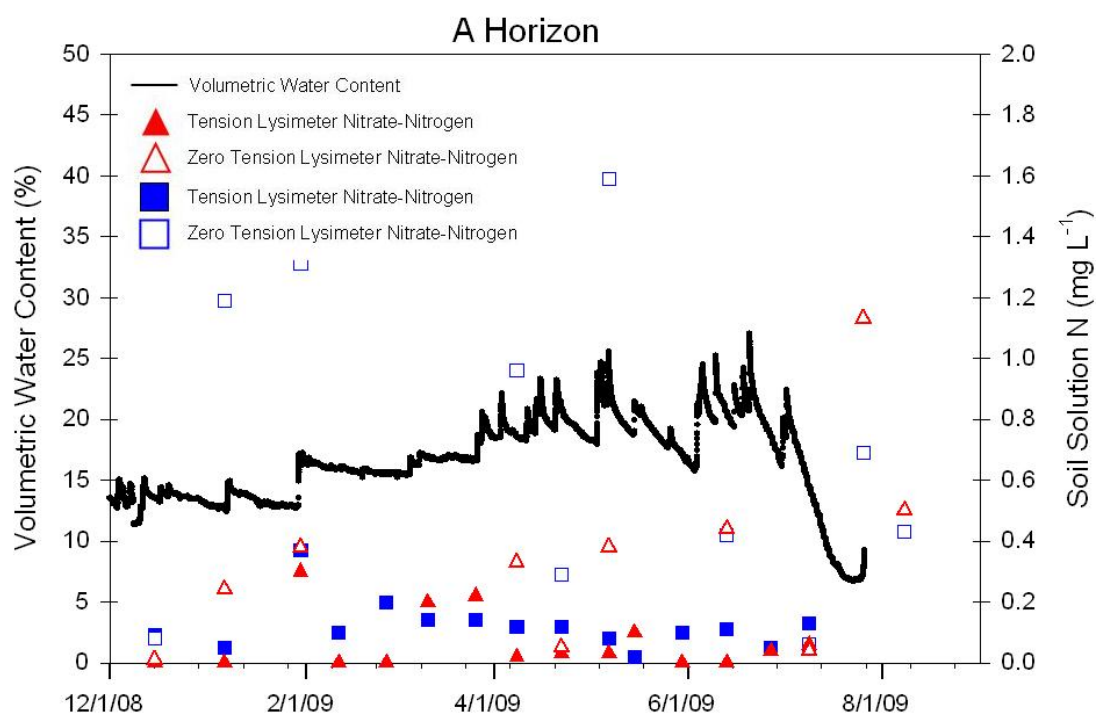
Transect 1, Ridgetop 2009



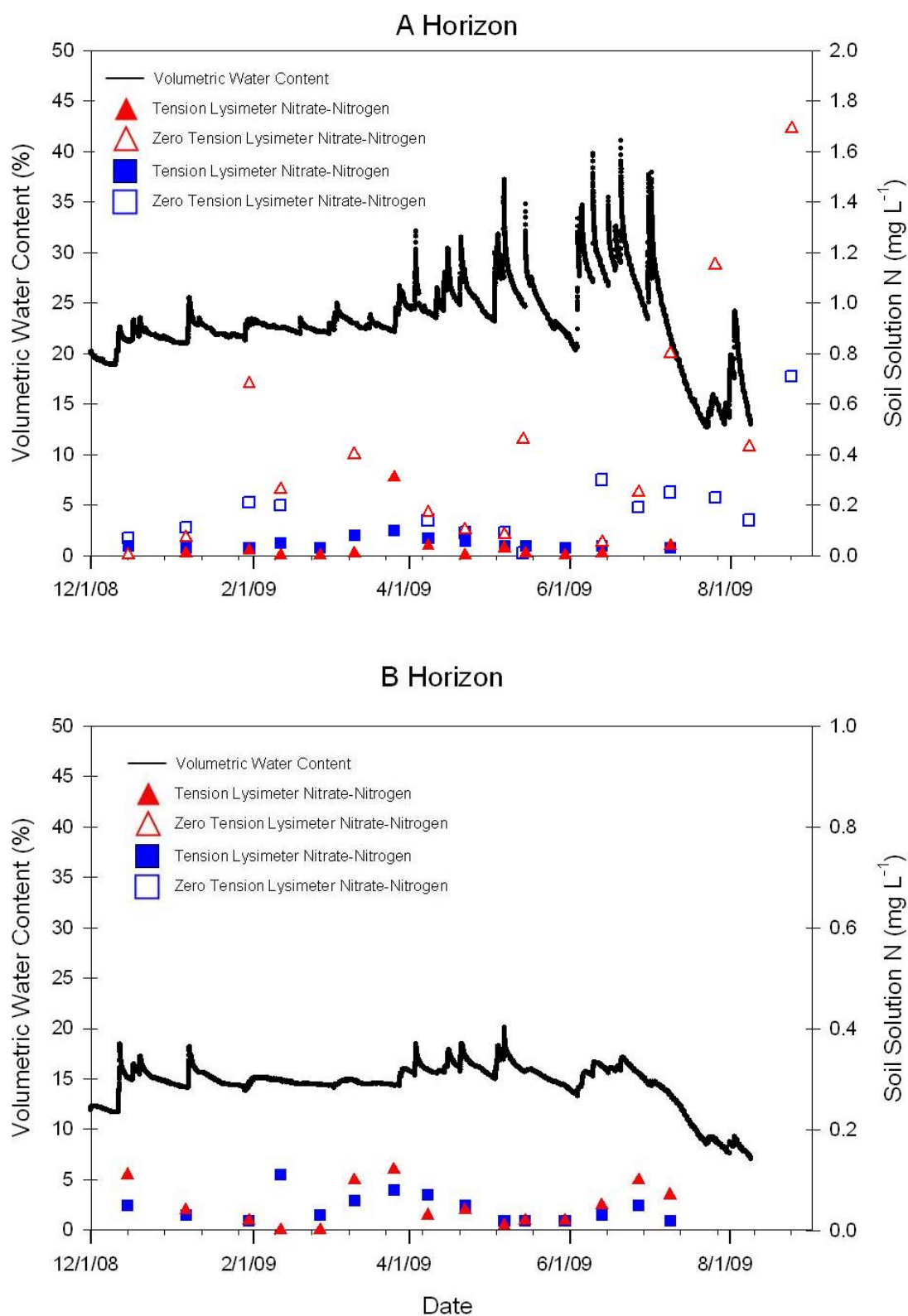
Transect 1, Hillslope 2009



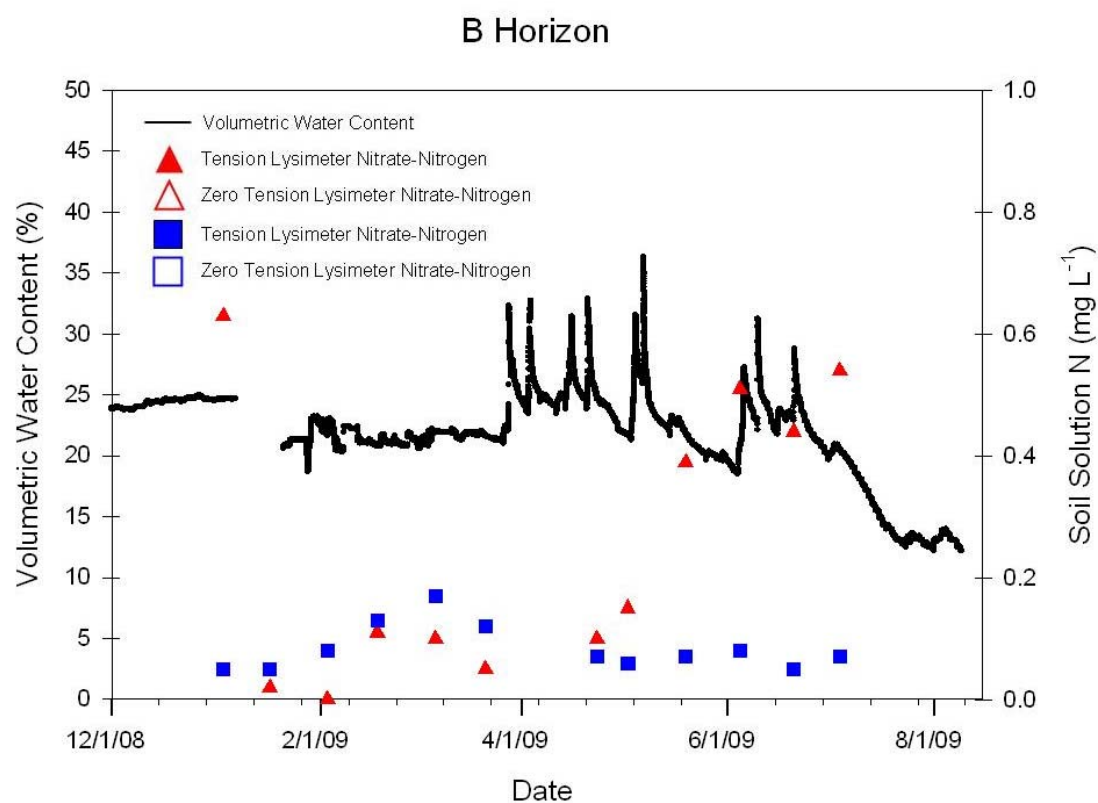
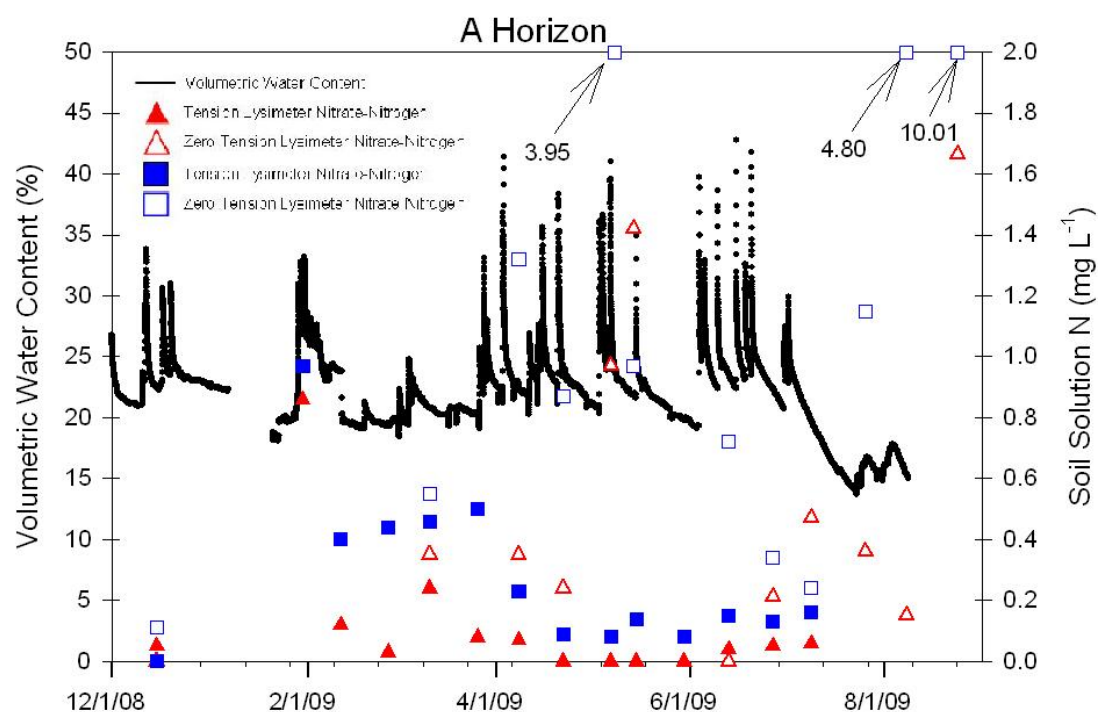
Transect 2, Ridgetop 2009



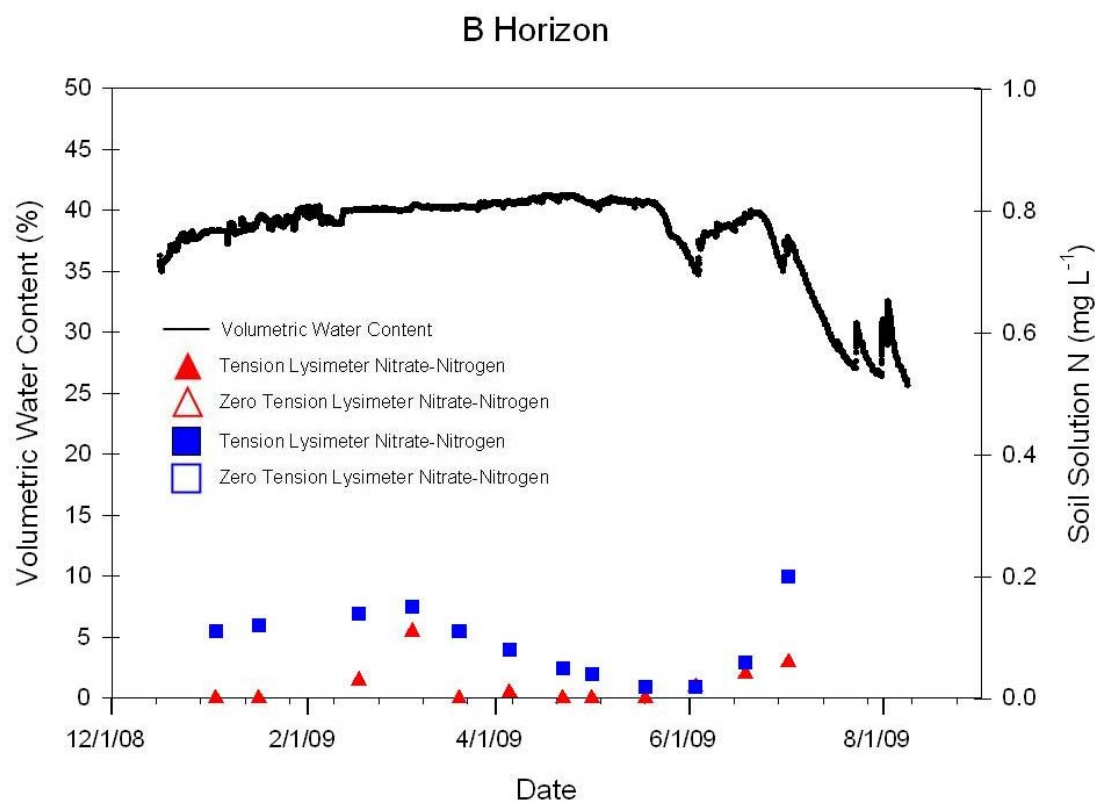
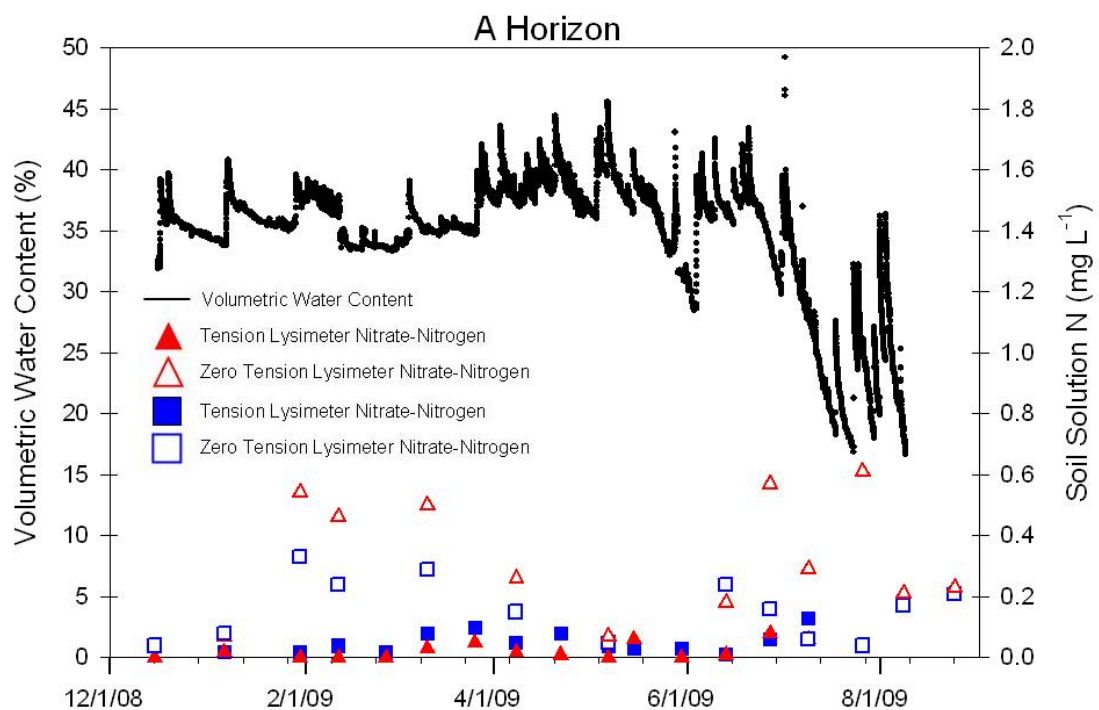
Transect 2, Hillslope 2009



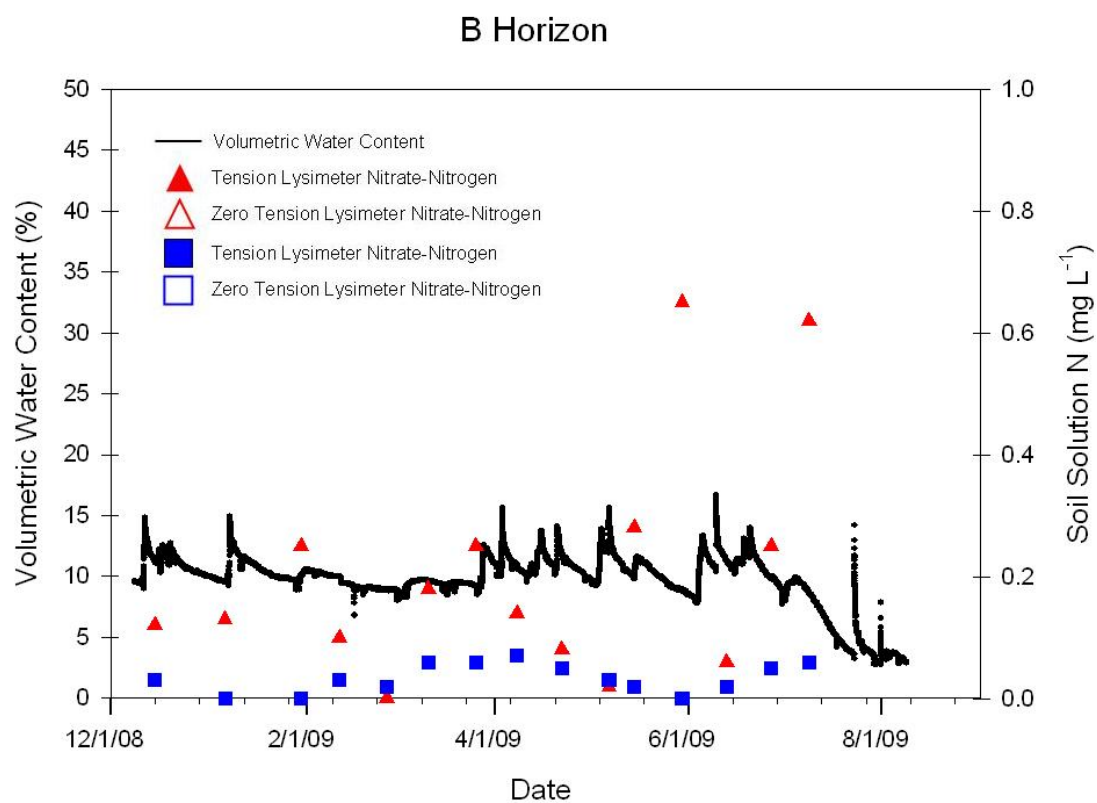
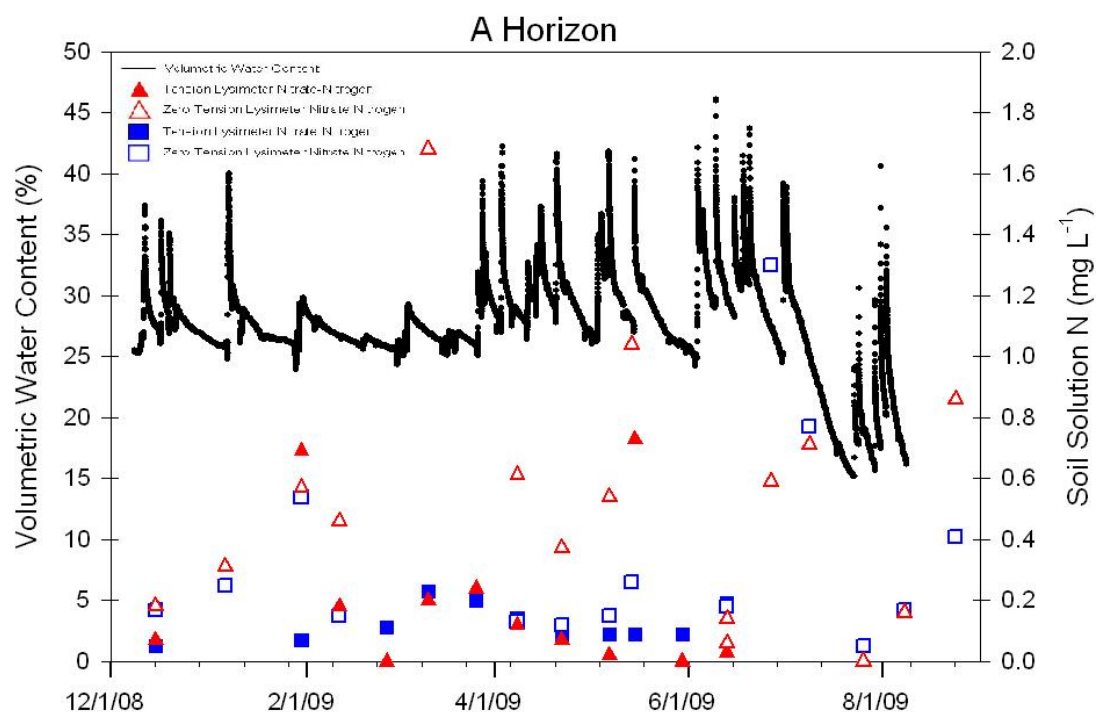
Transect 2, Toeslope 2009



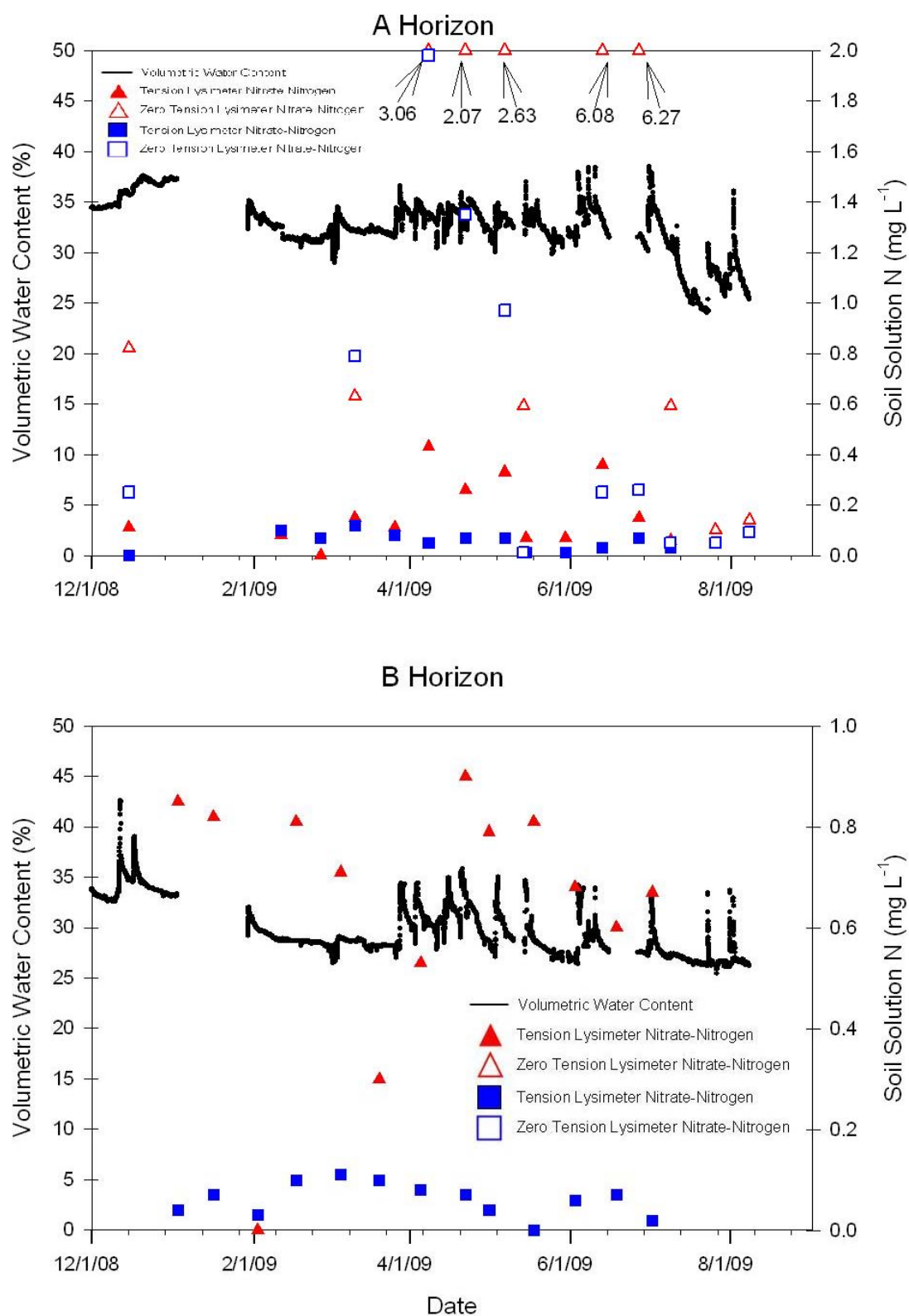
Transect 3, Ridgetop 2009



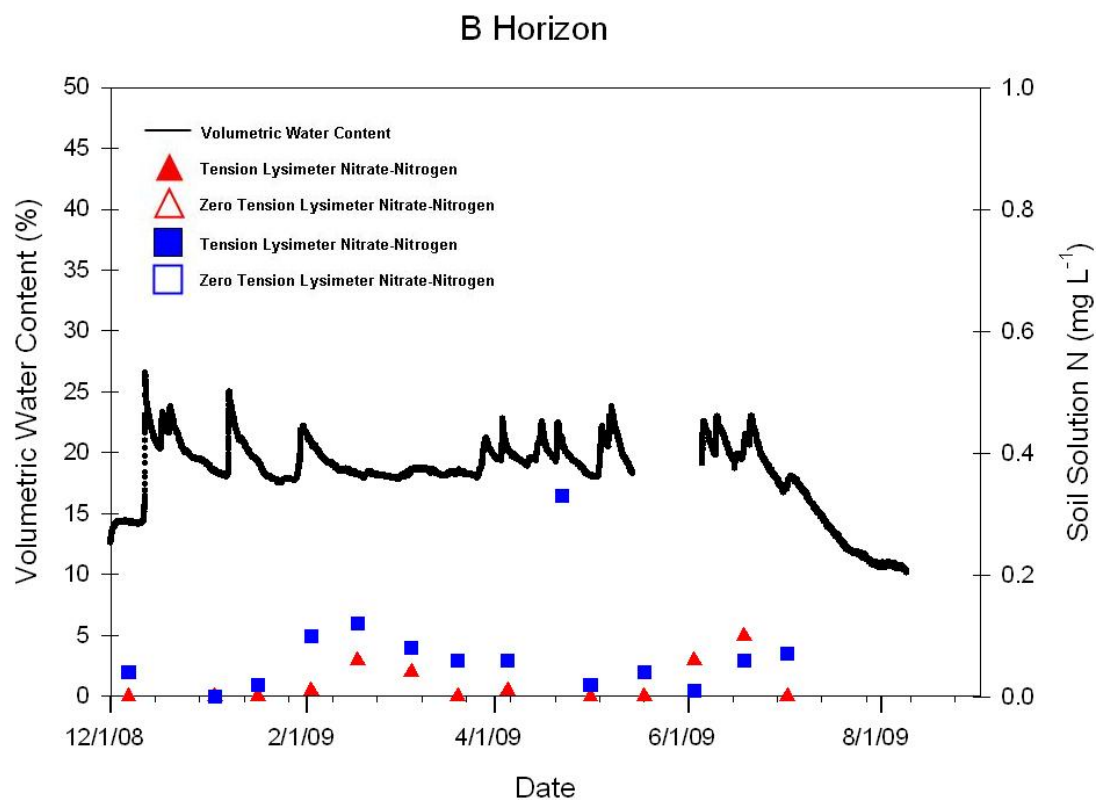
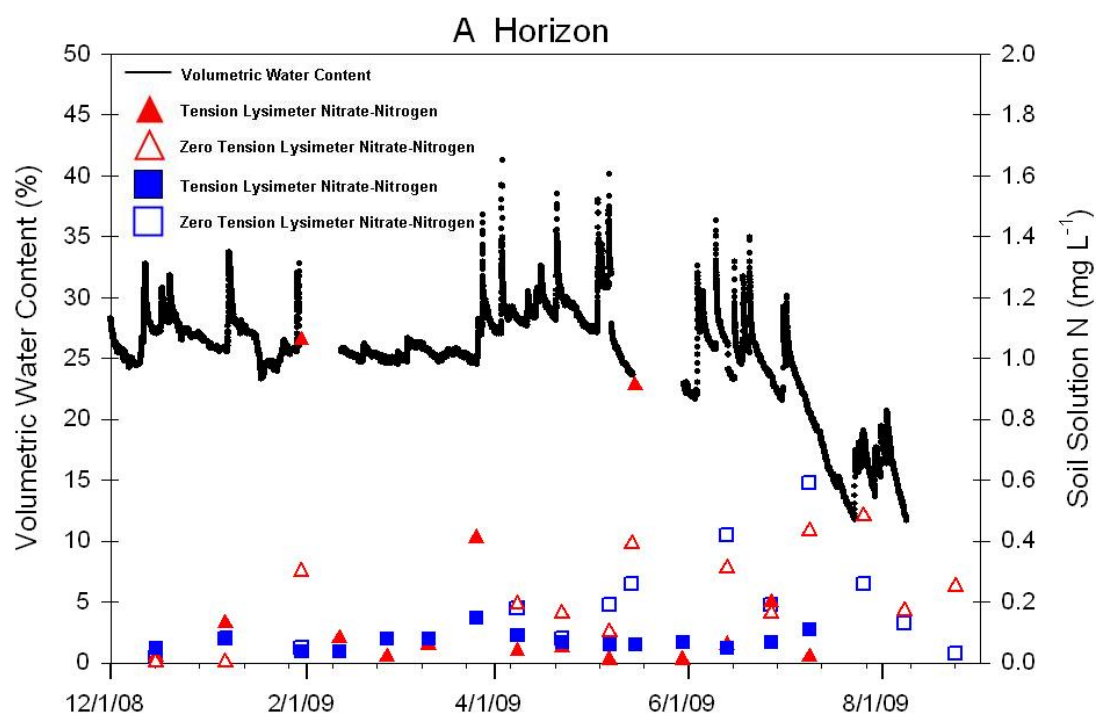
Transect 3, Hillslope 2009



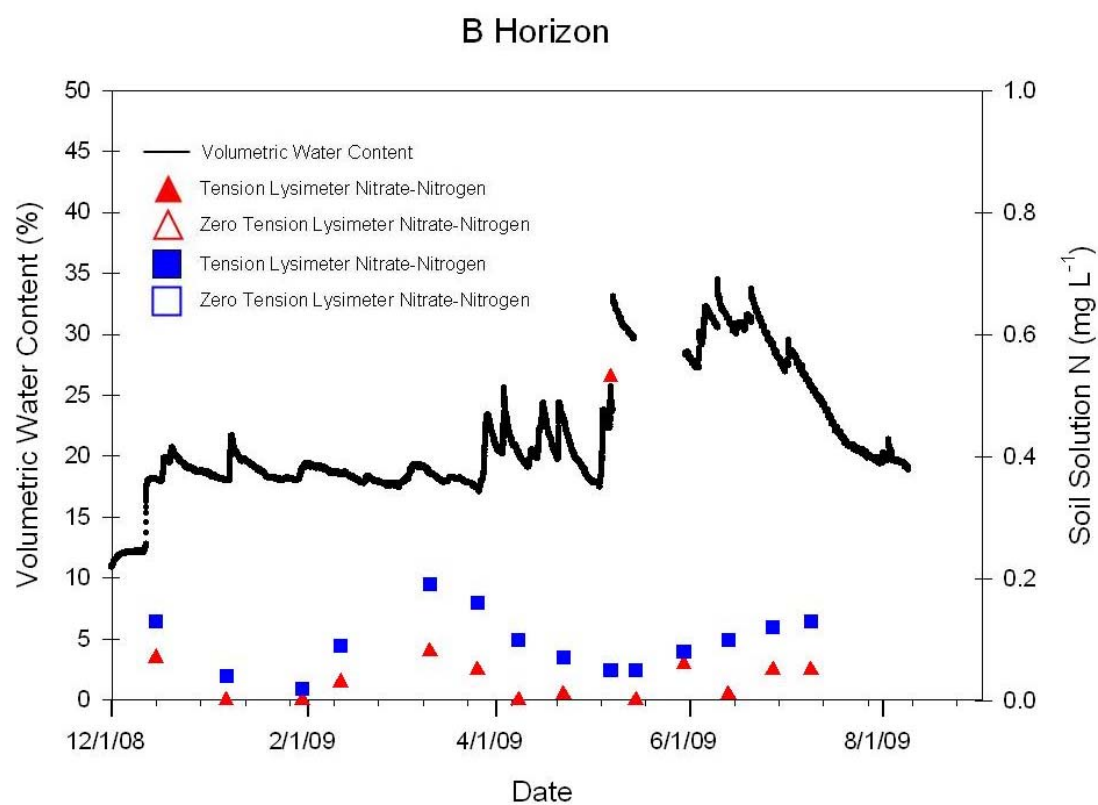
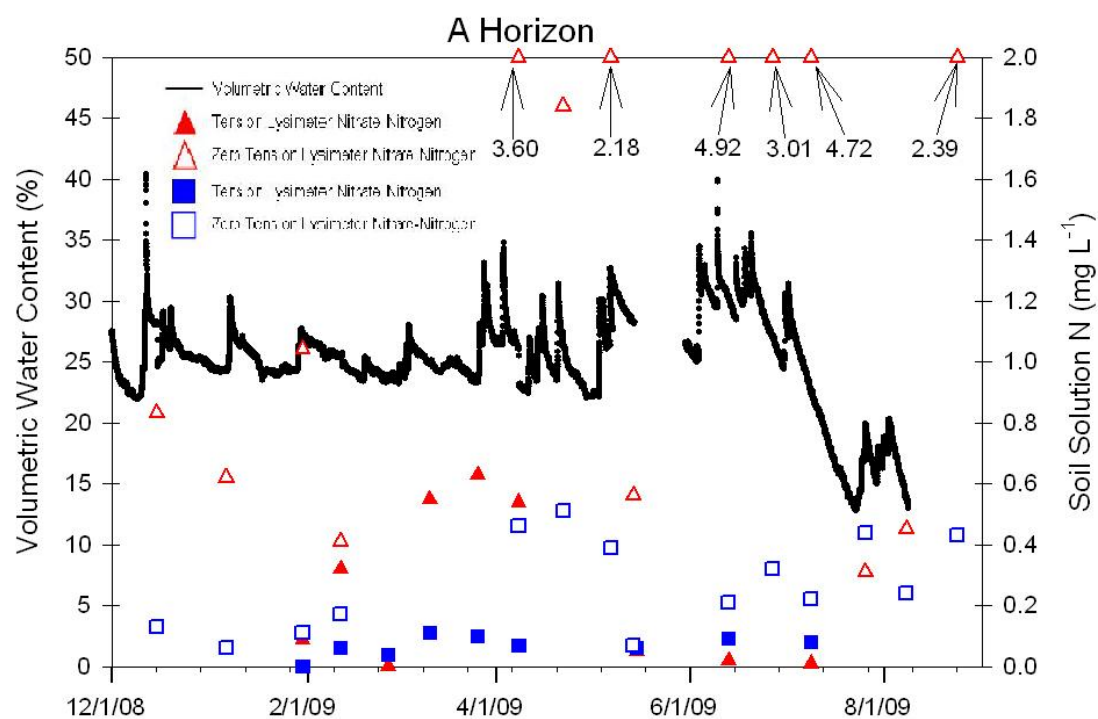
Transect 3, Toeslope 2009



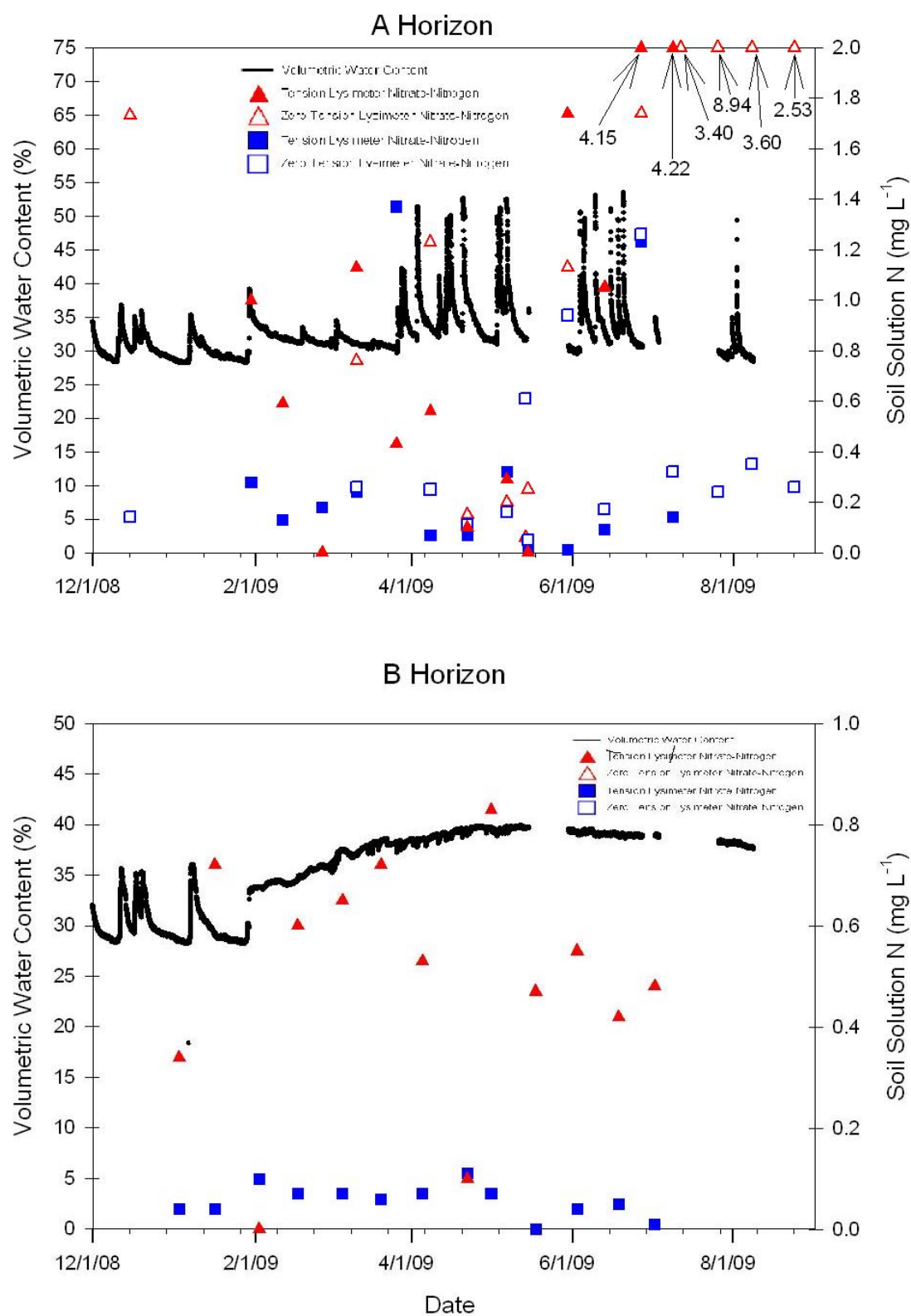
Transect 4, Ridgetop 2009



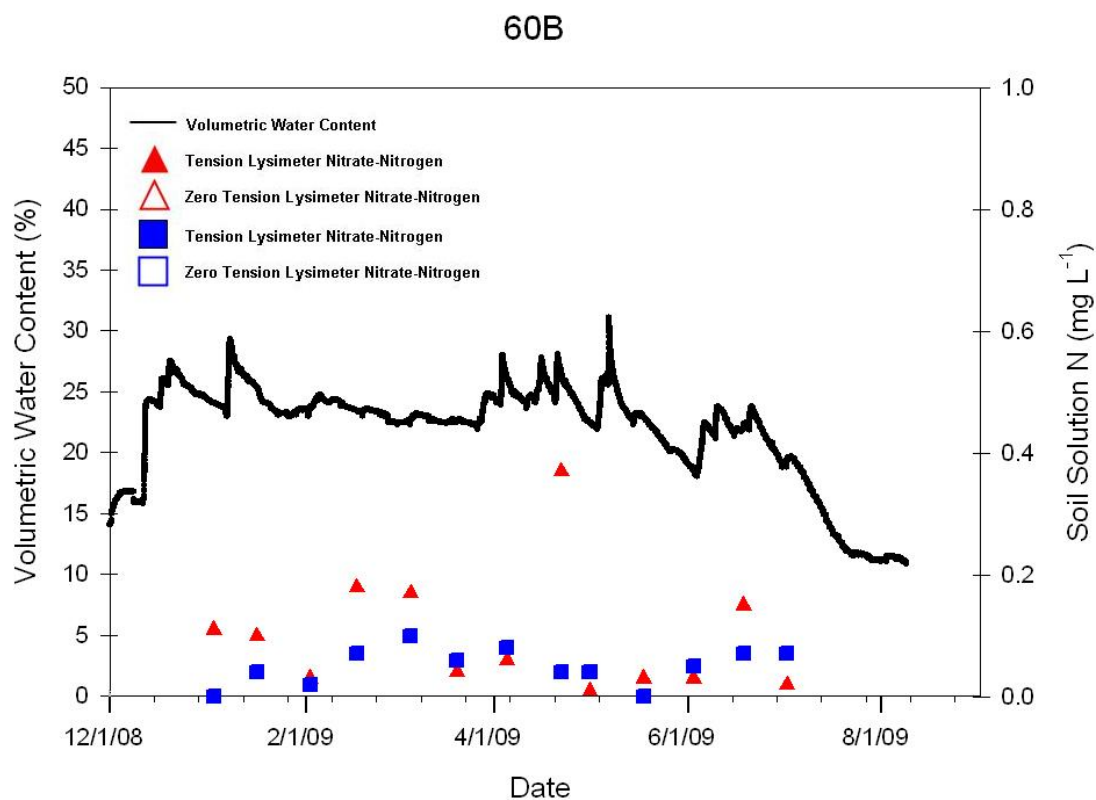
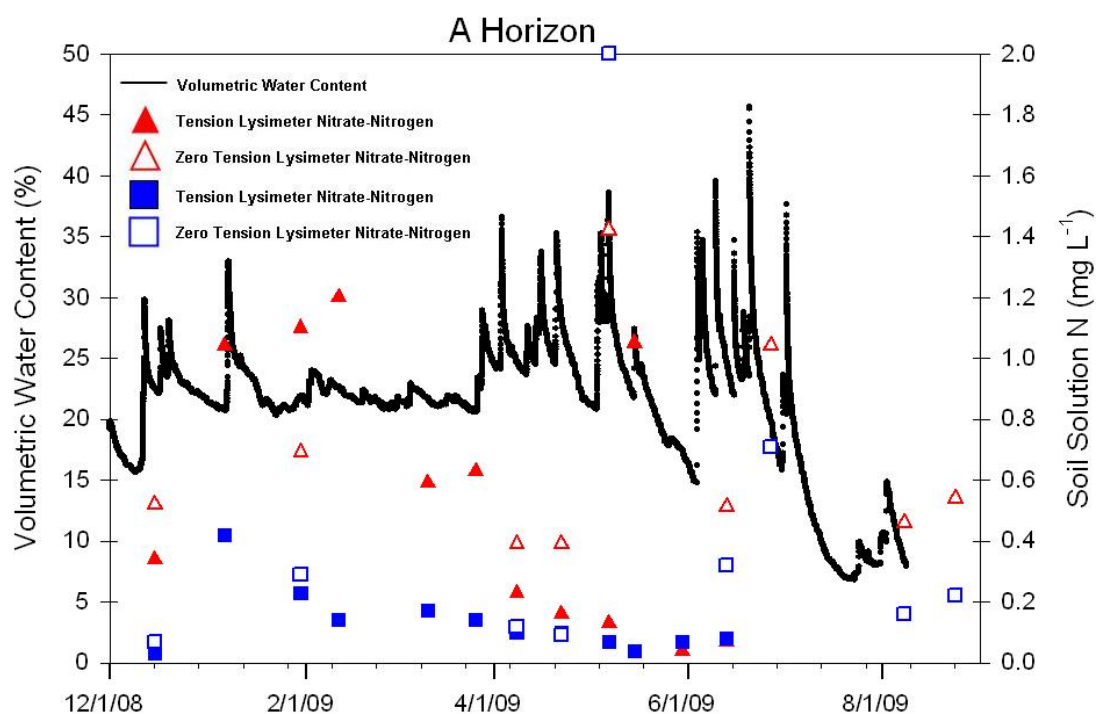
Transect 4, Hillslope 2009



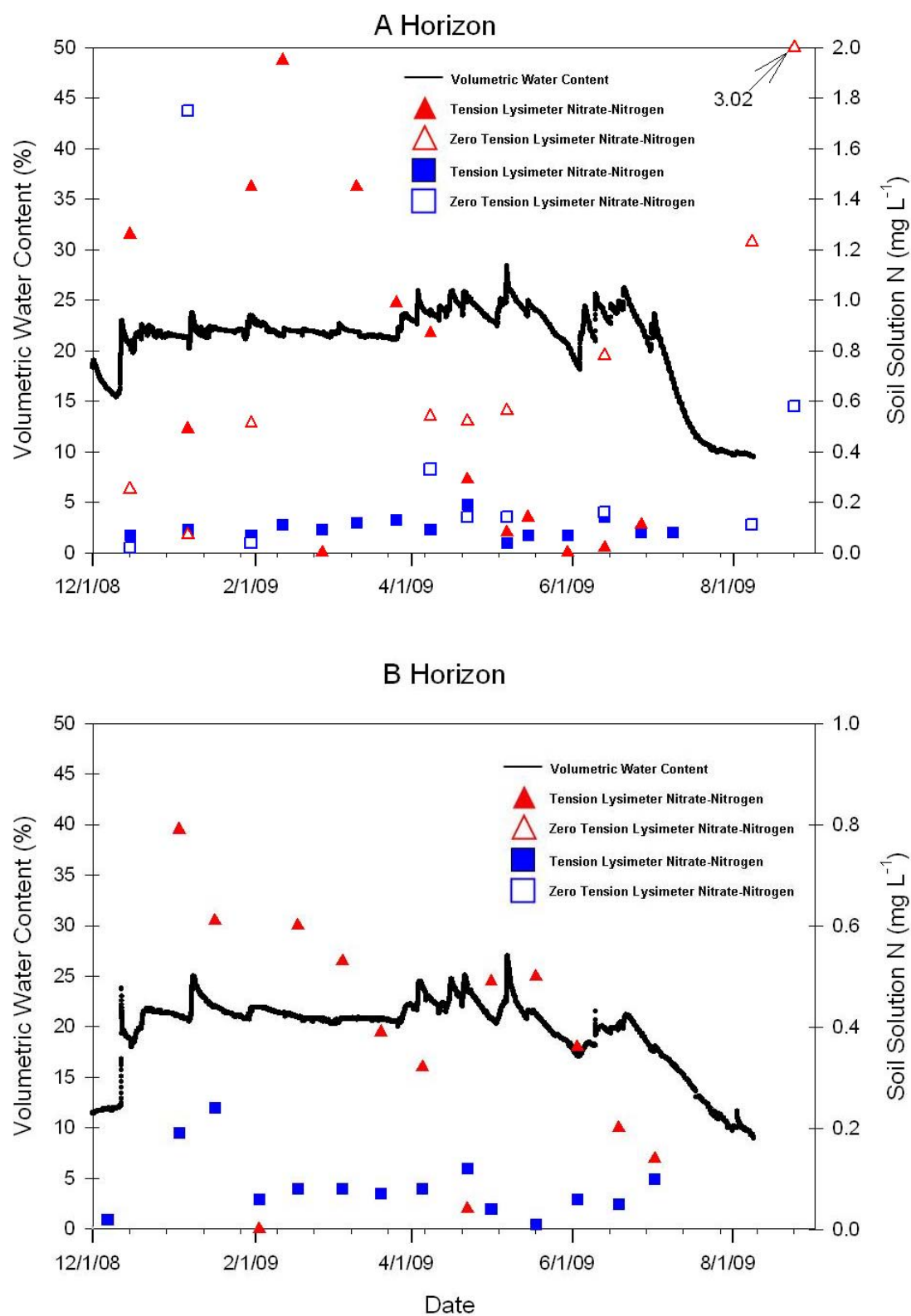
Transect 4, Toeslope 2009



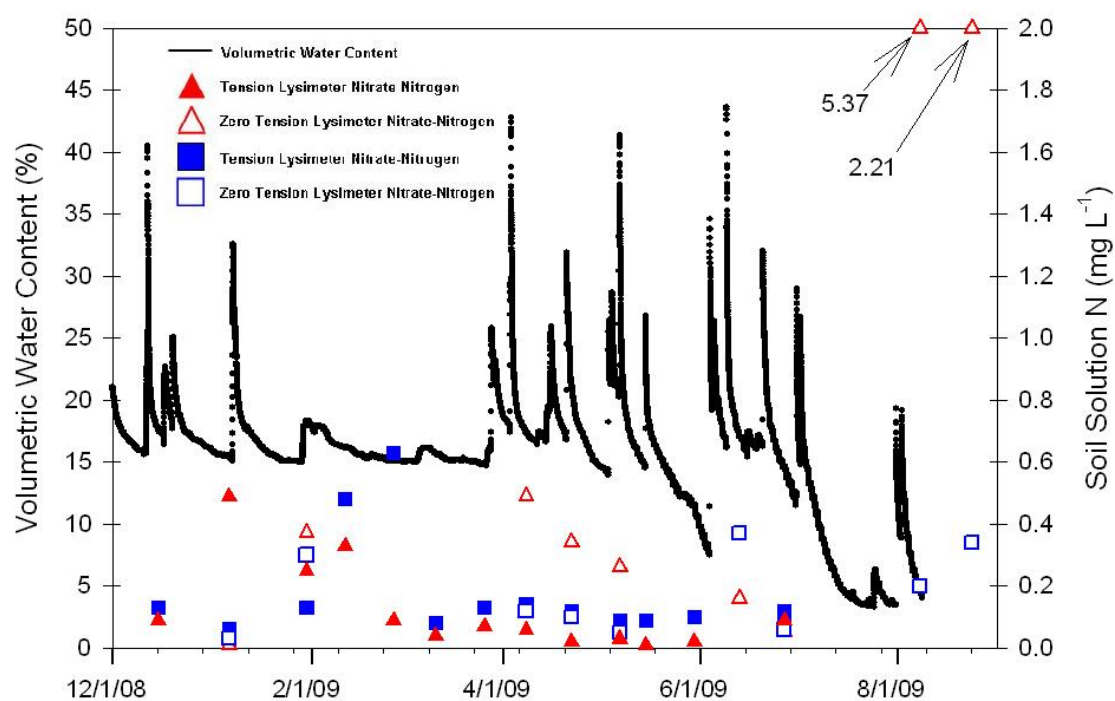
Transect 5, Ridgetop 2009



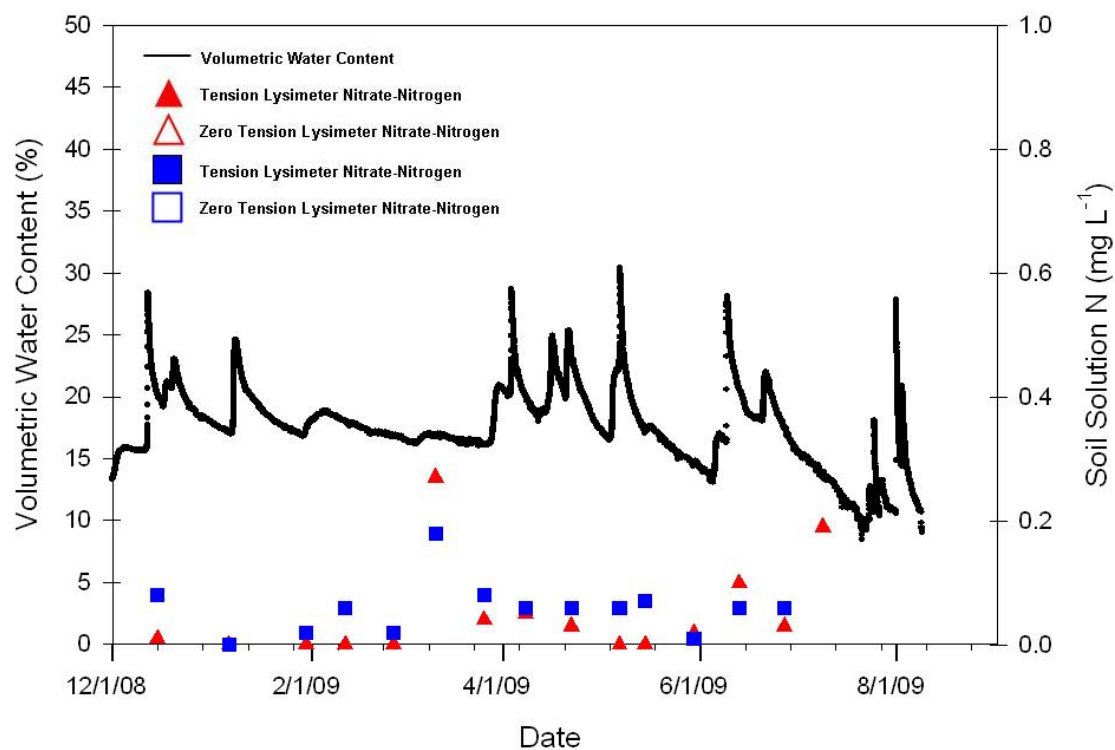
Transect 5, Hillslope 2009



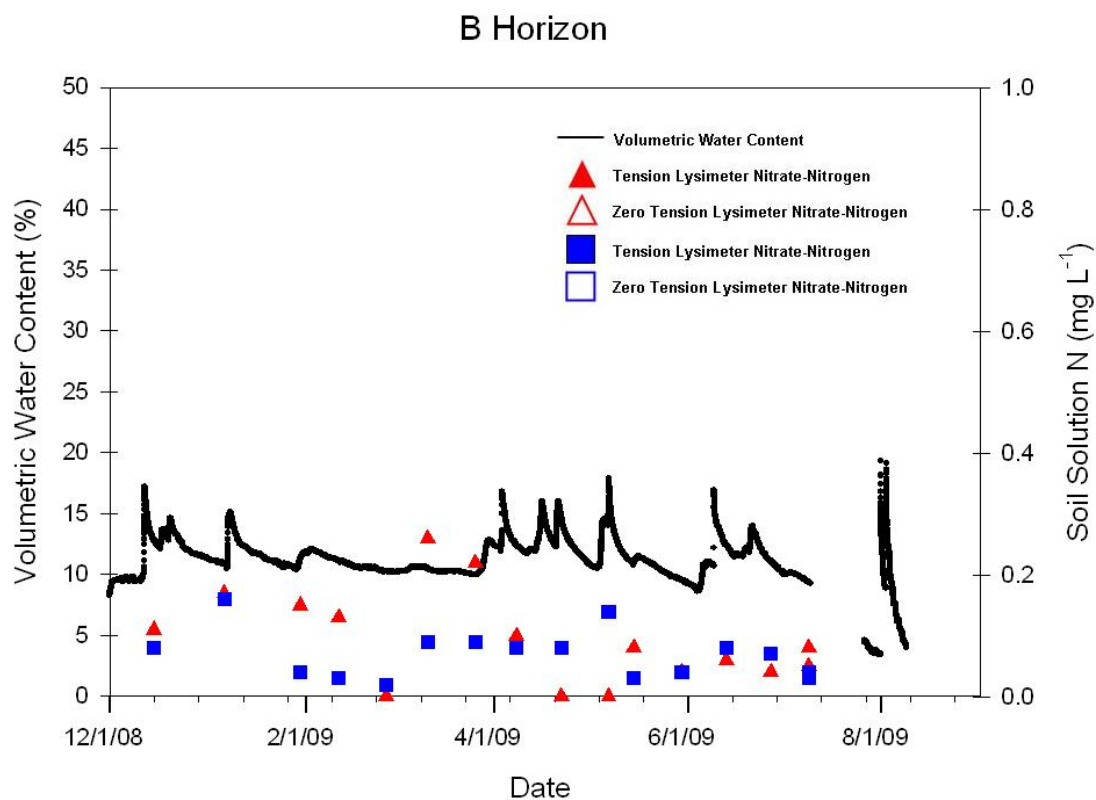
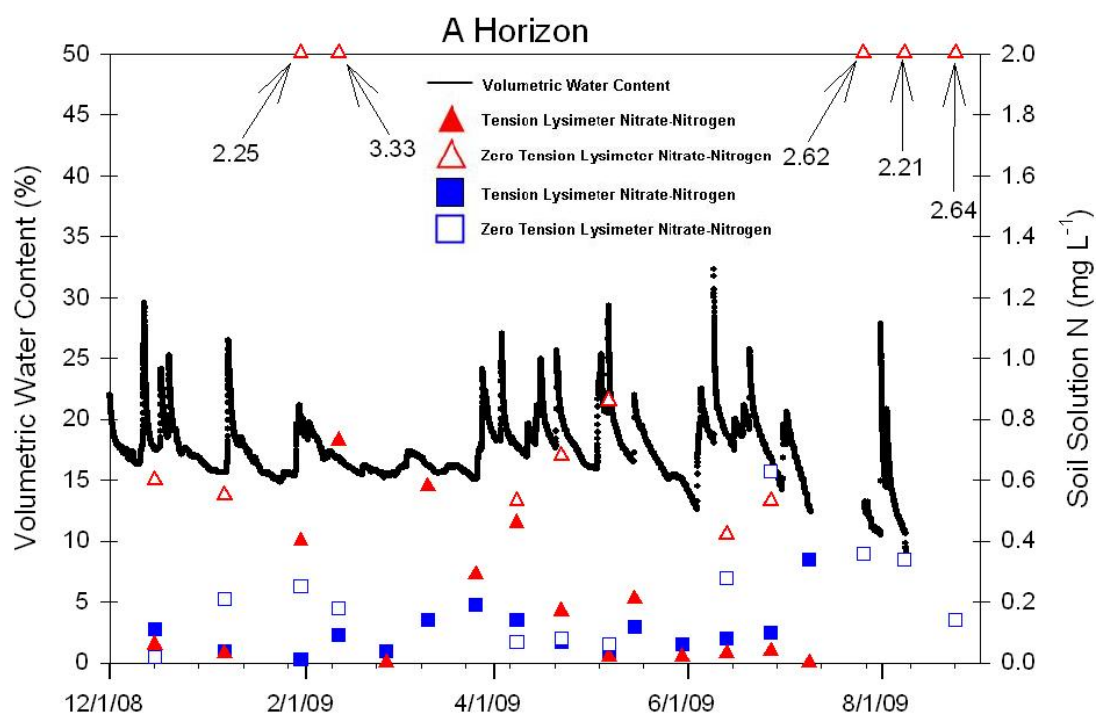
Transect 6, Ridgetop 2009



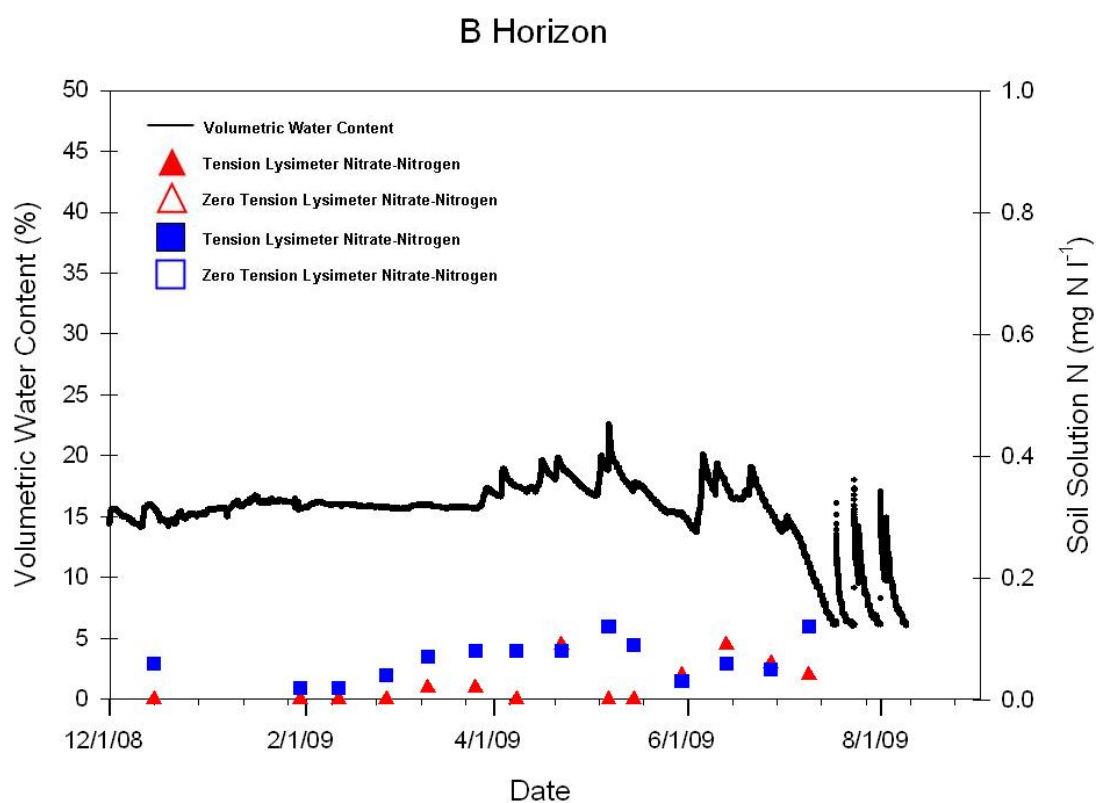
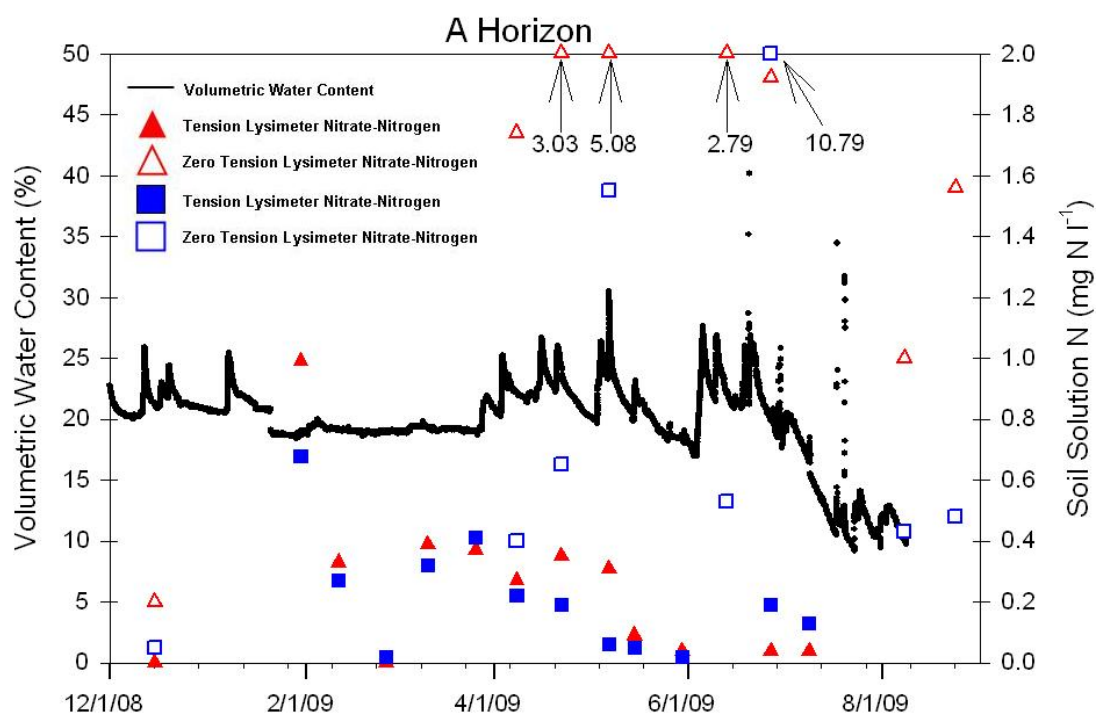
B Horizon



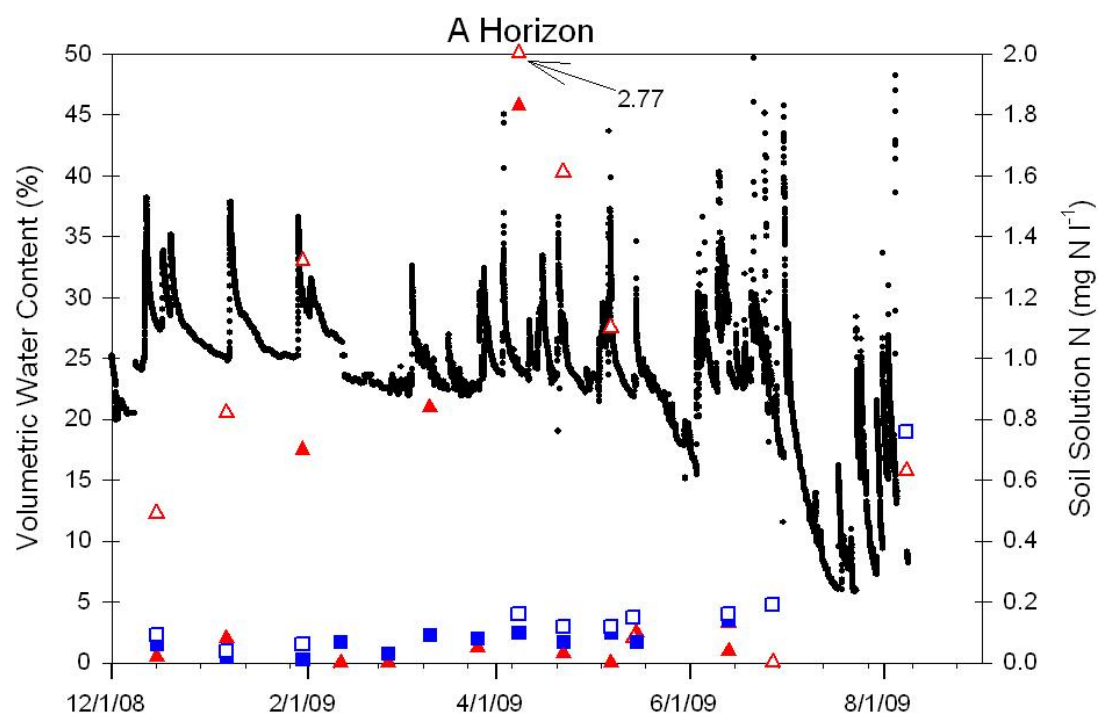
Transect 6, Hillslope 2009



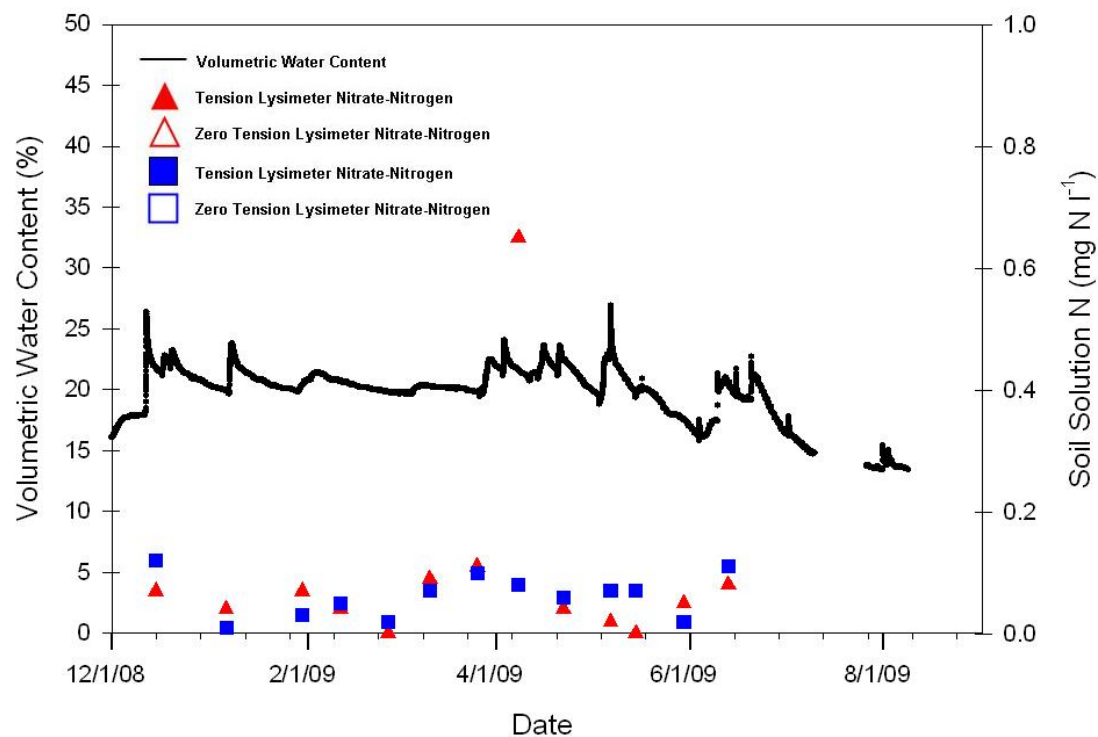
Transect 6, Toeslope 2009



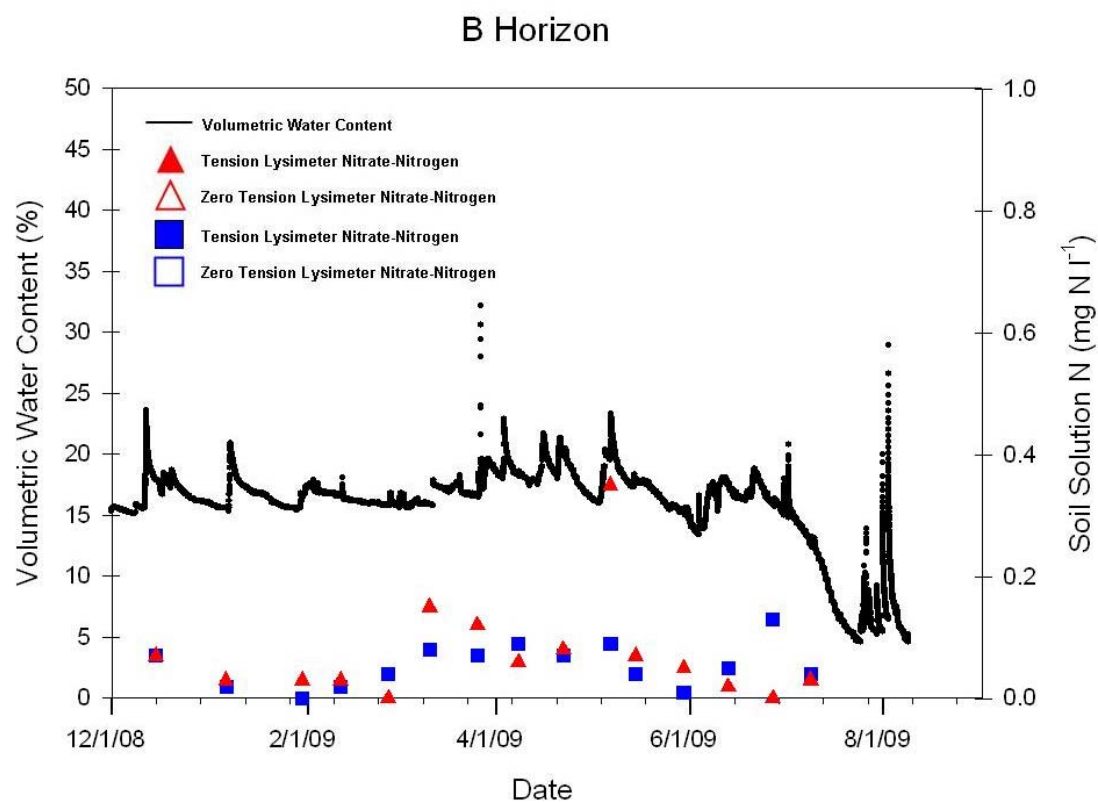
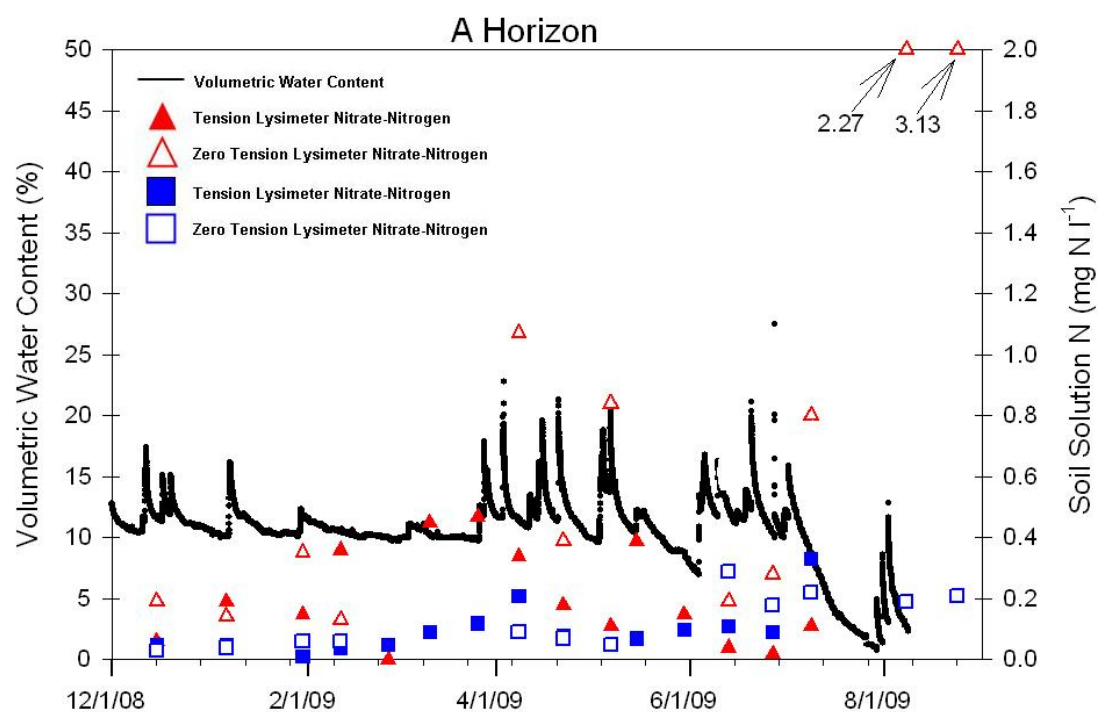
Transect 7, Ridgetop 2009



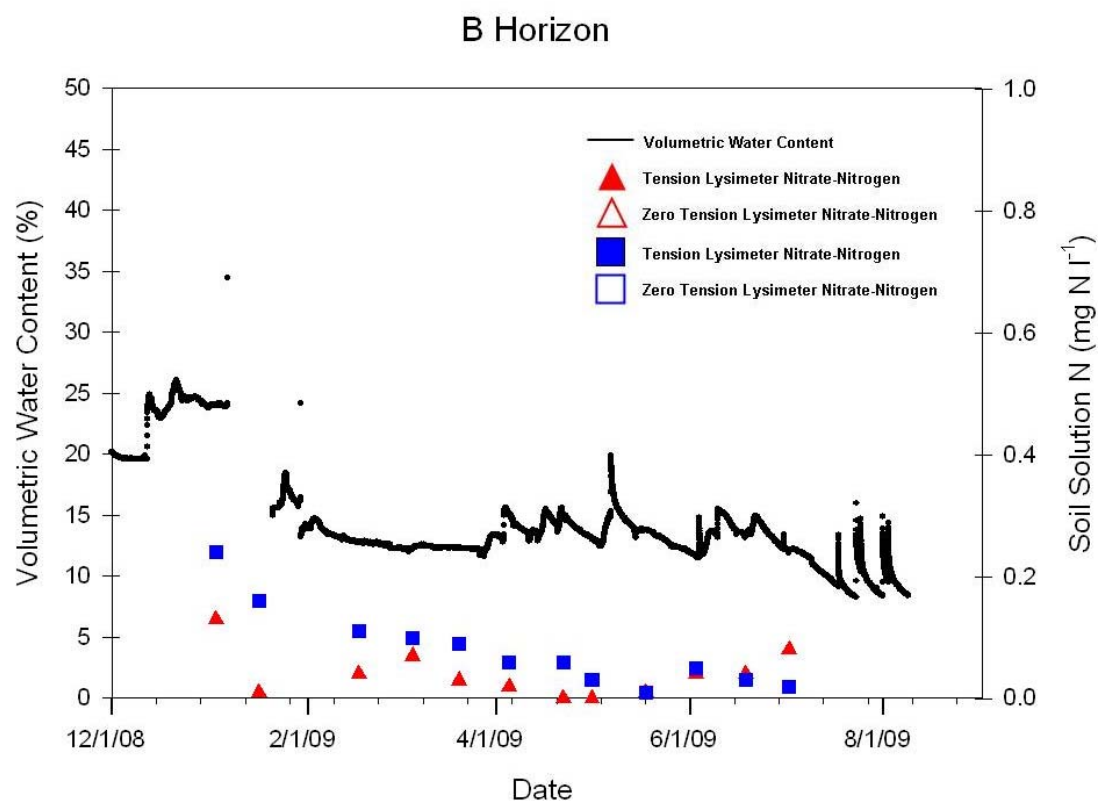
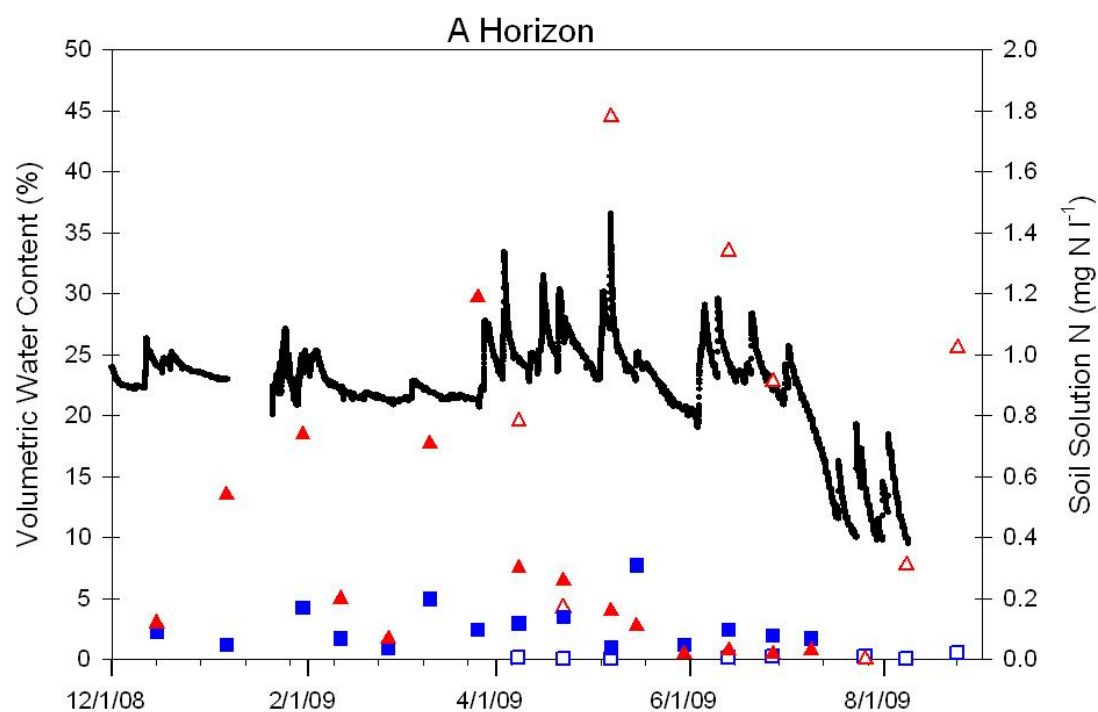
B Horizon



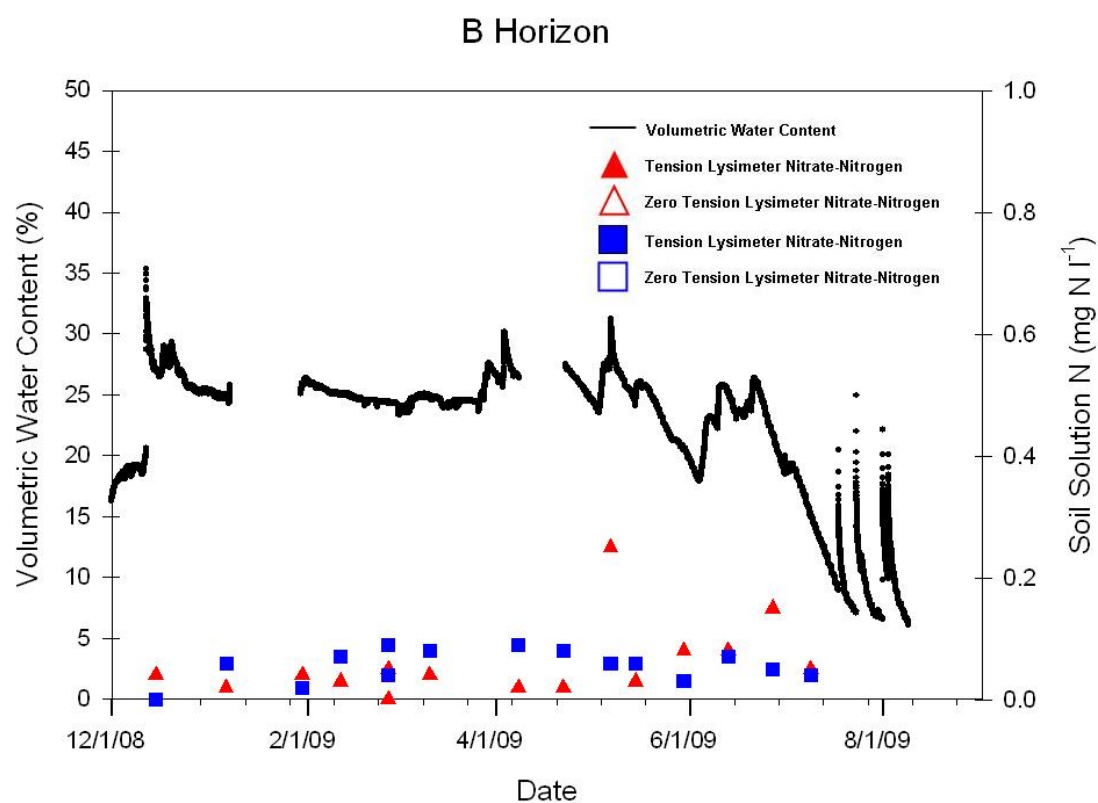
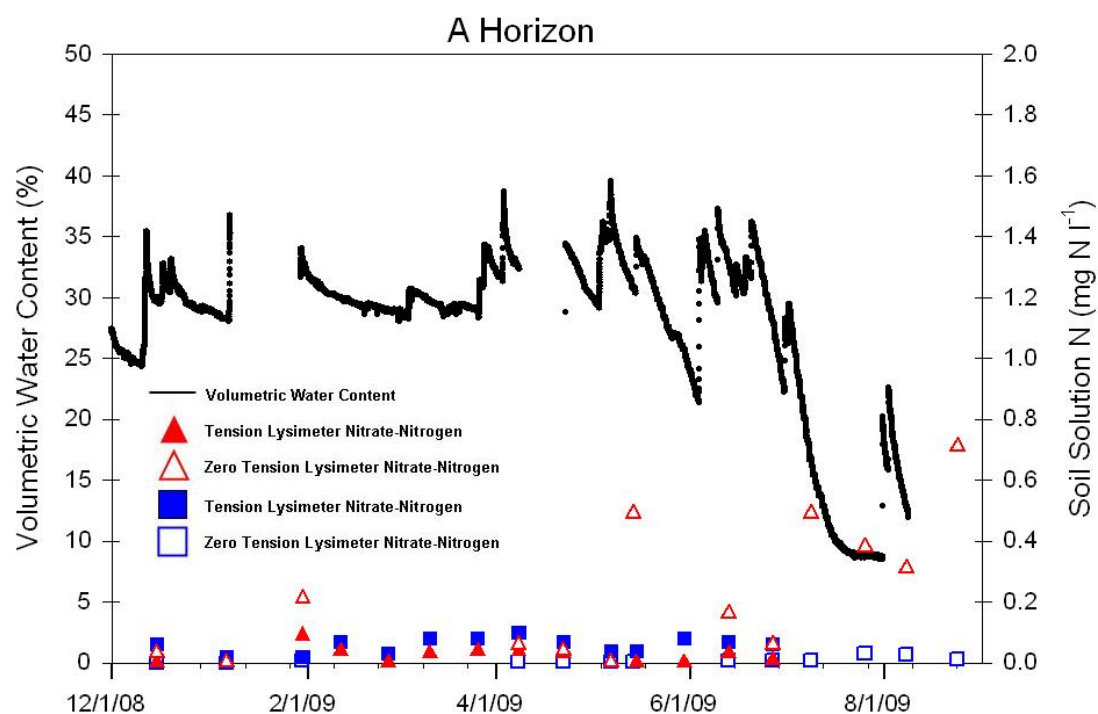
Transect 7, Hillslope 2009



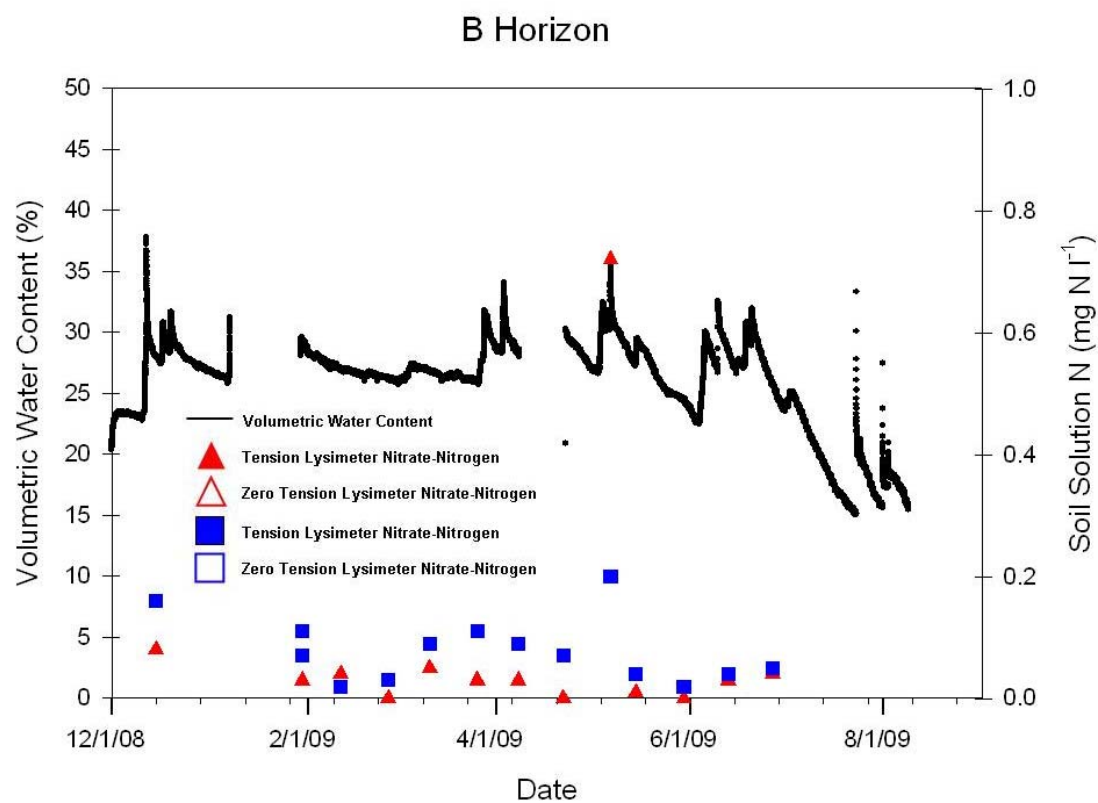
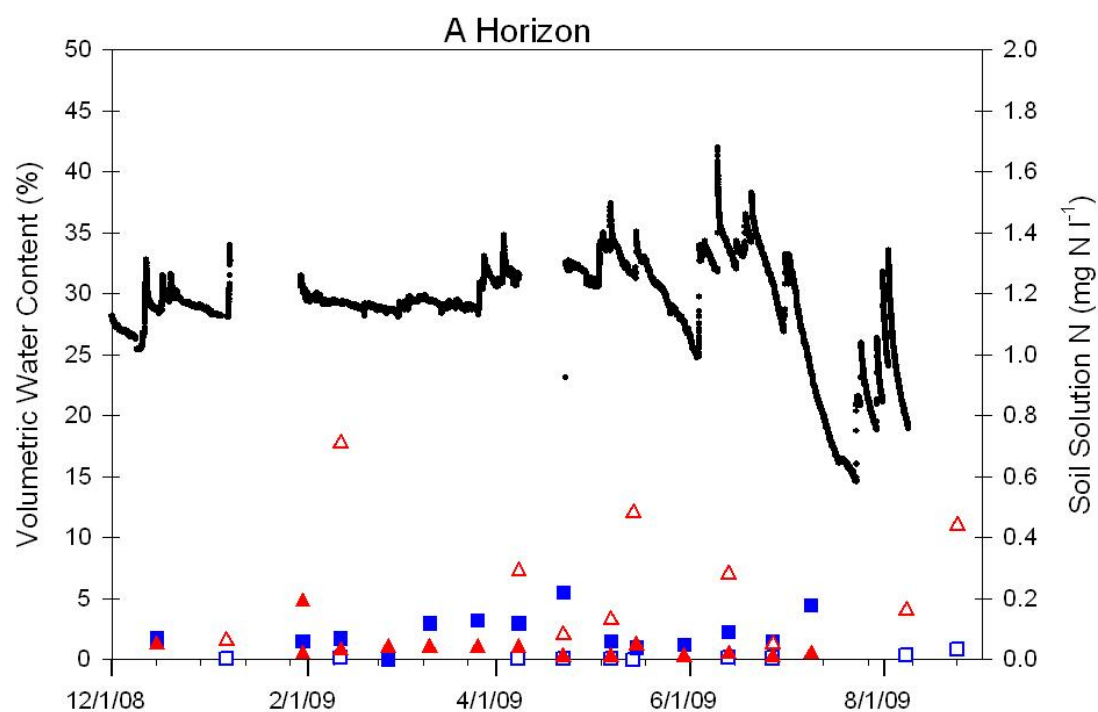
Transect 7, Toeslope 2009



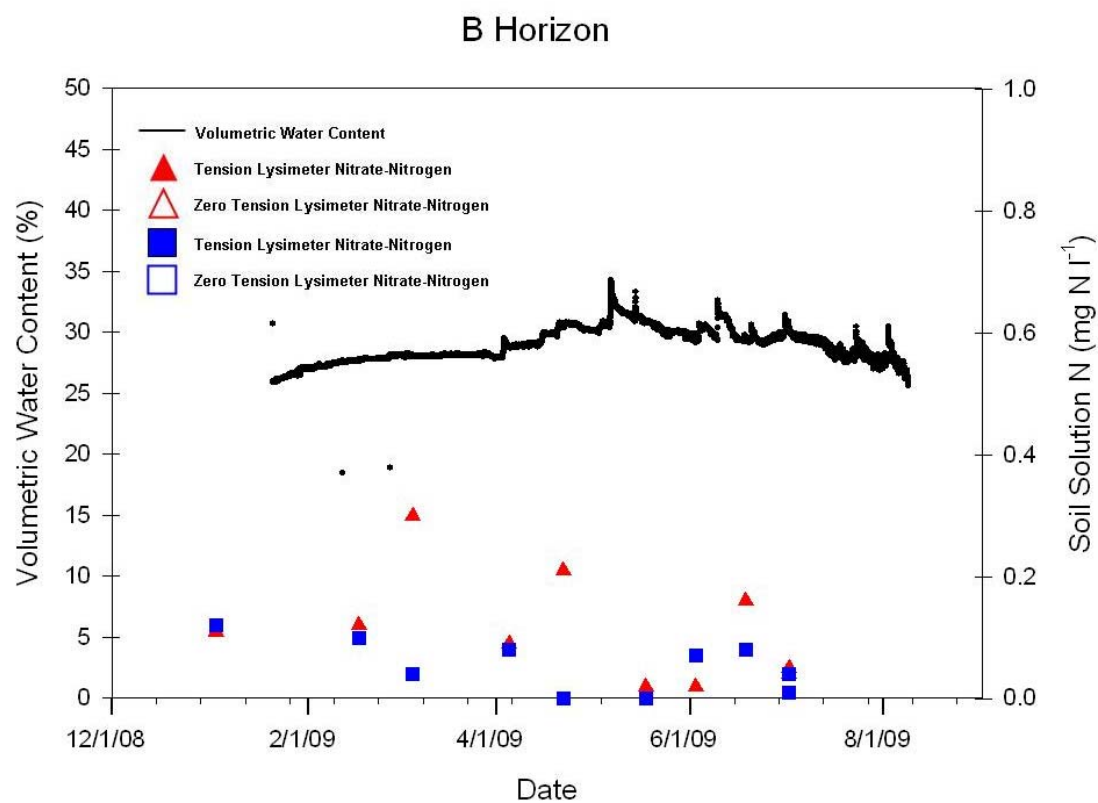
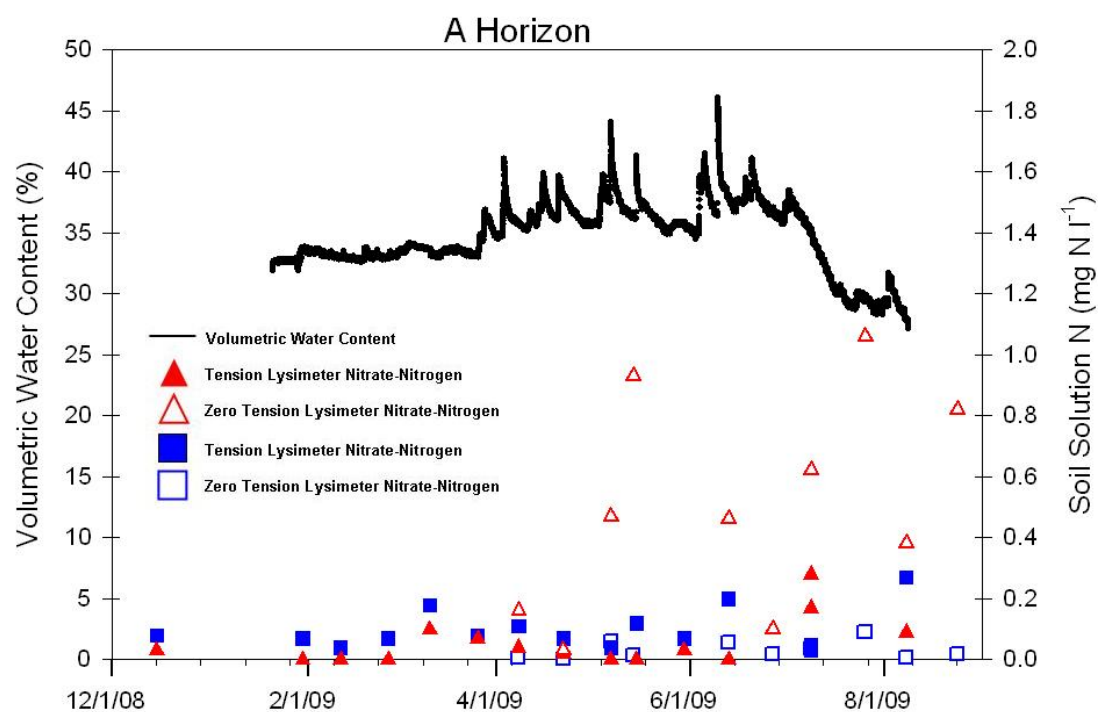
Transect 8, Ridgetop 2009



Transect 8, Hillslope 2009



Transect 8, Toeslope 2009



VITA

Michael J. Castellano

Education

Ph.D. 2009, The Pennsylvania State University

M.S. 2004, Saint Louis University

B.S. 2001, University of Rhode Island